The investigation of groundwater transport in a geological formation: West Park Cemetery, Johannesburg, South Africa.

Bomkazi Vava

Student number: 2016111847

Submitted in the fulfillment of the requirement for the degree

Master of Science in Geohydrology

in the

Faculty of Natural and Agricultural Sciences

(Institute for Groundwater Studies)

at the

University of the Free State

Supervisor: Prof Abdon Atangana

Bloemfontein, Free State

2023

Declaration

I, Bomkazi Vava, attest that the dissertation I submitted to the University of the Free State, Institute for Groundwater Studies within the Faculty of Natural and Agricultural Science to complete my master's degree under Professor Abdon Atangana supervision, titled "The investigation of groundwater transport in a geological formation: West Park Cemetery, Johannesburg, South Africa," is my original work and includes a list of references to acknowledge all sources cited.

In addition, I give the University of the Free State all rights to the dissertation and its contents.

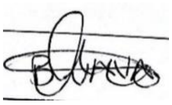

Bomkazi Vava

2016111847

Abstract

Groundwater is a source of fresh water for many people who live in communities with little surface water around the world. The major sectors of groundwater use are municipal; rural; agricultural irrigation; agricultural-livestock watering; industry and mining. The amount and quality of groundwater have nevertheless decreased because of anthropogenic activities, global climate change, and poor groundwater management. The use of fertilizers and pesticides, urban development, the dumping of household waste on the land, municipal waste discharge and laboratory waste disposal, the aquifer close to contaminated streams, mining operations, and the discharge of effluents with high concentrations of industrial chemicals and sludge on the land pose a concern on groundwater. Due to the migration of solutions from leachate to the soil, dumpsites are also regarded as important sources of groundwater pollution. Pollution from naturally existing toxins, such as arsenic or fluoride, should not be overlooked. Historically, contaminated drinking water has been known to be capable of transmitting dangerous chemicals and deadly diseases. In this thesis, we have considered contamination from cemeteries because they also contribute to contaminating groundwater, which spreads infectious diseases and dangerous substances. Many lives are lost because of the spread of some infectious diseases, resulting in a large number of burials that could pollute groundwater. The Johannesburg West Park Cemetery was selected as our case study location. We gathered a variety of data regarding the cemetery expect for water samples as the boreholes were dry. The collected data were subjected to numerous analyses, and a detailed presentation of the geological structure under the cemetery was made. A high rate of burials was seen between 2020 and 2022, primarily because of the spread of COVID-19. We presented evidence to support our claim that the crossover seen during the decay process cannot be replicated by the decay model with the classical derivative. To simulate the transition from fast decay to slow decay, a fractional model was utilized using a Mittag-Leffler function as the solution. The acquired results assisted us in choosing an appropriate mathematical formulation of the advection-dispersion equation, which was also numerically examined. Under certain hypotheses, we ran some numerical simulations utilizing the mass released within the geological formation as the beginning concentration. The cemetery's boreholes should be checked monthly to improve the environment, and additional boreholes should be dug to figure out the type of aquifer beneath the cemetery and the direction of flow since these details aren't currently known. This will help to ensure that the cemetery does not contaminate the environment, or the water supplies nearby.

Acknowledgments

"And we know that in all things God works for the good of those who love him, who have been called according to his purpose" – Romans 8:28.

I humble myself before the All-Powerful Lord, whose mercy led me throughout the course of this study from the beginning to its end. I have come this far because of your grace, tenacity, and faithfulness. It's a blessing that you directed me along this route. Thank you, God.

I owe a debt of gratitude to Professor Abdon Atangana for all of his assistance, support, and intelligence. His insightful advice and recommendations for adjustments, changes, and enhancements helped me become more flawless in how I carried out my work. Merci.

For their unwavering support, encouraging words, and genuine interest in my academic accomplishments, I would like to extend my sincere appreciation to my mother, Zoliswa Vava, and aunt, Zolelwa Vava. Hopefully, I have made you proud.

I dedicate my effort to my siblings, Siyasanga, Monelisa, Somila, and Yamkela as evidence that everything is achievable with faith, perseverance, and prayer.

Lastly, I would like to say thank you to Manna Mgijima, extended family, and friends for continually being beside me whenever life gets challenging. True friends are comparable to the oil of anointing which releases the aroma of the presence of God.

"Isipho somntu siyamgabulela, simse phambi kwabakhulu".

Table of Contents

List of Figures

Chapter 1: Introduction

1.1 Background Information

Groundwater is any water that is present in the saturated zone under the earth's surface which can be found in aquifers, porous rock, and silt with water in between, is the greatest freshwater reserve that is accessible to humans. The amount of groundwater that can enter a given area determined by the climate of the area, type of geology, the amount of vegetation, the vicinity of land usage and how well water retains. Approximately one-third of the world's populace gets their water for consumption from groundwater sources. In areas with minimal or no precipitation, groundwater is an important asset that can be utilized (Li, et al., 2017). Groundwater is essential for both sustaining water security and promoting economic growth in many South African rural and urban cities that rely entirely or partially on groundwater supplies. In South Africa, 22% of municipalities use groundwater as their only source, and another 34% use groundwater in conjunction with surface water (Department of Water and Sanitation, 2016). As industrialization and urbanization advance, South Africa's water usage rises, making it one of Africa's water-stressed nations. As a result, groundwater is more important and its function must be understood. Since groundwater typically provides a steady supply during dry spells and periods when there are no surface water resources, it can be defined as an ongoing source of supply if the recharge of aquifers is sufficient. Groundwater resource sustainability is essential for ensuring water security as it is a primary supply of drinkable, agricultural, and industrial water. The major sectors of groundwater use are municipal; rural; agricultural irrigation; agricultural-livestock watering; industry and mining. According to estimates from 2003 by (Foster & Chilton, 2003), groundwater resources account for about 50% of supplies of potable water, 40% of industrial water needs, and 20% of agricultural water.

1.2 Introduction

The city of Johannesburg is dependent on surface water supplies, but because of its high population density and demand in the semi-arid region, groundwater is becoming increasingly significant. Due to its water scarcity, this region is regarded as the economic centre of South Africa and is supported by inter-basin surface water supplies (Leketa, et al., 2018). In the semiarid environment of the Johannesburg region, where groundwater is especially important for socio-economic development, there are many factors at play. In fractured aquifers made of meta-sedimentary rocks like quartzite and dolomites, where groundwater flow and storage take place, the availability of groundwater is predominantly regulated by fractures and weathering zones (Abiye, et al., 2018). Aquifers composed of fractures and weathered crystalline basement rocks of low productivity and highly yielding Karstified meta-dolomites serve as the source of groundwater for extremely intensive farming, industrial, and rural residential activities. More water is present in the karstic aquifer than in the Vaal Dam, which is situated between the Witwatersrand Supergroup and the Karstified dolomites of the Malmani Supergroup of the Transvaal Supergroup. The karst system that stretches from the Northwest province to Gauteng into Mpumalanga and Limpopo Province can only supply towns, rural settlements, and farmland there. The aquifer is unable to provide water to the Witwatersrand's society and industries due to the contamination of surface water resources, the aquifer, and the sewage, industrial waste, and effluent from the region's gold mines (Durand, 2012). Hydraulic characteristics of the underlying fractured zone and the overlaying weathered zone affect the groundwater flow and the presence of aquifers with fractures, fissures, and joints (Witthüser & Holland, 2008). According to the structural features of the groundwater in the Johannesburg area, the mixing of fresh and contaminated groundwater occurs in shallow zones within weathered crystalline rocks and dissolution cavities in dolomites where the rocks are distinguished by lithological and structural complexity.

The amount and quality of groundwater have nevertheless decreased as a result of anthropogenic activities, global climate change, and poor groundwater management, as time passed, groundwater contamination became an urgent concern due to the health risks linked with its use as drinking water. The most frequent method by which people are exposed to hazardous substances of anthropogenic or geological origin is through their drinking water and due to the subsurface release of organic chemicals, groundwater supplies around the globe are exposed to an unpredictable risk of contamination (Murray & Douglas, 2001). Contamination is the existence of a constituent, impurity, or other unwanted element that could be harmful to the ecosystem or human health. Therefore, the addition of undesirable compounds to groundwater brought on by human activity is referred to as groundwater contamination and it is caused by the spread and storage of pollutants that can percolate to the ground or above the top of the soil (Iyyanki & Valli, 2017). Human activity can cause contaminants, such as toxic chemical spills or leaking gasoline tanks. Applications of pesticides and fertilizers infiltrate cultivated soil and end up in water obtained from a well. Additionally, bacteria can enter water through leaks from septic tanks and/or landfills. A danger to human health, ecological services, and sustainable socioeconomic development are contaminants like toxic metals, hydrocarbons, trace organic contaminants, pesticides, nanoparticles, and micro plastics, to name a few. Groundwater contaminants are typically tasteless and translucent. Furthermore, the harmful effects of polluted groundwater on human health are chronic and challenging to spot and once polluted, groundwater may continue to be unusable or even dangerous for centuries. Contamination from septic tank refuse can result in illnesses like hepatitis and dysentery. Exposure to human use of hazardous inorganic substances like arsenic and polluted water may also have other long-term effects, such as skin disorders, skin cancers, internal cancers (bladder, kidney, and lung), diseases of the blood vessels of the legs and feet, possibly diabetes, high blood pressure, respiratory infections and heart disease. The three main anthropogenic sources of environmental contamination are generally acknowledged to be agriculture, industry, and landfills. The discharge of acid mine wastewater from closed gold mines and the release of inadequately treated water that flows back from urban areas have reduced the amount of surface water available in the Crocodile River and Hartbeespoort Dam for leisure and farming purposes (Durand, 2012). Polluted surface water resources may also be impacting the quality of groundwater since they are sources of concentrated recharge. The quality of both groundwater and surface water is seriously threatened by seepage from tailings storage facilities, or mine waste dumps, in the Witwatersrand gold mine. Tailing's storage facilities are the most well-known pollutant in the Witwatersrand Basin because they are linked to large acid plumes that affect the nearby groundwater. However, the movement of contaminants from cemeteries into groundwater, surrounding water bodies, and water abstraction stations will be the main emphasis of this paper.

1.2.1 Factors Influencing Groundwater Quality

The safety of groundwater resources is a critical concern in countries where groundwater is the primary source of water for drinking, agriculture, and industry. Groundwater pressure has increased due to industrialization, rapid urbanization, and excessive irrigation, which has resulted in resource depletion and a decline in resource quality. As stated by (Mvandaba, et al., 2019), understanding the impact of climate change on groundwater resources, identifying potential at-risk areas, figuring out the implications for these vulnerable areas, and developing a workable set of guiding mitigation and adaptation strategies are all crucial for meeting the needs of both present-day and future communities. The mineral makeup of an aquifer, geology, weathering, water-rock interaction, topography, tidal effects, climate, anthropogenic activities, and the overall hydrogeological framework of an area are significant factors that affect groundwater quality. However, the characteristics of the soil and its filtration capacity are said to be the main factors that make groundwater vulnerable. These characteristics can either encourage or hinder the diffusion of environmental contaminants.

I. Cemeteries

Cemeteries as potential sources of pollution have not received much consideration (Jonker & Olivier, 2012). The increased interest in public health and sanitation during the first decades of the 19th century led to a widespread secularization of cemeteries in the Western world. Additionally, they have never been thought to have considerable potential for environmental damage. According to (Borstel, 2000) research, mineral-releasing burial loads are the primary contributor to cemetery contamination. The materials that are used to construct coffins deteriorate, releasing poisonous minerals. These minerals could spread into the soils nearby, seep out of the graves, and contaminate the groundwater, posing a health danger to anyone living near the cemetery. (Üçisik & Rushbrook, 1998) claim that given the lack of a thorough investigation into the role that decomposing bodies play in the contamination of groundwater, the transmission of dangerous chemicals, and the transmission of infectious diseases, the pollution risk posed by an improperly situated cemetery is just as serious as that posed by an improperly situated landfill.

II. Influence of geological factors

Due to the presence of minerals in aquifer rocks and sediments that can dissolve in groundwater when certain geochemical conditions are met, the structure and lithology of fractured bedrock aquifers can have significant effects on groundwater quality (United States Geological Survey, 2021). How much water can infiltrate the soil is influenced by its mechanical characteristics, such as the degree of fracture, particle size, and porosity, as well as its chemical and physical characteristics, such as cations, soluble chemicals, pH, and clay content. Sedimentary rock tends to have contamination more often than igneous or metamorphic rock. (Goeppert & Goldscheider, 2011) asserts that soil porosity affects how contaminated groundwater is. While non-porous karst soils are considered to be more sensitive and strongly impacted by agricultural activities, sandy soils may hinder the spread of microorganisms. The chemical composition of groundwater, which is affected by the solubility of the soil it passes through and the depth of the aquifer, also varies according to its quality.

III. Climate change impacts

A greater strain is anticipated on South Africa's groundwater resources due to the effects of climate change and population increase (Viljoen & Bosman, 2022). Water is thought to be the most important resource, even though climate change is anticipated to have an impact on many areas of the built and natural environments. Seasonal variations and meteorological conditions influence the quantity and quality of groundwater. The water quality, for instance, might be significantly impacted by high intensity or drought. Microorganisms are efficiently retained in groundwater and are only occasionally found there under typical environmental conditions. As a result, prolonged rain helps spread pathogenic bacteria to places where they had not previously been seen (Tornevi, et al., 2014). The consequences of climate change can also be felt in underdeveloped rural areas, which slows both local and global economic growth. Due to the reliance on groundwater for most extreme occurrences, such as intense flooding and frequent droughts, this is brought on by an increase in their frequency.

South Africa's runoff is particularly sensitive to fluctuations in precipitation, and it is estimated that in some regions, runoff would decline by up to 10% as a result of global climate change, according to research recently conducted in South Africa, Lesotho, and Swaziland (United States Agency, 2012). This occurs as a result of the region's overall aridity and significant spatial and temporal variability in rainfall. Climate change, therefore, affects the availability of water and decreases water flow for aquifer recharge, leading to a loss in groundwater resources or depletion as a result of significant groundwater abstraction by humans.

IV. Land-based activities

According to (Danielopol, et al., 2003), a significant environmental trend over the next 25 years will be the severe decline in the number of underground water reserves that are readily accessible due to ongoing water demand growth. The aquifers of South Africa are vulnerable as a result of land-use practices like active and abandoned tailings dams, municipal and industrial dumps, stockpiling of specific raw materials, storage tanks for fuel and chemicals, and even improper septic tank placement (Viljoen & Bosman, 2022). (Viljoen & Bosman, 2022) continues by stating that because they may alter the quantity, quality, availability, and occurrence of groundwater, all land-based human activities have an impact on the hydrogeological cycle, either directly or indirectly. As a result of population growth, and contamination brought on by anthropogenic activities including mining, urban development, industry, and agricultural practices, groundwater quality, especially of shallow groundwater, is becoming more prominent.

1.3.1 Problem Statement

It is well established that from recharge areas to discharge areas, water, and pollutants move in the topographic direction. A pollutant that has been released into the environment may or may not travel inside an aquifer in the same way as groundwater does, depending on its physical, chemical, and biological qualities. This natural impact is linked to the geology and the composition of the rocks that constitute the flow regime of the groundwater at a specific locality.

Since rock fractures are typically irregularly spaced and do not follow the contours of the land surface or the hydraulic gradient, groundwater, and pollutants can travel quickly through them. Also, the contamination is dispersed across a larger area by water movement and dispersion inside the aquifer.

- In a geological structure that displays crossover characteristics, how can we model the movement of contamination in space and time?
- How long does it take for the liquids produced by the decomposition of bodies to reach groundwater, water bodies, and water abstraction stations?
- What impact do graves beneath fracturing or voids in the rock have?

1.4.1 Significance of the Study

A geological feature known as an aquifer is composed of one or more layers of rock that serve to store and maintain groundwater levels in the soil. The sustainability of water resources is threatened when an aquifer produces a contaminated plume due to pollution and contamination of South Africa's metropolitan aquifers. The effects of groundwater contamination can be seen in socioeconomic development, environmental quality, and human health. Numerous studies in the field of health have revealed that exposure to high concentrations of fluoride, nitrate metals, and persistent organic pollutants puts people at risk for health problems, with new-borns and children being more at risk than adults (Ji, et al., 2020). Contaminated groundwater can result in soil contamination and a decline in the quality of the land, which has a detrimental effect on both the land and the forest. High groundwater salinity in agricultural areas affects the growth of vegetation and salinization of the soil (Jenifer & Jha, 2018). For sustainable economic development, the level of human demand and the rate of natural resource regeneration must be balanced. However, due to groundwater contamination, freshwater availability may decrease, disrupting the balance between water supply and demand and resulting in societal unrest and even conflict.

Groundwater transport in heterogeneous geological formations or groundwater transport in fractured formations has drawn more attention than crossover behaviour in geological formations. The interest in understanding and modelling the exchange between irregular flows and movements of pollution within complicated geological formations is a long-standing issue that is still not fully understood and for which a complete set of equations is still lacking. Over the past 10 years, various approaches to capturing these nonlocalities have been put forth, such as differential operators with power laws, exponential decay, and the generalized Mittag-Leffler function. The generalized Mittag-Leffler functions and exponential decay, however, were the only ones recognized to have crossover properties, both of which had the drawback of being unable to pinpoint the precise moment and location at which crossover takes place.

One of the main human-made sources of water pollution and contamination in urban areas and worldwide is cemeteries (Silva, et al., 2011). They can spread hazardous infectious diseases and have significant negative effects on groundwater. The consequences of cemeteries on the bacterial and viral contamination of groundwater have been studied in several geographical areas across the world. However, very little research has been done on the geology and hydrogeology of cemeteries being contaminated globally. Therefore, the proposed study will advance the field by generating fresh data, a fresh framework, and theoretical insights that can be applied to real-world problems. Numerous cemeteries were incorrectly localized, according to studies done in South Africa (Engelbrecht, 1993; Tumagole, 2006). Discovering burial sites where hydrogeological, geological, and climatic conditions are unfavourable to the process, will help by providing variables to be taken into account while choosing burial grounds. And also enables the creation of some suggestions aimed at safeguarding the health of cemetery team members and local inhabitants who live close to cemeteries, as well as maintaining the environment for future generations.

1.5.1 Aim and Objectives

The study aims to develop more accurate models for groundwater flow and transport, as well as to better predict abnormal behaviours of the flow and movement of pollution within complicated geological formations. The following objectives will be carried out to accomplish:

i. To observe the migration of human remains into the ground,
ii. To investigate the West Park Cemetery's groundwater contamination level,
iii. To determine the impact of cemeteries on groundwater,
iv. To determine the stability and accuracy of equations in complex geological formations,
v. To investigate the sensitivity of the previously discovered and proposed equations.

1.6.1 Thesis structure

Chapter 1	Covers background information on groundwater, discusses its significance, variables that affect groundwater quality, problem identification, the importance of the study, research goals, limitations of current methods, and the structure of the thesis.
Chapter 2	Cover a detailed literature review of groundwater flow systems and contamination models and groundwater contamination.
Chapter 3	Covers groundwater contamination in cemeteries
Chapter 4	Covers description of the study area
Chapter 5	Covers materials, methods, and results
Chapter 6	Covers groundwater transport model
Chapter 7	Covers discussion, recommendation and conclusion

Chapter 2: Literature Review

2.1 Introduction

The main interest in groundwater studies began in the first decades of the twentieth century with the discovering and use of the resources of groundwater. The environmental and engineering significance of groundwater has nevertheless grown along with the growth of businesses, water supply, and larger designed projects. As a result, industrial-scale water supplies are required, as is an understanding of how groundwater impacts structures such as tunnels, dams, and deep excavations. According to (Singh & Kaur, 2003), groundwater has been deemed to be among the greatest natural assets because it exists below the Earth's surface, as well as its formation in rock cracks. Around thirty percent of the planet's easily obtainable freshwater comes from groundwater, which is essential for biodiversity, health for humans, and the growth of the economy (Jha, et al., 2007). The Republic of South Africa (RSA) has many rural and peri-urban communities where there are no water distribution systems and subsurface water is the sole supply of usable water because surface water has become contaminated. As common in other countries, such as in rural Zambia, water for consumption is supplied through public and personal boreholes. Zambia's rural residents, who make up roughly sixty-five percent of the country's population, heavily rely on groundwater (Kapulu, 2012). The transportation and handling of substances, energy sources, and waste from industries were mostly unregulated before to the 1960s (Singh & Kaur, 2003) however, things changed as a result of population growth, economic expansion, environmental changes, shortages of water, and improved availability of clean water. Growing urbanization and the rise in population have contributed to groundwater contamination in numerous regions, improper subsurface utilization and the dumping of household and industrial waste. The contamination of groundwater is an important because of the health risks connected with its use as drinking water.

2.2 Groundwater Contamination

In recent decades, contamination of groundwater has grown to be a significant worldwide challenge. Numerous factors, such as urbanization, agriculture, industry, and climate change, have an impact on groundwater quality. As reported by (Engelbrecht, 1993; Akhtar, et al., 2021), the usage of nourishments and insecticides, urban development, dumping of household waste on the land, public waste discharge and laboratory waste disposal, aquifer in close to contaminated streams, mining operations, and the discharge of effluents with high concentrations of industrial chemicals and sludge on the land pose a concern on groundwater. Due to the migration of solutions from leachate to the soil, dumpsites are regarded as important sources of groundwater pollution.

They create toxins using various harmful chemical components. The increased levels of nutrients in streams and groundwater due to decades of residential growth, land use change, and urbanization have a negative influence on the water quality of streams and the health of their ecosystems (Groffman, et al., 2004). As a result, bacteria, viruses, and newly emerging infectious illnesses operate as environmental reservoirs in groundwater. The leaching of cationic and anionic compounds, such as fluorides, sulphates, heavy metals, and metalloids, can also be the outcome of natural processes like weathering and regional geology (Li, et al., 2018; Kaur, et al., 2020). In the words of (Kaur, et al., 2020), endemic fluorosis (skeletal and dental) and other consequences on children's neurological systems are all possible implications of fluoride in groundwater, which puts 200 106 people at risk. Furthermore, this issue is present in China, Tanzania, South Africa, and other nations as well. However, this section examines how cemeteries affect groundwater quality in saturated and unsaturated areas.

Many scientists believe that all cemeteries pose potential environmental risks. Numerous researches on the effects of graves on groundwater have been conducted in various locations, at various times, and with various environmental factors. (Van Haaren, 1951) became the initial researcher to detect high quantities of specific ions in underground water without assessing the soil properties in order to discover the effects of cemeteries on the groundwater regime. According to the data, there were 500 milligrams per litre of chlorides, 300 milligrams per litre of sulphates, 450 milligrams per litre of bicarbonates, with a higher conductivity of 2300 micro-Siemens per centimetre. Later, (Schraps, 1972) verified the elevated ion concentrations found only in nearby graves in Germany. His inquiry on the variations in ion concentrations according to the surface inclination and closeness to the places of rest focused on the chemical oxygen demand (COD), nitrate and ammonium concentrations, carbon dioxide, and gaseous ammonia concentrations. According to the findings, the proximity of the burial sites caused the high amounts of these contaminants to rapidly drop.

According to research done by (Gray, et al., 1974), there have been significant amounts of chloride in the area around and beneath cemeteries. In the range of 100 to 200 meters from a cemetery, the ion concentration decreased slowly, but quickly after. In 1978, Bouwer noted that wells near cemeteries in Paris had a sweet flavour to the water and an unpleasant odour (Bouwer, 1978). People who lived close to the graveyards in Berlin reported more cases of typhoid fever, but no assessments were done in Hamburg, where the decreased levels of pollutants were the results of having a denser unsaturated layer beneath the graves along with lower permeable soil (Hanzlick, 1994). The first records of cemetery-related public health problems were in the 1970s, where hygiene professionals identified outbreaks of typhoid epidemics near graves in places supplied by springs and aquifers (Franco, 2022). According to (Kemerich, et al., 2014) analysis, necro slurry contamination of the soil in the Brazilian town of Sebari, might potentially contaminate nearby residents. The report revealed higher-than-usual concentrations of ammonia, nitrate, nitrite, and pH.

In 2009, 114 monitoring sites for groundwater in Brussels, Belgium reported the presence of nitrate, which was concentrated within a 500-meter radius near cemeteries. Active artesian wells for human and industrial use were used to get the results (Mattern, et al., 2011). The findings of the (Jonker & Olivier, 2012) analysis of the presence of heavy metals such as copper, zinc, iron, and lead in the soil of the cemetery in Zandfonteim, South Africa, indicated a rise in the heavy metal as a result of the cemetery. When (Spongberg & Becks, 2000) examined soil samples from a cemetery in northwest Ohio, they looked for potentially harmful levels of pollution. The study found a sharp rise in arsenic, indicating pollution from graveyard leachates. The majority of the shallow aquifers formed in sand-grade (or coarser) alluvial, aeolian, or glacial deposits where burial grounds are located are contaminated.

There aren't many accounts from regions where the limestone is karstic or fractured. (van Allemann, et al., 2018) claims that coffin materials contain toxins that have been shown to contaminate groundwater and soil in cemeteries. An attenuated saline plume in the groundwater was found by (Knight & Dent, 1995) observations at Australia's Botany Bay Cemetery. It was discovered that the leachate plume had higher average pH values, and processes of decay were high in ions such as chloride, nitrate, nitrite, ammonium, orthophosphate, sodium, potassium, and magnesium. According to a report from (Pacheco, et al., 1991), three cemeteries have been found in Brazil with shallow water tables. In groundwater, there was a significant number of indicator organisms including Total and faecal coliforms, and faecal streptococci. However, there was also a high concentration of lipolytic or proteolytic bacteria in the groundwater at the cemeteries, but no lipolytic or proteolytic bacteria were found in the groundwater at the control site outside the cemeteries. This suggested that the presence of organic decomposition active substances migrated from the cemeteries to the water table. A study carried out by (Amuno & Amuno, 2014) at the Gisozi cemeteries using spatial-temporal analysis found that the concentration in the cemeteries is higher than in the mines, particularly for As, Cr, Pb. The trace element analysis contained Ba, Cr, Cs, Ga, Rb, Sc, Th. V, Y, and Zr.

The coffin materials do corrode and leach out through the soil column, according to a laboratory study of the compositions of the leachate from a few different metals found in South African cemeteries. The study was carried out under various conditions that resembled common South African temperatures, rainfall intensities, and pH values. Zn was the most easily corroded and mobile coffin material in all types of soils, and Fe was less corroded from coffin materials and moved slowly through sandy soils. The corrosion rate varied between different soils and under diverse environmental conditions, and the selected metals in leachates revealed this (van Allemann, et al., 2019). Cemeteries located in warm, humid regions, such as RSA and Brazil, have the greatest contamination indexes. (Engelbrecht, 1993) researched a cemetery built on loose sands in the Western Cape province of South Africa during the beginning of the 1990s and subsequently discovered that the levels of TOC or ions containing nitrogen had dramatically increased in the groundwater contamination indicators.

A cemetery in Ditengteng, South Africa, north of Tshwane, (Tumagole, 2009) discovered considerable chemical and microbiological contamination of shallow groundwater, along with elevated quantities of iron and manganese. In a study carried out by researchers in South Africa, bacteria and viruses were identified as the two main risks associated with cemeteries (Engelbrecht, 1993; Wright, 1999). According to (Trick, et al., 1999), current pollution is the cause of the bacteria and viruses that infect groundwater in graves. Microorganisms in these leachates from human corpse decomposition have the potential to contaminate soil, surface water, and groundwater. The majority of the time, pathogenic intestinal bacteria like E. coli, Pseudomonas aeruginosa, C. perfringens, and Salmonella spp. are the sources of environmental contamination.

Additionally, according to (Jonker & Olivier, 2012), if there is no infrastructure in place to collect and handle necro-leachate, cemeteries might be thought of as possible sources of soil and groundwater contamination, and high levels of precipitation and poor management can accelerate the spread of necro-leachate depending on the location. From the first autopsy and embalming to the final disposal in cemeteries or cremations, the entire process of treating corpses produces many possible toxins that could spread to the urban environment. Based on the study conducted by (Silva, et al., 2020), heavy metals and toxic organic pollutants that seep into the soil, and water table, and migrate to water bodies can damage human neurological systems, cause liver disease, gastrointestinal tract corrosion, and liver cirrhosis; they can also cause problems for the central nervous system; cause lung cancer in humans; and they can also lead to osteoporosis.

High-ranking officials and experts have noticed that cemeteries harm the quality of drinking water. Therefore, additional studies must be done and generated to decrease and prevent groundwater contamination linked to cemetery contamination. Due to poor urban planning and a lack of accessible space, homes are often built next to cemeteries, which poses major health risks to people. International cooperation is required to advance research that takes into account varied environmental factors and enables method standardization and additional investigation is required to evaluate contamination evidence such as amino acids, chemical compounds, formaldehyde, and arsenic.

(Neckel, et al., 2021) have demonstrated that the leachate, also known as necro slurry, found in conventional burials has a direct impact on the soil and subsurface water. Further research should focus on characterizing the local necro slurry and gas as well as the uses of the separation processes to ensure a clean effluent and the possibility of any economic gain. The majority of scientists believe that the greatest danger posed by cemeteries is posed by bacteria, viruses, and ions that contain nitrogen and phosphorus as well as other elements. And, the primary by-product of breakdown is thought to be ammonia. Given it is obvious that graveyards are sources of pollution and that different contaminants seep through them and become mobile under controlled laboratory circumstances, the contamination of metals in graves continues to be a matter of concern. This can potentially contaminate the nearby biotic receptors, water reservoirs, and soils of a cemetery (van Allemann, et al., 2018).

2.3 Groundwater flow and solute transport

In several related fields, such as groundwater hydrogeology, contaminant transport, reservoir engineering, chemical engineering, and earthquake hydrology, the study of groundwater flow through porous media is crucial. The selection of an acceptable geometry for the geological system in which the flow occurs presents a challenge in groundwater research. This groundwater-flowing geological formation is dynamic in both space and time.

2.3.1 Dynamics of the groundwater flow system

According to (Alley, et al., 2002), there are a variety of dynamic elements that affect groundwater flow networks, their recharge, and interactions with surface water and the land surface. A groundwater system is made up of parts that let water move through them and be stored there. The subsurface water, the geological media containing the water, flow limits, sources like recharge, and sinks like wells or springs are the parts of the groundwater system. Water can flow from places of recharge to areas of discharge for over a million years or less under natural circumstances. The hydraulic conductivity, porosity, and spatial and temporal gradient of the hydraulic head all affect how quickly water moves through a system. In contrast to systems with unconsolidated porous media, including sands and gravels, flow velocities in fractured-rock systems can be rather high (Long, et al., 1996). Understanding groundwater flow requires taking into account long-term climate and geologic change, which influences all geologic processes like diagenesis, ore mineralization, and petroleum development. Hydrogeological analyses of aquifer water supplies have been carried out during the past 20 years, but as concerns about water quality have increased, it has become vital to predict how contaminants will move through the subsurface environment. The migration of pollutants within a groundwater system is significantly influenced by the period of passage of water. The vast majority of groundwater contamination from surface sources occurs on a global scale, which is a reflection of shallow groundwater's relative shortage of a few decades or less. Contaminant transport durations to wells can be further decreased by hydraulic gradients created by large-capacity wells (Alley, et al., 2002). The distribution of void sizes along linked flow channels as well as the path lengths will have an impact on the residence duration of solutes.

For several months or years, water moves from one aquifer unit to the next and travels from the recharge zone to the discharge zone. According to a study by (Carrillo-Rivera & Cardona, 2012), it is necessary to evaluate groundwater flow systems using an integrated wide system-view analysis of partial evidence represented by surface as well as hydraulic, isotopic, and chemical groundwater characterization in the relevant geological media where the depth of actual basement rock is crucial as well as discharge areas. A gap exists in more recent methods for evaluating the heterogeneity of subsurface hydraulic systems. This would contribute to better modelling tools, a clearer understanding of model uncertainty, and a better understanding of the role that climate plays in surface-water interactions. The complexity of the flow pattern is further increased by geological heterogeneities like structural components, heterogeneity, and anisotropy of deposits.

The earliest flow system studies were developed by (Toth, 1963) using the idea of hierarchical groundwater flow systems, where the topography of the water table and the topography of the land surface are closely coupled. Theoretically, he discovered that there are hierarchically integrated groundwater flow systems and that topography, geology, and climate play key roles in determining gravity-driven flow in homogenous and isotropic groundwater basins (Zhou & Li, 2011). Topography, or the elevation differences of the water table, which create gravitational or topography-driven flow systems, is the most common and dominant fluid flow-driving factor near the surface in terrestrial regions. Ground-water flow networks at the local, intermediate, and regional levels can all be found in an aquifer system. Areas for recharge and discharge are close by in the local groundwater flow system. An intermediate groundwater flow system has one or more topographic highs and lows separating the recharge and outflow zones. Recharge zones in a regional groundwater flow system are found along groundwater divisions, and discharge zones are found at the bottom of significant drainage basins (Toth, 1963).

The handling of migration is the greatest advantage of the dynamic groundwater flow system method, as it allows for quantitative and distributed evaluation of the groundwater flow paths that migrate substance and heat. According to a study by (Simmons, et al., 2001), the geologic environment has an impact on solute transport processes on a variety of length scales, especially for coastal aquifers where variable-density flow and transport are prevalent. Concerning the findings, the geometry of heterogeneity plays a crucial role in modelling and has an impact on the rates and patterns of groundwater flow as well as the creation of sanity distributions in coastal aquifers. The spatial patterns of discharge in heterogeneous systems can be complex, making it challenging to quantify and model the process. (Adindu, et al., 2015) states that several models have been developed to calculate infiltration rate because it requires time to measure this variable. (Abubakr, 2012) also presents the Infiltration equations as a basic, mathematical, and empirical model. Geologic media contained in the water, flow boarders, sources like recharge and infiltration, sinks like springs, inter-aquifer flow or wells, and underground water are all parts of groundwater systems (Alley, et al., 2002).

2.3.2 Characterization of aquifers

Water-bearing zones or layers in the subsurface are referred to as aquifer and confined layers. An aquifer is a permeable and porous geologic formation or a fracture zone that enables significant fluid flow and serves as a below reservoir for groundwater. An aquitard known as the confined layer is a semi-confining unit that enables restricted water flow. An aquiclude is an impermeable geologic unit that hinders the flow of water. According to (Charles, 2002), aquifers are layers with greater hydraulic conductivity than aquitards, which are layers with lower hydraulic conductivity. Aquiclude has a hydraulic conductivity layer with a very low value. Aquifers can be categorized as unconfined or confined. An aquifer that is contained between two aquitards is known as a confined aquifer. An aquifer in which the water table serves as the top boundary is referred to as an unconfined aquifer or water-table aquifer (Wang & Manga, 2021).

2.3.3 Aquifer Properties

The composition of the aquifer has a significant impact on the aquifer's qualities. The two primary variables that affect an aquifer's ability to release water into pores and ease of flow transfer are its porosity and specific yield and the characteristics that make it an aquifer will be covered in this section.

I. Porosity

Porosity is defined as the ratio of a material's overall volume to its pore volume. It can be expressed mathematically using the equation given as:

$$n = \frac{V_v}{V_t} = \frac{V_v}{V_s + V_v} \qquad 1$$

where V_s represents the volume of mineral solids in a specific amount of material and V_v represents the volume of voids in a total volume of material V_t (Fitts, 2013). A related dimensionless parameter known as the void ratio e, which is defined as follows, is frequently used by geotechnical engineers.

$$e = \frac{V_v}{V_s} \qquad 2$$

where V_s represents the volume of mineral solids in a specific amount of material. Porosity can also be expressed mathematically as $V_t = V_s + V_v$. There are three basic types of porosity, and they display themselves differently in various geologic materials. As shown in the Figure, the term inter-granular refers to the formation of pores as spaces between grains or particles in compact materials such as silts, sands, gravels, and porous sandstones, and joint fissures or fractures refer to net fine fissures due to cooling of the rock. Vugular porosity refers to the formation of large, irregular pores as a result of material dissolution, particularly in limestone. Porosity is greater in granular materials than it is in fractures, where it is often much less than matrix porosity (Fitts, 2013).

Figure 1: In a properly sorted granular material (left), inter-granular matrix porosity is present. Poorly sorted granular material (middle) is linked to lower porosity. Porosity at fractures in crystalline rocks (right). Extracted from *(Fitts, 2013)*.

II. Specific Yield and Specific Retention

The amount of water that drains by gravity (V_D) about the total volume of the sample (V_T) is referred to as the specific yield (S_y). Different soil types have different specific yields, with some showing a stronger molecular attraction to the water contained in their pores than others. The equation is shown as follows:

$$S_y = \frac{V_D}{V_T} \tag{3}$$

where S_y is the specific yield (dimensionless), V_T is the volume of the sample (L^3), and V_D is the amount of water that drains by gravity (L^3).

When gravity drains a porous material, a fractional volume is left behind. This fractional volume is referred to as the specific retention or S_r, and it is calculated as the ratio of the volume retained (V_R) to the volume of the entire sample, or V_T (Woessner & Poeter, 2020). The following is the specific retention formula:

$$S_r = \frac{V_R}{V_T} \tag{4}$$

where S_r is the specific retention (dimensionless), V_T is the volume of the sample (L^3), and V_R is the volume of water remaining after drainage stops, against gravity (L^3).

III. Transmissivity

The ability of an aquifer to transfer water is frequently referred to as transmissivity. Transmissivity measures how quickly water flows through an aquifer with a given width and hydraulic gradient. According to (Cheremisinoff, 1997), transmissivity is defined as being equal to the product of hydraulic conductivity (K) and aquifer thickness (b), and it is measured in $\left(\frac{L^2}{T}\right)$ as shown in the equation

$$T = K.b \qquad 5$$

where T is the transmissivity, or the ability of an aquifer to transport water (L2/T); b is the aquifer's saturation thickness (L); and K is the hydraulic conductivity.

IV. Hydraulic Conductivity

In terms of science and engineering, the hydraulic conductivity of a material is determined by how easily a fluid may move through its pores and fractured networks (Saravanan, et al., 2019). The inherent permeability (k, unit: m2) of the substance, the level of saturation, as well as the density and viscosity of the fluid, all affect how easily water can flow through an aquifer. Henri Darcy calculated hydraulic conductivity in 1856 by calculating the rate of water flow as a function of the hydraulic gradient. He carried out several tests using various sediments and varied hydraulic gradients (Woessner & Poeter, 2020). According to Darcy's law, the movement of liquids in and through soil can be explained as follows:

$$q = \frac{Q}{A} = -KI \qquad 6$$

where q represents the liquid flux or flow rate (L T− 1); Q is the volumetric flow rate of the liquid $(L^3.T^{-1})$; A is the total cross-sectional area of the soil (solids plus voids) perpendicular to the direction of flow (L^2); K is the hydraulic conductivity or coefficient of permeability $(L.T^{-1})$; and I is the hydraulic gradient (dimensionless).

There are several ways to calculate hydraulic conductivity, but the two that are most frequently used are the empirical technique, where hydraulic conductivity is associated with soil parameters like pore size and particle size distributions, and soil testing. and experimental method, where the hydraulic conductivity is calculated from hydraulic experiments using Darcy's law, such as Laboratory tests using samples of soil that have undergone hydraulic experiments, Field tests, and so on.

2.3 Flow in Fractured Media

When two rough surfaces are partially in touch, they form a crack or mechanical discontinuity in the rock that serves as a flow and transport channel, and the cracks are known as fractures. They are frequently packed with transported materials or mineral precipitates and have complex forms. In different types of media, fractures operate as key conduits or barriers for fluid flow because they have an impact on flow and transport. Underground rocks have fractures that were created by tectonic action. These tectonic fractures are characterized as systematic fractures because of their consistent occurrence, lengthy extension wing, and uniform orientation. There are two types of fractured formations: those with impervious blocks, like granite, and those with pervious blocks (matrix), also known as double porosity such as limestone and sandstone. It is more challenging to forecast the flow of pollutants in fractured clay formations than in unfractured formations. In addition to making, it more difficult to foresee and characterize fractured systems, they also make it more difficult to optimize several crucial subsurface energy production and anthropogenic waste disposal activities. The fracture network aquifers in fractured formations with impervious blocks are unable to hold a great deal of water due to their low porosity, but because of the relatively high permeability of the fractures, harmful substances can get transported quickly through the fracture structure and contaminate nearby aquifers (Carol, 2009). Conductive fractures in a porous media can produce an effective permeability that has a greater magnitude in secondary permeability than the primary permeability provided by linked pores.

2.4 Mechanisms of Contaminant Transport in Aquifers

A groundwater resource may get contaminated by contaminants that were emitted at or close to the earth's surface and travelled through the soil's unsaturated zone (Zhuang, et al., 2021). Numerous biotic or abiotic mechanisms control the movement and fate of contaminants in soils, and they are influenced by several variables, including soil properties (such as mineralogy, organic matter content, pH, and moisture), chemical compound properties (such as hydrophobicity, vapour pressure, and chemical stability), biota activity, sequestration, and environmental factors (such as temperature and precipitation). The majority of pollutants in groundwater are reactive by nature, and they permeate through the vadose zone, reach the water table, and then continue to weaken as groundwater flow continues. In this context, the movement of substances in soils and groundwater aquifers is referred to as "solute transport," and it is crucial to many other processes, including biogeochemical cycling (Sukop & Dentz, 2022). When a chemical interacts with soil or aquifer solids, retardation might cause the transport to slow down. Since aqueous pollutants frequently reside in the dissolved phase, it is also crucial to understand the mechanics of solute transport in groundwater. It is not always easy to determine the concentration of a solute since the transport of a dissolved component (solute) depends on the strength and directions of the solvent flow. There is a substantial amount of diversity in groundwater flow and contaminant migration patterns, and these behaviours and patterns vary depending on the geographical and temporal distribution aspects of environmental elements in the groundwater environment for each location.

The patterns in the penetration curves for environments with porous media were notably different, and (Silliman & Simpson, 1987) found that the dispersion coefficients increased with migration distance when they utilized tabular fine sand and a coarse sand medium. Migration in saturated porous media is either directly or indirectly affected by ionic strength and ion type, pH, flow rate, and surfactant. This was demonstrated by (Lyu, et al., 2019), who investigated the effects of perfluorooctanoic acid migrations in saturated groundwater under varied ionic strength, ion type, and pH circumstances. An experiment on the transport of pollutants has been developed based on Darcy's experiments. To calculate the basic rules of percolation in porous media, (Darcy, 1856) used macroscopic techniques rather than microscopic averaging. In Slichter's study of 1909, it was found that not all solutes are transported in the soil at the same speed (Slichter, 1905). Mechanistic investigations, which included sand column tracer experiments and laboratory-based contaminant leaching migration simulation experiments, were the first to investigate the migration of organic contaminants in a subsurface inhomogeneous porous medium. In porous media, this research determined the existence of organic pollutants as well as their mode of migration, hysteresis effect, wettability, and infiltration pattern. To solve the advective dispersion transfer equation for reactive transfer through the layered porous medium, including equilibrium adsorption and first-order degradation constants, a physical model that represents a layered porous medium and an implicit finite difference numerical technique was developed.

Unsaturated soils display greater solute dispersivity than fully saturated soils, whereas fully saturated soils demonstrate constant solute dispersion. The dispersion process is known to be strongly influenced by the texture of the soil and the distance travelled. A non-monotonic relationship between dissolved dispersivity and soil content has been established in laboratory studies carried out using repacked soil columns. A tracer that has been dissolved tends to disperse, which lengthens the tracer's transit time across a porous medium. The dispersion coefficient in unsaturated porous media changes with non-linear Darcy's velocity and the amount of water present. Meandering through the partially saturated pore complex, (Toride, et al., 2003) discovered how solutes disperse relative to the mean displacement location during water flow in soils. The convection-dispersion equation (CDE), which describes the spreading, uses the hydrodynamic dispersion coefficient. Due to large-scale soil variability, soil layering, the occurrence of fractures and macropores, and geographic variations in the flow velocity within the transport domain, more uncertainties will be expected for field-scale undisturbed soils. When a pollutant enters the environment several mechanisms may aid in its spread, including advection, diffusion, mechanical dispersion, and hydrodynamic dispersion. According to (Shackelford, 1993), groundwater contaminant migration mostly occurs through seepage, which, as shown in Figure 2, is caused by both molecular diffusion and advection-dispersion in the pore medium.

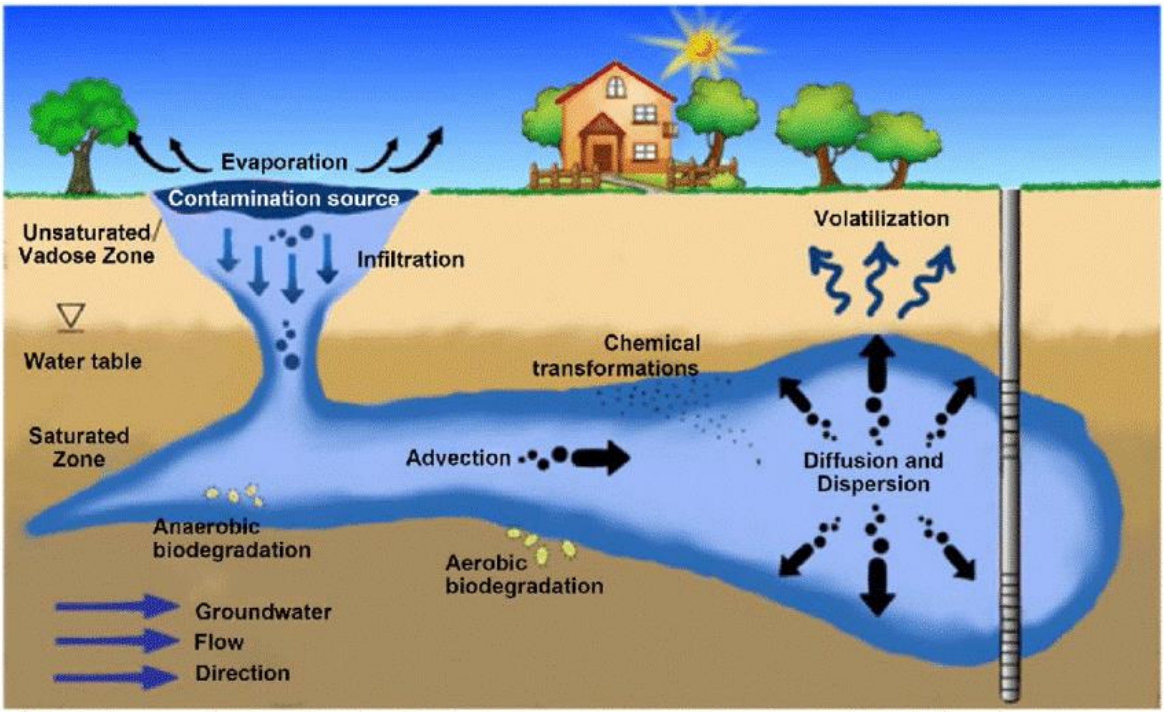

Figure 2: Main processes that occur in an aquifer. Obtained from *(Talabi & Kayode, 2019)*.

To characterize the mechanisms of groundwater contamination, the primary framework of mathematical models has been created and to choose an appropriate mathematical model, one must take into account the physical characteristics of the fluid such as heterogeneous flow or saltwater intrusion in the groundwater region and the geographic characteristics of the different porous media such as saturated and unsaturated groundwater.

I. Advection – Dispersion Equation

The combined advection and dispersion processes cause groundwater to move from locations with higher hydraulic heads to areas with lower hydraulic heads, delivering dissolved solutes. The advection-dispersion-reaction equation, which describes solute transport in many groundwater transports models, can be used to compute the dispersion coefficients by adding the effects of mechanical dispersion, molecular diffusion, and macro dispersion.

The ADE for the transport of non-reactive solutes is provided by

$$\frac{\partial C}{\partial t} = D\frac{\partial^2 C}{\partial x^2} - v\frac{\partial C}{\partial x} + R_C \quad 7$$

where C is the solute concentration, v corresponds to the mass velocity of the pore water, D is the horizontal hydrodynamic dispersion coefficient, t is time and x is a spatial coordinate, R_C is the retardation factor.

Two components make up the coefficient of hydrodynamic dispersion.

$$D_l = \alpha_l \bar{v} + D^* \quad 8$$

where $D^*$is the coefficient of molecular diffusion for the solute in the porous medium [L2/T], and α_l, is a characteristic attribute of the porous media known as dynamic dispersivity, or simply dispersivity [L]. Figure 3 illustrates how mechanical dispersion and molecular diffusion both contribute to the spreading out of the concentration profile and breakthrough curve of tracers or pollutants moving through porous materials. The graph demonstrates that mechanical mixing is the dominant dispersive process at high velocity, in which case $D_l = \alpha_l \bar{v}$. At low velocities, diffusion is a significant contributor to dispersion, and as a result, the coefficient of hydrodynamic dispersion equals the diffusion coefficient $D_l = D^*$. The solute front advances while mixing more when the medium's dispersivity increases.

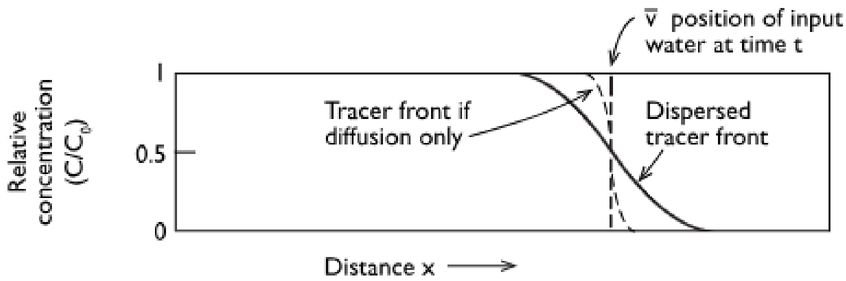

Figure 3: A diagram illustrating how mechanical dispersion and molecular diffusion both contribute to the spreading out of the concentration profile and breakthrough curve of pollutants or tracers moving through porous materials.

II. Diffusion

The process of diffusion involves the movement of ions or molecules from regions with high solute concentrations to regions with low solute concentrations, and the outcomes of diffusion are outlined by Fick's First Law. The law states that the flow has a magnitude proportionate to the concentration gradient (spatial derivative), moving from areas of high concentration to areas of low concentration. One-dimensional mass-flux due to mechanical dispersion is typically represented mathematically as follows:

$$J = -D\frac{\partial C}{\partial x} \qquad 9$$

where J is the diffusion flux (amount of substance per unit area per unit time), D is the diffusion coefficient or diffusivity (area per unit time), C is the concentration (substance per unit volume) for ideal mixtures, and x is position, whose dimension is length.

III. Retardation

Retardation is the process of a solute transport decreasing relative to the advective groundwater velocity at any location on the travel path at any given point in time. It can happen through a variety of processes, namely adsorption and precipitation. Chemical retardation is measured in dynamic research as the difference between the water (w) and species-of-interest (M) velocities through a control volume. A solute plume's concentration and spread depend on the retardation factor, which reduces the plume's velocity as the transit time increases. (Vermeulen & Heister, 1952) initially came up with the idea of a retardation factor for application in chemical engineering. Retardation factor usage was expanded to include the movement of reactive solutes inside geological materials. According to (Bosma, et al., 1996), the ratio of a solute's total mass including adsorbed mass and solution phase mass in a bulk soil volume to the mass of the solute in the solution phase of the same soil volume is frequently used to define a reactive solute's retardation factor, denoted by R and can be expressed as:

$$R(x,t) = \frac{T(x,t)}{c(x,t)} = 1 + \frac{s(x,t)}{c(x,t)} \qquad 10$$

Where $R(x,t)$ stands for a volume-averaged retardation factor because $c(x,t)$) and $s(x,t)$ are defined on a volumetric basis.

IV. Sorption

The process by which a material is adsorbed or absorbed on or in another substance is referred to as sorption. The sorption process has three retention mechanisms: adsorption, precipitation, and desorption. Adsorption is an ion exchange process that occurs in the diffuse layer as a result of electrostatic forces whereas desorption is the process whereby chemical substances are released from the surface into the soil environment (Landrot & Sparks, 2022). It is possible to predict contaminant distribution and movement in the subsurface by studying the complicated sorption processes that occur in subsurface systems. An adsorbed solute can be transported in one dimension using the ADE, which can be expressed as follows:

$$\frac{\partial C}{\partial t} = \frac{\rho}{\theta}\frac{\partial S}{\partial t} = D\frac{\partial^2 C}{\partial x^2} - v\frac{\partial C}{\partial x} \qquad 11$$

where C is the solute concentration, S is the adsorbed concentration, which is expressed as the solute's mass per dry soil mass. By assuming that the concentration of the contaminant in the liquid phase and the concentration of the contaminant in the solid phase are taken onto the soil particles at constant temperature are proportional, this equation is formed.

Chapter 3: Groundwater contamination in cemeteries

3.1 Introduction

The global problem of groundwater contamination, which has a significant adverse effect on health and environmental services, is being caused by the increasing number of people in cities as well as rapid urbanization and deterioration of natural resources in rural areas (Li, et al., 2021). Historically, contaminated drinking water has been known to be capable of transmitting dangerous chemicals and deadly diseases. In addition, cemeteries also contribute to groundwater pollution leading to the spread of communicable diseases and hazardous chemicals (Engelbrecht, 1993). This chapter will cover the anatomy of the human body, the effects of cemeteries on groundwater systems, as well as decomposition and burial remains' leaching.

3.2 Anatomy of the human body

The complete structure of the human organism, including every living cell, tissue, and organ, is made up of both living and non-living parts, collectively known as the human body (Dutfield & Rettner, 2021). There are approximately 200 bones, 650 muscles, 79 organs, and a large number of blood arteries. The human body is a complex biological and chemical mechanism that constantly interacts with its environment below the surface.

It is helpful to first study the compounds that are present in the human body before deciding whether or not seepage is a potential cause of pollution. The average adult male, who weighs 70 kg, possesses 42 litres of water in his body, which equals 60% of his weight, and the average adult female, who weighs 55 kg, has 55% of her body weight in water, which is less because she has more fat. (Dent & Knight, 1998) found that the average adult male weighing 70 kg has a body composition of between 70 and 74% water, 16,000 grams of carbon, 1,800 grams of nitrogen, 1,100 grams of calcium, 500 grams of phosphorous, 140 grams of sulphur, 140 grams of potassium, 100 grams of sodium, 95 grams of chlorine, 19 grams of magnesium, and 4.2 grams of iron. The majority of the other elements, including heavy metals and trace elements, rapidly decline in proportion to milli- and micromole quantities. In addition to the dose, route, and chemical species, its toxicity is also influenced by the age, gender, genetics, and nutritional state of the exposed individuals. For example, mercury is very variable based on lifetime exposure and dental fillings, while cadmium is 0.05g.

There are around 650 muscles that make up the body's muscular system, which is important for movement, blood flow, and other biological processes, as shown in Figure 4.

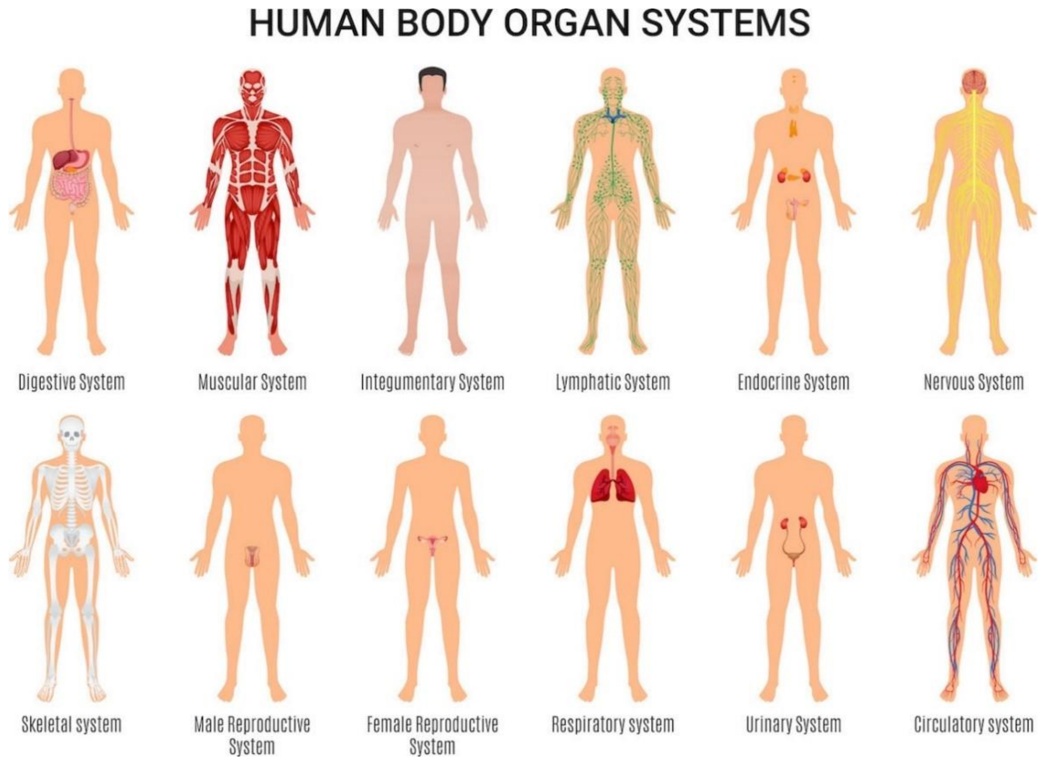

Figure 4: View of the human anatomy extracted from *(Dutfield & Rettner, 2021)*.

There are two different types of reproductive systems. The male reproductive system consists of the penis and the testes, which generate sperm. The ovaries, which generate eggs, the uterus, and the vagina make up the female reproductive system. As we breathe, the respiratory system enables us to inhale oxygen that is essential for life and release carbon dioxide.

The lungs, diaphragm, and trachea make up the majority of it. The body produces urea as a waste product when certain nutrients are digested, and the urinary system aids in the removal of urea from the body. Two kidneys, two ureters, the bladder, two sphincter muscles, and the urethra make up the entire system. The skin, also referred to as the integumentary system, is the biggest organ in the body. It protects us from the outside world and serves as our first line of protection against bacteria, viruses, and other disorders. Additionally, our skin aids in controlling body temperature and removing waste through perspiration.

3.3 Decomposition of the human body

A deceased person's body decomposes at varying rates and in different ways depending on a variety of conditions. The decay of human remains produces leachate, which is a liquid containing microorganisms, which causes groundwater contamination in cemeteries (Engelbrecht, 1993). (Bouwer, 1978) claims that there have been several reports of groundwater contamination caused by normal fluids found in decaying bodies. A body will gradually decay in a coffin or casket. The body often experiences active decay, putrefaction (the breakdown of organic substance by the activity of microbes producing a foul odour), and blackening during the first few months underground. The tissue and organs will keep on deteriorating and liquefy over many years, leaving only the teeth. Figure 5 illustrates the five stages of human decomposition.

Figure 5: Presentation of human decomposition. From *(Cohen, 2023)*

The amount that decomposition can be slowed down or accelerated depends on a variety of external factors, including the body's size, temperature, moisture, oxygen, pH, and whether it is buried below and above the ground. The intrinsic aspects, such as gender, age, body type, intestinal flora, illnesses and treatments, cause of death, embalming, and whether or not an autopsy was conducted, are also implicated in the decomposition of human bodies (Oliveira, et al., 2013). The biological and chemical process of decomposing a human body is highly complicated and involves the interaction of many different enzymes, bacteria, fungi, and protozoa. Each of these organisms' functions best within a certain spectrum of environmental circumstances. There have been attempts to develop a "universal formula" for calculating how long it will take for a body to decompose. However, this has not yet been accomplished.

According to an investigation conducted by (Young, et al., 1999), a 70 kg corpse buried in a 10 kg chipboard coffin has the following proportions that are degradable to various degrees:

- 60% degrade easily
- 15% moderately degradable

- 20% degrade bit by bit
- 5% are non-degradable

3.1.1. Timeline of a human body decomposition before and following Burial

The four stages of a body's decomposition include colouring, emphysematous, liquefaction, and skeletonization. The decomposition process is initiated by autolytic processes. Figure 6 illustrates the timeline of the body before and after burial adapted from (Häggström, 2022).

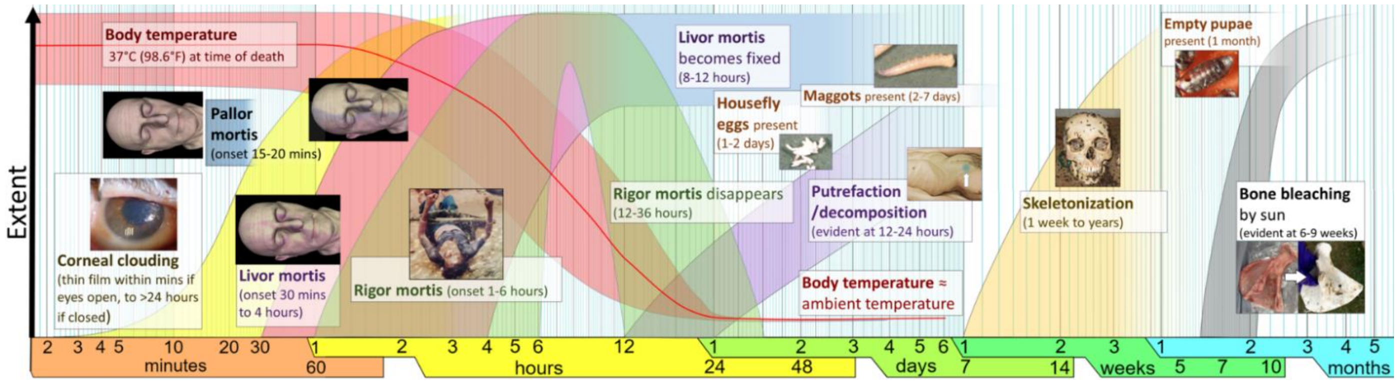

Figure 6: Postmortem development timeline (death stages). From *(Häggström, 2022)*

The following are the five phases of decomposition:

I. Stage 1- Autolysis: Initial decomposition that takes place from 24 to 48 hours during death

After death, the lack of oxygen sets off a series of events that cause cell necrosis, the start of autolysis, and eventually putrefaction (Gill-King, 1997). As a result of the body's inability to handle waste, an acidic environment develops, leading to membrane rupture and the release of enzymes that subsequently go on consuming the cells. The body turns pallid and stiff when the blood flow stops. These enzymes convert biological polymers into hydrolysed proteins, lipids, and carbohydrates. Putrefaction begins once this stage has produced an adequate quantity of nutrient-rich fluid due to cellular disruption.

II. Stage 2- Bloating: 48 hours to 2 weeks

Bloating, which commences 4 to 10 days after death, is the following step of decomposition. Once the bacteria in the body of the deceased change from aerobic to anaerobic, the bloat stage starts. When bacteria are no longer suppressed by the immune system and enzymes released by the cells during the fresh stage, gases like methane, carbon dioxide, nitrogen, and hydrogen sulphide are generated (Cohen, 2023). The inside cavity is filled with gases, which increases the internal pressure and forces bodily fluids out of natural openings like the mouth, nose, and anus, causing the body to grow to twice its original size. The most noticeable amount of odour is produced during the decaying process by the release of gases and liquids. However, the decomposition of the body will be postponed if the deceased's relatives opt to have it embalmed.

III. Stage 3- Active Decay

After 10 to 25 days, the body enters the active stage, also known as liquefaction, during which the decomposition odour intensifies (Janaway, et al., 2009). The greatest bodily mass is lost as a result of bacteria and insects breaking down the body's components and releasing liquids into the environment while insects and maggots feed on the body, further destroying it. The skin turns black. The majority of the liquid evaporates from the body and sinks into the ground or forms a pool.

IV. Stage 4- Advanced Decay

Between 25- and 50-days following death, this stage takes place. The body’s soft tissues, including the skin, hair, muscles, and connective tissue, have been completely broken down by maggots and other insects (Kazmeyer, 2023). Scavengers cause the insert activity to decline by eating the last nutrition of the body. Insects like beetles and different kinds of flies that have chewing mouthparts are drawn to the area and ingest the bones, hair, cartilage, ligaments, and sticky residues of decomposition that are left behind.

V. Stage 5- Skeletonization

A deceased organism after going through decomposition is said to be in a skeletonized form. In the latter stages of decomposition, the skeleton becomes apparent, changes colour, and is later reclaimed by the earth. The only chemical weathering that occurs on the remains is inorganic (Dent, et al., 2004). The loss of organic (collagen) and inorganic components affects the skeleton's rate of breakdown as well.

3.4 Decomposition of a casket

The rate at which caskets degrade varies because they are made of biodegradable materials like wood, metal, fiberglass, and plastic. Numerous variables affect how long it will take for a coffin to deteriorate underground, including:

- The material used - wood eventually rots because it ages more quickly than metal.
- The soil's temperature and humidity when the casket is buried - caskets rust more quickly in warm, humid conditions.
- The soil's ability to support insects, germs, and other microbes.
- And whether a burial vault is used to protect the coffin.

Regardless of the material used to construct the casket, no casket will remain intact underground for more than 80 to 100 years. In general, Cheaper coffins may decay in as little as 10 years, and biodegradable coffins made of materials like wicker typically take three to four years to dissolve.

3.5 Hydrogeological interactions

The interactions that occur between land use and hydrological cycles take place when rain falls on a cemetery (Dent & Knight, 1998). Surface water and groundwater interact in a range of physiographic and climatic environments and are not separate elements of the hydrologic system. (Tóth, 1970) uses the impacts of topography, geology, and climate on groundwater flow systems to describe the interactions between groundwater and surface water. The geographical, geological, and climatic factors all have an impact on groundwater flow. A groundwater flow system will arise, driven by a water-table surface that is an attenuated duplicate of the land surface, assuming a uniform precipitation and infiltration rate over an uneven surface.

The distribution of hydraulic conductivity in the rocks as well as the layout of the water table both affect how the groundwater flows as a result. In cemeteries, groundwater is created as water seeps through the ground surface and travels vertically to the water table. The flow system along which groundwater travels is composed of flow routes that are arranged spatially. Groundwater and streams may be affected by the interaction of cemetery solutes with water systems (Dent & Knight, 1998). Some components of the buried remains will be carried by the waters that percolate through cemeteries. The diversity of geology and hydrogeology that are present for different cemetery sites will significantly influence the potential impacts of any dissolved materials that migrate into the environment. Figure Figure *7*: Demonstration of the hydrological cycle in cemeteries. Obtained from . uses a conceptual landscape to illustrate the interaction of groundwater and the movement of water in cemeteries.

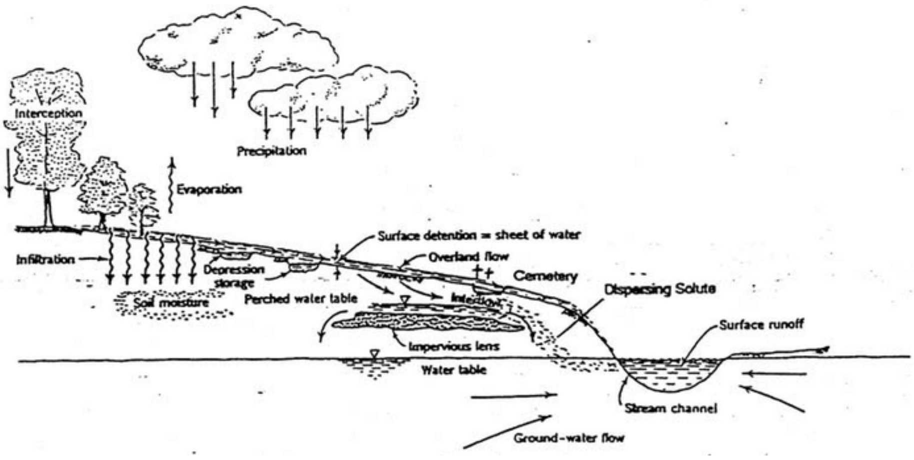

Figure 7: Demonstration of the hydrological cycle in cemeteries. Obtained from *(Dent & Knight, 1998)*.

3.6 Impact of cemeteries on the environment and public health

Numerous researches have examined the potential environmental impact that cemeteries can cause, with the majority of these studies focusing on non-metallic contaminants and being conducted on cemeteries in Europe and the South (Spongberg & Becks, 2000). The results have been published, and they refer to research done in various geographical and climatic contexts, types of cemeteries, etc.

The state of the surrounding environment has a significant impact on how burials affect the ecosystem. The decomposition of human bodies emits gases like carbon dioxide and ammonia as well as bacteria that seep into the soil and reach the groundwater, which has a significant negative influence on the ecosystem. Due to the lack of knowledge on the makeup of their degradation products, the decomposition of the coffin also affects the environment. The materials used in funeral rituals consist of different microbial organisms that live on buried bodies, heavy metals, and chemical compounds. According to (Üçisik & Rushbrook, 1998), the contamination may get into the groundwater if the cemetery is located on soil that is susceptible to contamination or if the soil approaches its limit for depuration. In South Africa, more than forty percent of cemeteries contaminate water resources. The cemeteries that are located in warm, humid climates, such as South Africa and Brazil, have the most contamination indicators. The majority of scientists believe that bacteria, viruses, and ions containing nitrogen and phosphorus as well as those found in graves offer the biggest harm.

If the geology, hydrogeological, and environmental factors are ignored, the decomposition of human bodies causes a saline contamination plume that gradually spreads below burial sites in the path of the hydraulic gradient. The dispersion of this plume is based on many dynamics namely characteristics of the source of contamination, infiltrating rainfall, hydraulic conductivity, and the water table (Franco, 2022). The effects of cemeteries on the environment are linked to the contamination of the soil, surface water, and groundwater, as well as the emission of odours when the earth above the grave is porous to gases or when the condition of burial vaults or chambers is unsatisfactory. The chance of contamination is low when surface water is active and oxygenated, and the risk is increased by rains and washing from the interior region of the cemetery. The use of a variety of chemicals during procedures including formalization, embalming, thanatopraxy, and mummification that involve the human body could increase environmental dangers, and solutions of formaldehyde are the most often employed items in these processes.

According to (van Allemann, et al., 2018), formaldehyde is a known carcinogen that is dangerous when inhaled, comes into touch with the skin, or is ingested; nonetheless, formaldehyde's ability to pollute has gone undiscovered. Although it is unknown whether formaldehyde seeps into the soil and groundwater, formaldehyde remains the primary embalming solution used in South Africa (Chiappelli & Chiappelli, 2008). For grave digging and body decomposition, the soil's qualities are crucial. (Özkan, et al., 1996) argues that flat land is undesirable for burials because it may cause drainage issues; consequently, cemeteries with slopes must be between 0 and 10%. Cemetery locations should not be chosen in areas with slopes of more than 15%. The burial loads can be thought of as an anthropogenic source of contamination because they are a direct contributor to soil mineral composition. Due to the toxic poisons that are generated during coffin degradation and corpse decomposition, they represent a threat to both the environment and human health. They result in water-borne diseases and health hazards if the discharged fauna or flora gets into human lungs or if the leachate containing dangerous chemicals migrates into groundwater or a nearby water source. The types and quantities of pollutants discharged by each burial are displayed in Table **Table *1***.

In conclusion, a cemetery shouldn't be built in the lowest portion of a place where rainwater runoff accumulates and the infiltrated water comes into touch with the interred remains because this would allow more decomposition products to be transferred into the groundwater. A cemetery cannot be built on exceptionally hard, rocky, or unsteady ground. Both the soil's microorganism activity and the cemetery's ground surface must be sufficiently permeable to water.

Table 1: Contaminant decay rate in human body and coffin

Contaminant	Mass per burial (g)	Available mass for release (g)	Release start year	Release end year	Kinetic release model	Release rate per burial (gy^{-1})
Calcium	1100	1100	10	100	Zero-order	12.22
Carbon	16000 + 10000[a]	14800[b] + 10000[a]	0	10	Zero-order	2480
Carbon	1200[b]	1200[b]	10	20	Zero-order	120
Nitrogen	1800 + 500[a,d]	1400[c] + 500[a,d]	0	10	Zero-order	190
Nitrogen	400	400	10	20	Zero-order	40
Mercury	3	3	0	2600	Zero-order	$1.12x10^{-3}$
Phosphorous	500	500	10	100	Zero-order	5.55
Formaldehyde	180	180	0	0.25	As a single event	NA
Formaldehyde	500[dd]	500[d]	0	10	Zero-order[d]	50

[a] assumed from coffin of mass 15kg
[b] assumes that of the 16,000g body total then 1,200g are present in collagen in bone etc. and so degraded after skeletonization and completely lost over the subsequent decade
[c] assumes that of the 1,800g body total then 400g are present in collagen in bone etc. and so degraded after Skeletonization and completely lost over the subsequent decade
[d] relies on catalytic hydrolysis of resin in situ

Chapter 4: Description of the Site

West Park Cemetery is a well-built cemetery in Johannesburg that is 10 kilometres to the northwest of the city and is surrounded by Montgomery Park, Sophiatown, and Emmarentia (Commonwealth War Graves Commission, 2023). In the past, it was a part of one of Johannesburg's first farms and became operational in 1942. West Park is 100 hectares in size, and each hectare has 2000 graves. After it opened in 1942, they have taken up nearly 85% of its 100 hectares, and due to its facilities, it has been designated as a category A cemetery. Following this, graveyards in Johannesburg were separated into categories A, B, and C, with categories A and B containing graveyards that are situated in locations with developed infrastructure, while Category C cemeteries are primarily found in townships with poor infrastructure and low maintenance levels. **Error! Reference source not found.** shows the geographical map of Johannesburg where West Park Cemetery is located.

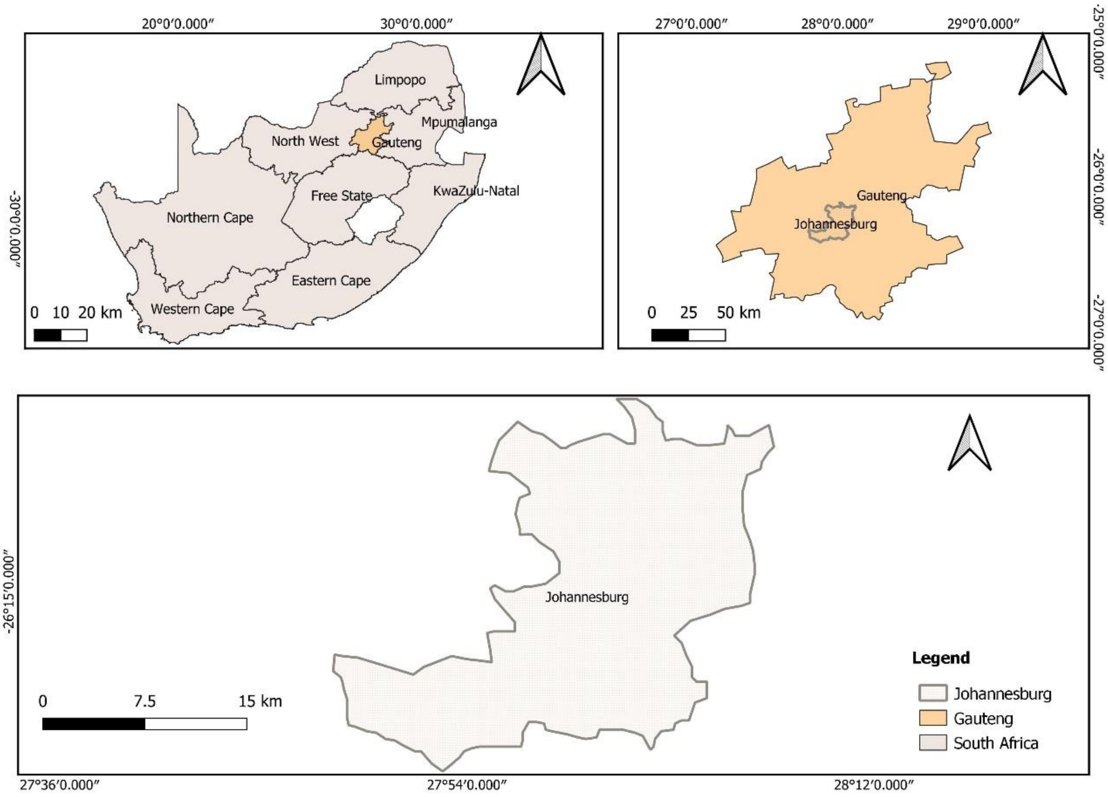

Figure 8: Geographical map of the study area created using GIS.

Some of the nation's most well-known residents are laid to rest in West Park Cemetery, which is a non-denominational approved burial ground with spaces for Chinese, Jewish, Muslim, and Christian graves. It holds 617 Second World War Commonwealth graves. In addition, the Commission is responsible for 21 cemeteries from various nationalities that were used in battle, as well as seven non-war graves. 69 service members who were interred in Johannesburg's Braamfontein Cemetery during World War II are remembered by the Johannesburg (West Park) Cremation Memorial. The following picture presents the main entrance of West Park Cemetery taken by (Fourie, 2018).

Figure 9: West Park Cemetery. Adapted from *(Fourie, 2018)*.

4.1 Climate and Rainfall

The subtropical climate of Johannesburg, South Africa's largest city, features moderate, sunny winters, but evenings are chilly, and comfortably warm summers that are mostly sunny but occasionally cloudy in the afternoon. In June and July, the average temperature ranges from 10 degrees to 21 degrees. The average annual precipitation ranges from 600 to 800 millimetres, placing it in the moderate range, as shown in Figure 10. In the driest months (July and August), it is 5 mm, while in the wettest (January), it is 125 mm.

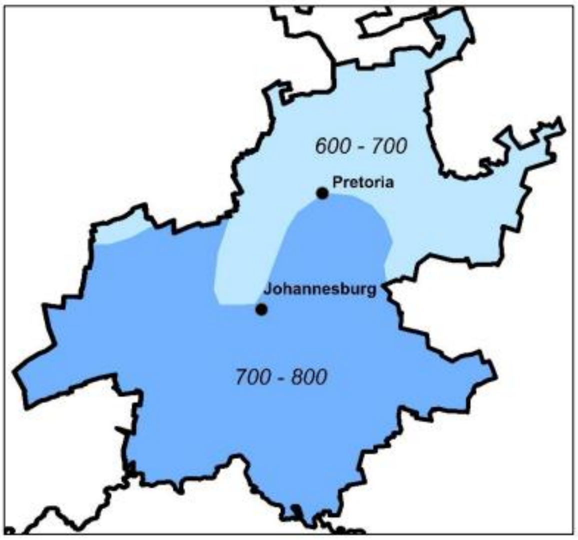

Figure 10: Average annual rainfall (mm) is based on data from 1991 to 2020 and geography. Adapted from *(Kruger & Mbatha, 2021)*.

In Gauteng, semi-bushed and grassland vegetation coexist with summer showers and cold summer weather. The West Park Cemetery climate region is classified by SAWS as a high-highveld grassland with very changeable winds, however easterly and westerly winds are more common (World Climate Guide, 2023).

4.2 Geological Setting

The West Park Cemetery is sited in the Witwatersrand area. The Witwatersrand, often known as Rand, is a 56-kilometer-long, steep slope that faces north in South Africa. It was created by faulting or erosion, dividing two usually flat zones of varying elevation as shown in Figure *11*. The Witwatersrand plateau was deposited over some time of roughly 260 million years ago. The Witwatersrand Supergroup, which is made up mostly of sedimentary rocks between 5000 and 7000 meters in thickness is what makes up this formation and the Witwatersrand rocks exhibit the fractured regime's characteristics.

Figure 11: West of Johannesburg, at the base of the Witwatersrand Supergroup, White Orange Grove Quartzite forms the northern scarp face of the Witwatersrand plateau. Extracted from *(Tucker, et al., 2016)*.

The largest subterranean geological structure to arise from the Witwatersrand is the Witwatersrand Basin, which is also identified as the world's leading gold province in South Africa. It is one of the planet's oldest geological formations, dating back to the Archean Aeon. It has yielded approximately 40000 tonnes $(1.3 \times 10^{9}\ ozt)$, or nearly 22% of all the gold found above ground (Norman & Whitfield, 2006). The Witwatersrand Basin lies either conformably or unconformable on tholeiiticandesitic lavas, quartzite, and conglomerate units of the Dominion Group, as well as the Archaean basement in some locations where the Dominion Group is absent.

4.2.1 Stratigraphy

The Witwatersrand Basin consists of eight goldfields that are currently producing gold, namely East Rand, South Rand, Central Rand, West Rand, West Wits Line, Klerksdorp, Free State (Welkom), and Evander goldfields. The West Rand group, which is part of the Johannesburg subgroup, is where the West Park Cemetery is located in the Roodepoort formation (Figure 12). On the northern edge of the Witwatersrand Basin, 40 kilometres from the west of Johannesburg centre, lies the West Rand goldfield.

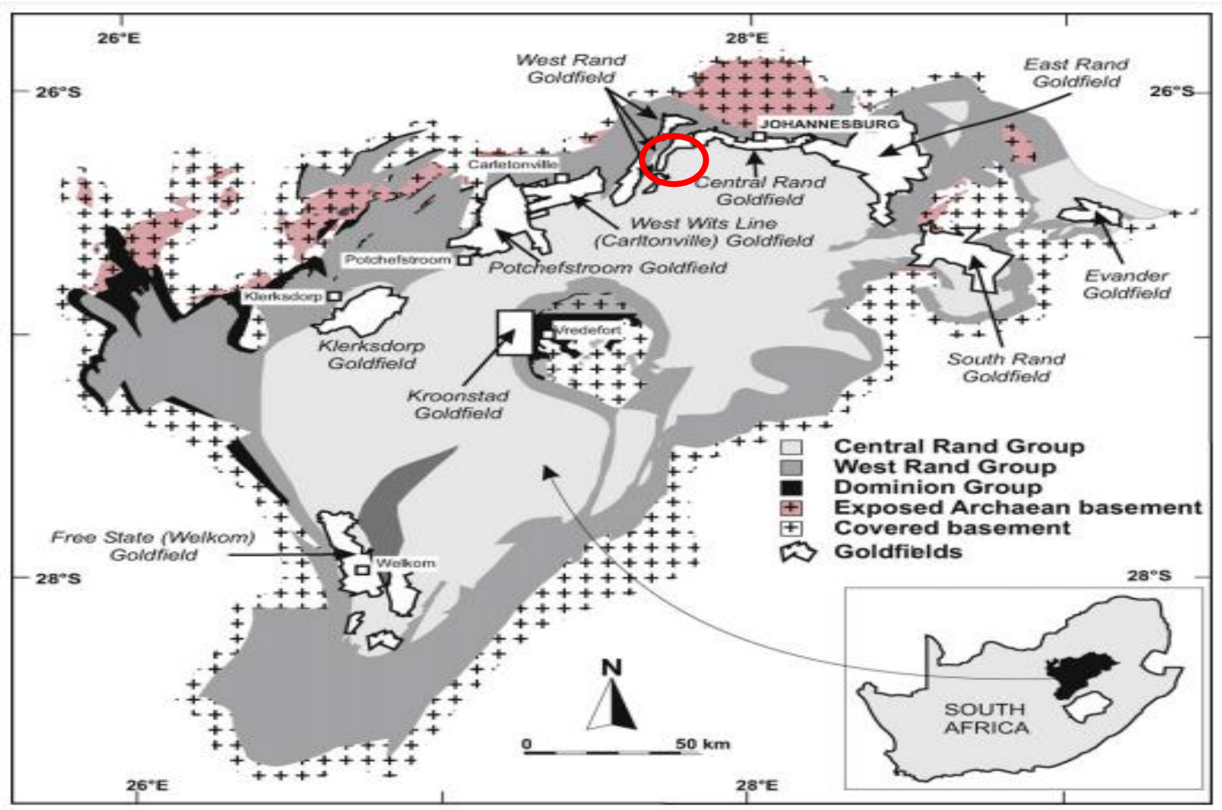

Figure 12: Geological map showing the distribution of the Archaean basement and the location of goldfields in the Witwatersrand Basin's Ventersdrop Supergroup. Adapted from *(Rance, et al., 2006)*.

The structural geology description of the West Rand goldfield, there are numerous significant faults and folds. Figure 13 shows the four regional faults known as the WNW-trending extension of the Rietfontein Fault Zone, the arcuate Witpoortjie and Roodepoort-Saxon-Panvlakte faults, the north-trending West Rand fault, the WSW-trending Doornkop fault, and the WSW-trending faults south of Westonaria.

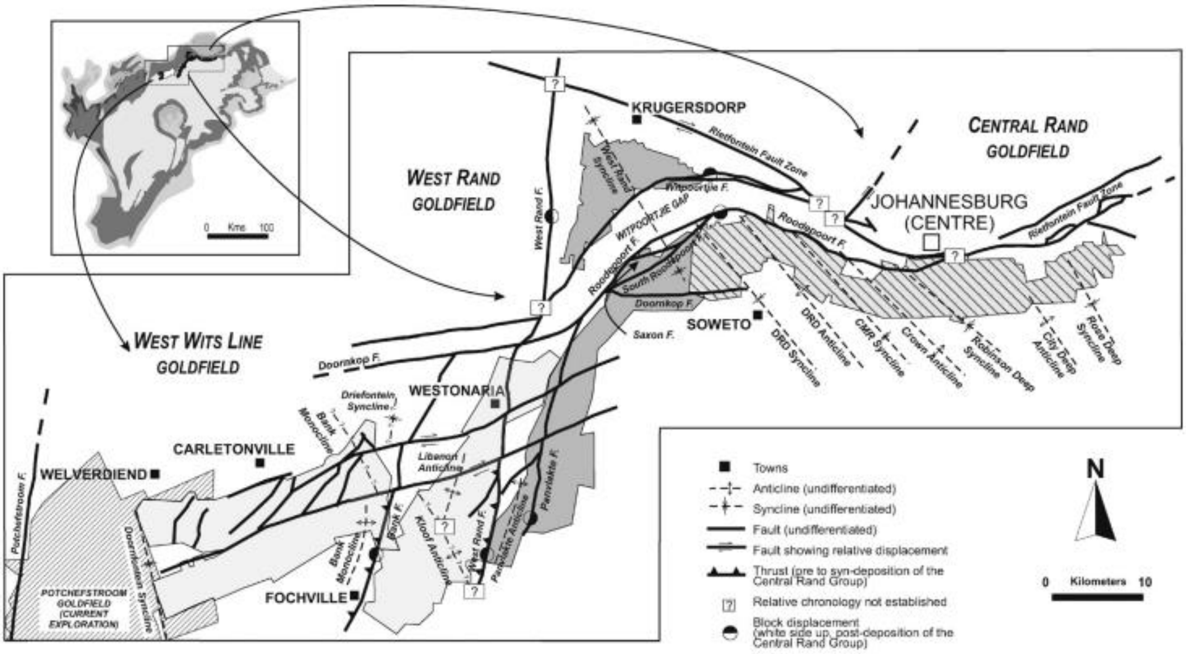

Figure 13: The Witwatersrand Supergroup geological map adapted from *(Stewart, et al., 2004)*.

4.2.2 Lithology

The Witwatersrand Supergroup is separated into two groups: The Lower West Rand Group, which is primarily composed of quartzites and shale, and the Upper Central Rand Group, which is composed of a variety of quartzites and shales, with conglomerates making up the majority of the sequence (McCarthy, 2006). The West Rand Group contains three major depositional-facies that may be distinguished: marine self, fluvial brand plan, and debris flow. It is further divided into the Hospital Hill, Government, and Jeppestown Subgroups.

The Hospital Hill Subgroup is primarily composed of marine inner and outer shelf deposits, which were first formed during widespread transgressive, wave-dominated (mesoidal) conditions. The initial development of shale horizons signalled the transition to low-energy tide-dominated (macro tidal) depositional conditions.

There are two types of sandy inner shelf orthoquartzites: deposits dominated by currents and deposits dominated by storm waves. In the currently dominant, it comprises orthoquartzites with subordinate pebble layers that are well sorted, medium to coarse-grained, or gritty, on a small scale, and cross-bedded. The inner shelf, which is dominated by storm waves, is made up of medium to coarse-grained orthoquartzites with hummocky cross-stratification and huge symmetrical wave ripple markings that are crowned by wave-ripple, crossed-laminate quartzites, and siltstones. The deposits on the outer shelf are indicated by mudstones that range in size from enormous to delicately laminated.

In the Government Subgroup, fluvial braid plain deposits are widespread and predominately composed of sand, with modest intrusions of transgression shelf orthoquartzites. Particularly in the upper portions of the Roodepoort and Maraisburg Formations, portions of the Jeppestown Subgroup are also regarded as fluvial braid plain deposits. Figure 14 shows the lithology of the research area, which is denoted by a red circle.

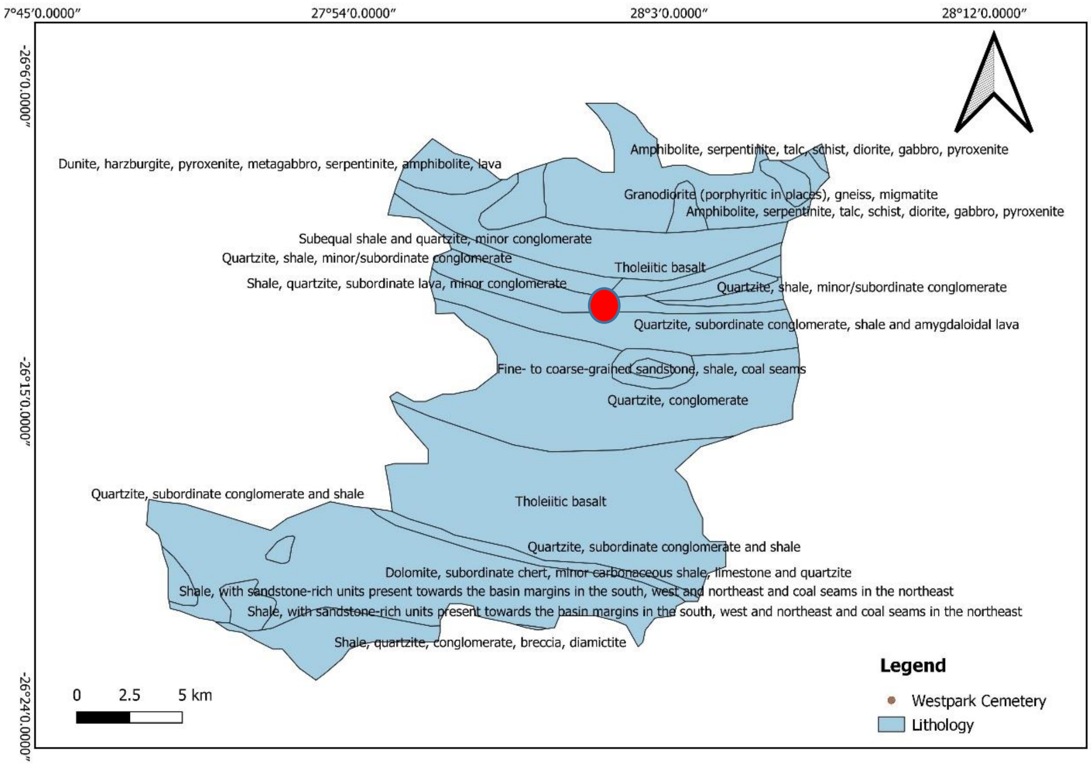

Figure 14: Simplified geological map of the West Park Cemetery, Johannesburg.

4.3 Hydrogeological Setting

The hydrogeological map of Johannesburg scaled 1: 500 000, hydrogeological investigations by (SRK, et al., 2013) and (Abiye, et al., 2011) show that the region has one aquifer type identified as:

- Fractured aquifer associated with fractures, fissures, and joints.

Aquifer yields in the area surrounding West Park Cemetery are estimated to be between 0.1 and 0.5 l/s, which is regarded to be poor to minor. The rocks found in the West Park contain the following characteristics:

- The permeability ranges from medium to low.
- They contain aquifers with limited water resources compared to porous (sand, gravel, sandstone, sedimentary rocks, etc.) and karst (limestone rocks)
- They also have minimal porosity or no area for water to pass through the rock.

The weathered aquifer often has low hydraulic conductivity and storativity, which makes groundwater flow through this aquifer slow. The Witwatersrand rocks are weathered and fractured sedimentary rocks that are shallow water-bearing horizons however, there are isolated high-yielding boreholes in which essential fractures, rarely deeper than 60 m below the surface, tend to be intersected. The aquifers in the Witwatersrand Supergroup have different groundwater types such as calcium-magnesium-bicarbonate for the majority of their aquifers in this regime and magnesium bicarbonate in this regime. The EC values, which vary from 26 to 60 mS/m, indicate that all of the aquifers in the fractured regime have good groundwater quality (Department of Water and Sanitation, 2000).

The Witwatersrand Supergroup's exposed quartzitic rocks act as a continental divide between rivers draining southward to the Orange River, which empties into the Atlantic Ocean, and rivers draining northward to the Limpopo River, which empties into the Indian Ocean. This division regulates the regional hydrology and hydrogeology (SRK, et al., 2013). A suitable medium for vertical recharge can be found in the Witwatersrand Group's fragmented Black Reef quartzites, which make up the water divide (Abiye, et al., 2011). Granitic gneisses and quartzites found in this group have huge structures with broad fracture networks compared to shales which have extremely tight fractures across sloping beds to the south. Waste is frequently kept in rocks with low permeability. As a result, pollutants cannot be easily transported by water, which can rarely pass through.

4.4 Topography and drainage

The slope of the research region is generally flat, and the elevations range from 1600 to 2000 meters above mean sea level. The hill's slope, however, is quite steep, with an elevation between 2,000 and 2500 meters above sea level. Groundwater hydraulic gradients always follow topographic gradients and slopes. The movement of groundwater frequently parallels that of surface drainages and is most likely to be observed at stream confluences on downhill slopes (Toth, 1963). Joints, faults, and lineaments, among other minor and major characteristics, regulate the drainage of the region.

4.5 Vegetation

The area is covered in a medium to dense number of grasses, shrubs, and various tree species around and between the graves. The predominant type of vegetation is grasses.

4.6 Types of burial practices at West Park Cemetery

As a non-denominational authorized burial ground, West Park Cemetery has Christian, Jewish, Muslim, and Chinese burial spaces.

4.6.1. Christian Burials

Christian funerals often occur roughly a week following a death, and because of the religion's beliefs regarding death and burial customs, embalming is permitted, allowing the casket to be displayed at a wake. The wake is held at a funeral home, where family members can pay their final respects to the deceased.

For several reasons, the body of a deceased Christian is frequently placed in a casket before burial. They believe that the body is a temple of the Holy Spirit and should be handled with respect, therefore it is a method of respecting the deceased. Second, it shields the body from deterioration by keeping it away from substances that accelerate decomposition. Thirdly, it allows the family members to see the body before the funeral.

Cremation and Believes

The majority of Christians do not believe in cremation because they hold to the belief in an afterlife and bodily resurrection. As opposed to believing that God will return and raise all the corpses, Christians oppose the idea of burning a body. Nevertheless, some Christians choose cremation over burial because it is less expensive and because they would like their ashes to be dispersed at a location they treasured while they were living (Jones, 2013).

4.6.2. Jewish Burials

Once someone has passed away, the body is properly cleaned, all bleeding is stopped, and any remaining blood is buried with the deceased. The jewellery is all taken off. The body is then dried after being immersed in water or having water poured over it during a ritual bath called taharah. White funeral shrouds are then placed over the deceased (Goodman, 2003).

Before placing the body inside the casket and wrapping it with the winding sheet, the casket must first be prepared by removing any lining or other decorations. In Israel and many other sections of the Diaspora, particularly in Eastern Europe and Arab nations, caskets are not used unless obliged by law. Rather, the body is brought directly into the grave while being covered in a shroud and tallit. Embalming or cosmetic surgery is not permitted unless legally required. Similar rules apply during autopsies, but if required by law, a rabbi may be present.

Cremation and Believes

According to the Jewish sect, cremation is typically permitted, and cremation is forbidden in Orthodoxy. They think the body ought to be interred whole. Reform Rabbis are typically willing to preside over a funeral or burial in Judaism because the religion has become more accepting of cremation.

4.6.3. Muslims

A muslin's body must be ritually cleansed before the ceremony can be performed, according to religious law. An individual of the same gender strips off clothes and covers the body with the white cloth (Gatrad, 1994). Religion forbids post-mortems, yet when the law of the land requires one, there is no other option. The body is said to be afraid and to belong to God. Muslims do not use embalming, so the deceased is buried as quickly as possible to prevent deterioration and the development of an offensive odour.

A plain white fabric in three parts is used to cover the body. Before the body is put on top of them, they are stretched out and piled one on top of the other. The left hand of the deceased is placed on the chest, then the right hand is placed on top of the left, and finally, the sheets are placed one at a time over the body. After that, ropes are tied to the top of the head, the bottom of the feet, and possibly around the middle of the body (Cremation Institute, 2023). The individuals doing this function are hepatitis B immunized and knowledgeable about the risks associated with AIDS. Typically, gloves are used, and a sponge is employed.

The community oversees maintaining the plain wooden boxes used for interment, which are undecorated. After the funeral, four family members carry the casket to the burial place with the body already inside. The body is laid out in a grave that has been dug parallel to Mecca with its right-side facing Mecca. The cemetery is filled after the body has been lowered by family members, and a small, unassuming marker is permitted. Coffins and burial caskets are not allowed in the Islamic faith.

Cremation and Believes

Islamic law forbids cremation because it is viewed as disrespectful to the deceased. A Muslim must not participate in, watch, or condone any form of burning. The sole exception is if the victim passed away as a result of a communicable disease.

4.6.4. Cremation

Cremation is a procedure done in a crematorium with a closed furnace (cremator) that employs high heat to reduce a deceased person's body to ash. Nowadays, the cremation operation is carried out in specialized incinerators, however, some nations, such as India or Nepal, still use open cremation (Matthews Cremation Division, 2006). The remains are safe to handle and can be legally taken by family members, buried, or preserved in crematories. Figure 15 depicts the Braamfontein location of West Park Cremation.

Figure 15: West Park Crematorium in Braamfontein.

Procedure

Cremation takes place inside a cremator, which is a large industrial furnace capable of producing temperatures between 871 and 982 °C to ensure the breakdown of the corpse (Wilkinson, 2016). Oil, natural gas, and propane are all acceptable fuels for modern crematories. The time it takes varies from body to corpse, with an adult body taking an average of 90 minutes to be cremated. It automatically monitors the cremation process and signals when it is finished.

To decrease health risks to the operator and to prevent heat loss, the body must be placed within a coffin or other combustible container and inserted into the cremator immediately and carefully. The cremation chamber, which is lined with heat-resistant refractory bricks, is located inside the cremator and is used to place the body. The fire bricks' exterior layer is shielded from the combustion process by an insulating layer that is periodically changed. The ashes are then deposited within a simple container and returned to the family.

Figure 17: Casket with a body inside waiting to be inserted inside the chamber (right).

Figure 16: Automatic cremator controller showing primary and secondary burner, the temperature inside and time (left). Carbon emission canals releasing to the atmosphere (right).

Figure 18: Excess ashes are disposed of in this location after being collected in the ash chamber.

4.7 Environmental Impact of Cremation

Cremation is a source of carbon emission however depending on the local custom, it is better for the environment compared to burial. According to research (Keijzer, 2017), both cremation and the more recent alkaline hydrolysis technique have a smaller environmental impact than cremation. When compared to burial, cremation requires approximately seventy-four percent less land. When the long-term impacts on the environment are considered, burials at Centennial Park were found to have a 10% greater effect as opposed to cremations, according to the study conducted there at Centennial Park in Adelaide. A Cremation produces roughly 160 kilograms of carbon dioxide comparable to four times as much carbon dioxide as a burial (which produces 39 kilograms of carbon dioxide) (Adelaide Cemeteries Authority, 2021). About 110L of fuel is used for cremation, which emits 240kg of carbon dioxide into the atmosphere. The annual production of 2,400,000 tons of carbon dioxide in the US from the cremation of nearly 1 million bodies is greater than the annual emissions of CO2 from 22,000 typical American homes (Herzog, 2016).

The PCDD, Fs, and Hg, as well as fine particulate matter (PM2.5), which can have a severe effect on the heart and lungs, are just a few of the pollutants emanating from crematoria that are hazardous to humans and can accumulate in tissues. The fine particulate matter (PM2.5) is also linked to various chronic illnesses and poor birth outcomes. Based on annual cremation records and emissions factors unique to crematoria, estimates from (Trozzi, et al., 2019), indicate that about five percent of Canada's PCDD/Fs, six percent of its Hg emissions, and 0.25 percent of its PM2.5 emissions come from crematoriums.

A crematorium's proportional impact on the surrounding air quality depends on a variety of factors, including the other potential sources of pollutants nearby, the volume of cremations and the nature of the remains, the system's design, the cremator's performance, and emission control measures. In addition, the cremation process releases greenhouse gases from coffin coatings and fasteners, which contain carbon dioxide and mercury, as well as from body implantations and treatments, dental fixture which contain mercury and various kinds of metallic element and polymers in prostheses and implants.

Chapter 5: Methodology and Results

5.1 Materials and Methodology

The main objective of the study was to develop a precise model for the flow and movement of pollution within a geological formation in West Park Cemetery by analysing the movement of human remains, investigating the degree of groundwater contamination and aquifer recharge, and finding out how cemeteries affect groundwater. To achieve this, proceeded in three steps:

First, conducted an in-depth scientific literature review to understand the current state of groundwater contamination, contamination in cemeteries, flow of groundwater and solute transporting models, characterization of aquifers, and existing mechanisms of contaminant transports. The desktop study was also carried out to identify any work done on the geology of the area, geotechnical investigation, and use of a Geographical Information System (GIS) to create the lithology of the study area, as well as hydrogeological analysis of West Park Cemeteries and the Witwatersrand basin.

The second step involved conducting an interview with the area manager, environmental researcher, and crematorium operators at the West Park Cemetery to learn more about the cemetery's specifics, including its size, number of burials, and distance between graves, as well as any potential groundwater zones, seepage, ecosystems, and the process of cremation. Recognize the commercial, regulatory, social, cultural, technological, and regulatory opportunities and limitations at the cemetery. Both telephone and in-person interviews were conducted.

Thirdly, a site visit was made to the West Park Cemetery to validate the geology of the area, identify springs, collect data, identify available faults and fractures, determine the water levels and flow directions, and identify the boreholes that may be used for sampling. However, no water samples were collected as one of the boreholes had extremely low water, and the others were reported to be dry, making it impossible to collect samples. This study will make use of information on boreholes that was also gathered from the prior report prepared by the local water department.

An Excel spreadsheet was used to evaluate the data collected from West Park, presented in graphs, did calculations, and used descriptive statistics to list and classify a data set's features. The data was then evaluated using the advection-dispersion reaction equation to investigate the flow of the contaminants emanating from the graves. The advection-dispersion-reaction equation, an analytical solution that can be applied to numerous groundwater transport models, was used to characterize the solute transport, and sensitivity analysis was carried out.

5.2 Results and Analysis

The information regarding West Park Cemetery and the cemeteries in Johannesburg presented in this section was sourced from (Greaves, 2023) and (Breedt, 2022), respectively.

5.2.1 Cemeteries

a) **Table 2: Total number of burials over five years in Johannesburg Cemeteries.**

Total number of burials over five years in Johannesburg Cemeteries		
Period	**Number of Deaths**	**Percentage (%)**
2018-2019	14876	17
2019-2020	15540	18
2020-2021	20822	24
2021-2022	20620	23
2022-2023	16582	19
Total	**88440**	**100**

Figure 19 illustrates the total number of burials in Johannesburg cemeteries over five years (Greaves, 2023).

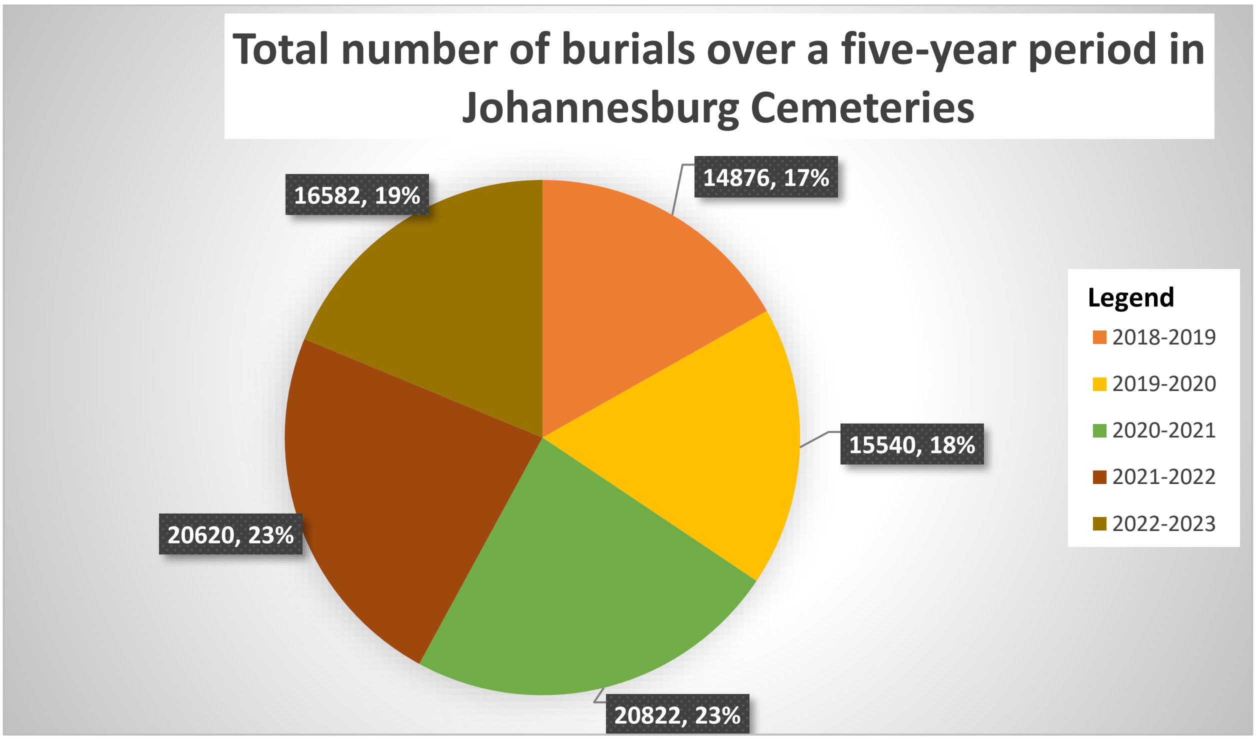

Figure 19: Total number of burials in Johannesburg cemeteries over five years. Based on *(Greaves, 2023)*.

According to the graph, the years 2020–2021 had the highest percentage of burials over the previous five years (24%), followed by 2021–2022 (23%) and 2022–2023 (19%). In Johannesburg, there were incredibly few burials during the years 2018–2019. Many interments occurred because of the COVID-19 coronavirus epidemic and other circumstances. A total of 88440 people were buried between 1st March 2018 and 28 February 2023.

b) **Table 3: Total number of burials in Johannesburg Cemeteries.**

Total number of burials in Johannesburg Cemeteries	
Cemeteries	**Number of Deaths**
Olifantsvlei	6297
West Park	4101
Waterval	2249
Avalon	2003
Lenasia	440
Doornkop	234
New Roodepoort	276
Eldorado Park	287
Newclare	164
Diepsloot	245
Other Cemeteries	246

The graph shows that Olifantsvlei cemetery had the highest percentage of graves (6297; 38%), followed by West Park Cemetery (4101; 25%) and Waterval Cemetery (2249; 14%). In comparison to other cemeteries, the Olifantsvlei, West Park, Waterval, and Avalon are thought to be more accessible and have more room for burial. To meet the demand for burial space as the city continues to develop and grow, new cemeteries were built, including Waterval Cemetery, Diepsloot Memorial Park, and Olifantsvlei (Kaapu, 2021).

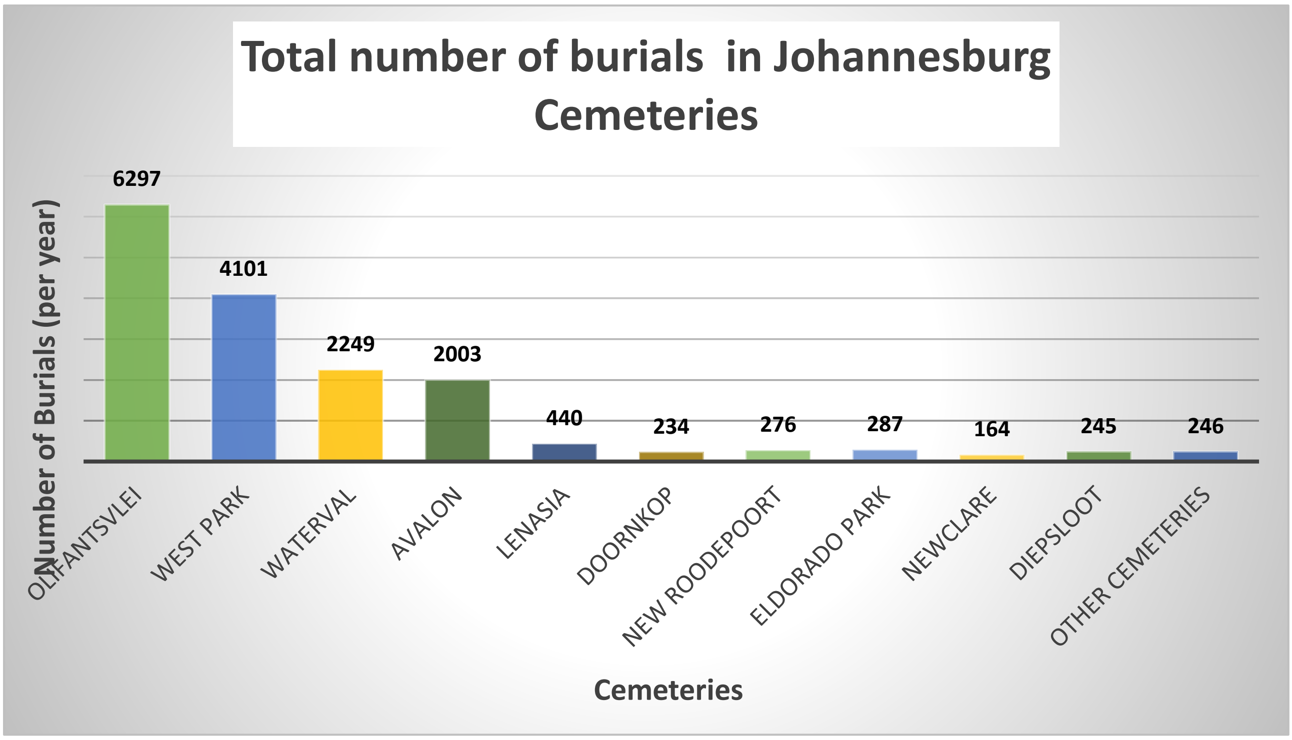

Figure 20: Total number of burials in Johannesburg Cemeteries, *b*ased on (Greaves, 2023).

c) **Table 4: Total number of burials in West Park Cemetery.**

West Park Cemetery Burials from 1st March 2022 to 28 February 2023	
Time (quarter)	**Number of Deaths**
1st Quarter	1075
2ndQuarter	937
3rd Quarter	957
4th Quarter	1132
Total (2022-2023)	4101
Total (2021-2022)	5491

Figure 21 shows the total number of burials in West Park Cemetery throughout the financial year, according to (Greaves, 2023).

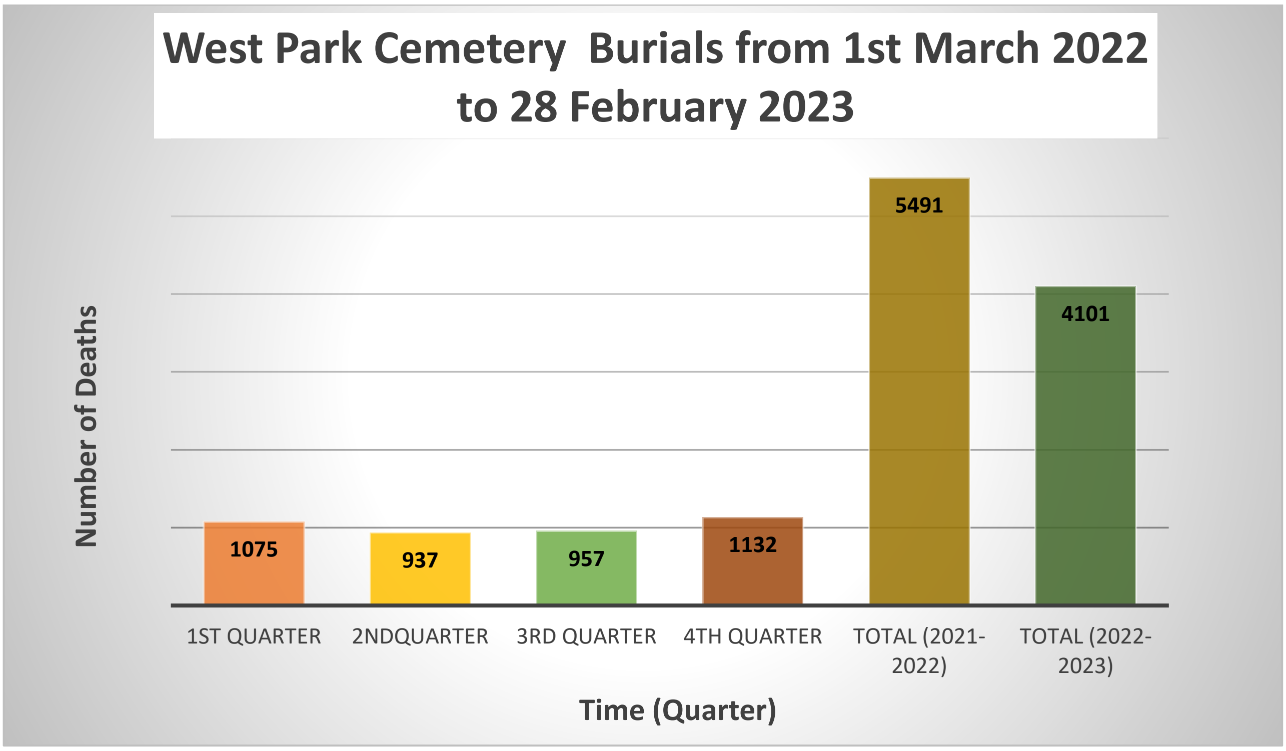

Figure 21: Total number of burials in West Park Cemetery throughout the financial year, according to *(Greaves, 2023)*.

According to the graph above, the fourth quarter of the financial year displays the largest number of burials, followed by the first and second quarters, which have the lowest number. In comparison to 2022–2023, there were more burials overall in the years 2021–2022. The findings show that external causes of morbidity, including assault, contact with an object, home or place of residence accidents, and traffic accidents, as well as certain infectious diseases like intestinal infectious diseases, COVID-19, tuberculosis, and HIV, and respiratory system diseases, including influenza and pneumonia, are the main causes of death during the fourth quarter and first quarter. One can see the effect of COVID-19 spread as the primary cause of death from 2021 to 2022.

5.2.2 Statistical analysis

To derive predictions from data that are prone to random fluctuation such as standard error and population variance, descriptive statistics are used to examine the data from the West Park Cemetery. These statistics describe population data using indices such as the mean and standard deviation.

6.1 Descriptive statistics

Descriptive statistics will be used to illustrate the features of the population data, including measures of central tendency and variability. Variability is described by the terms range, standard deviation, variance, and interquartile range, whereas central tendency is described by the terms mean, median, and mode.

Table 5: Measures of central tendency of West Park data

Measures	Value
Mean	1025
Median	1104
Mode	0

Between the first of March 2022 and the last day of February 2023, the estimated median and average burial numbers were 1016 and 1026, respectively. There is no mode measurement in this data because it is a record of the number of funerals at West Park Cemetery throughout the specified time.

a) Measures of variability

Table 6: Measures of the variability of West Park data

Measures	Number of Burials
Minimum	937
First Quartile	952
Second Quartile	1016
Third Quartile	1089
Maximum	1132
Range	195
Standard Deviation	94
Sample Variance	8772

For better comprehension, the box and whisker diagram (Figure 22) provides a summary of Table 6. The first quartile of the box represents the first 25% of the burials done at the cemetery and the third quartile is 75% of total burials at the West Park graveyard for the financial year which lies closer to the 4th quarter. The middle value which is 50% of the data lies closest to the lower quartile, which lies in the 1st quarter.

The standard deviation, which was computed using the data gathered, was found to be 94, which is large, and indicates how widely the data deviate from the mean. The more variance there is in the data set, the higher the standard deviation. The variance was calculated to be 8772 and the data is more dispersed.

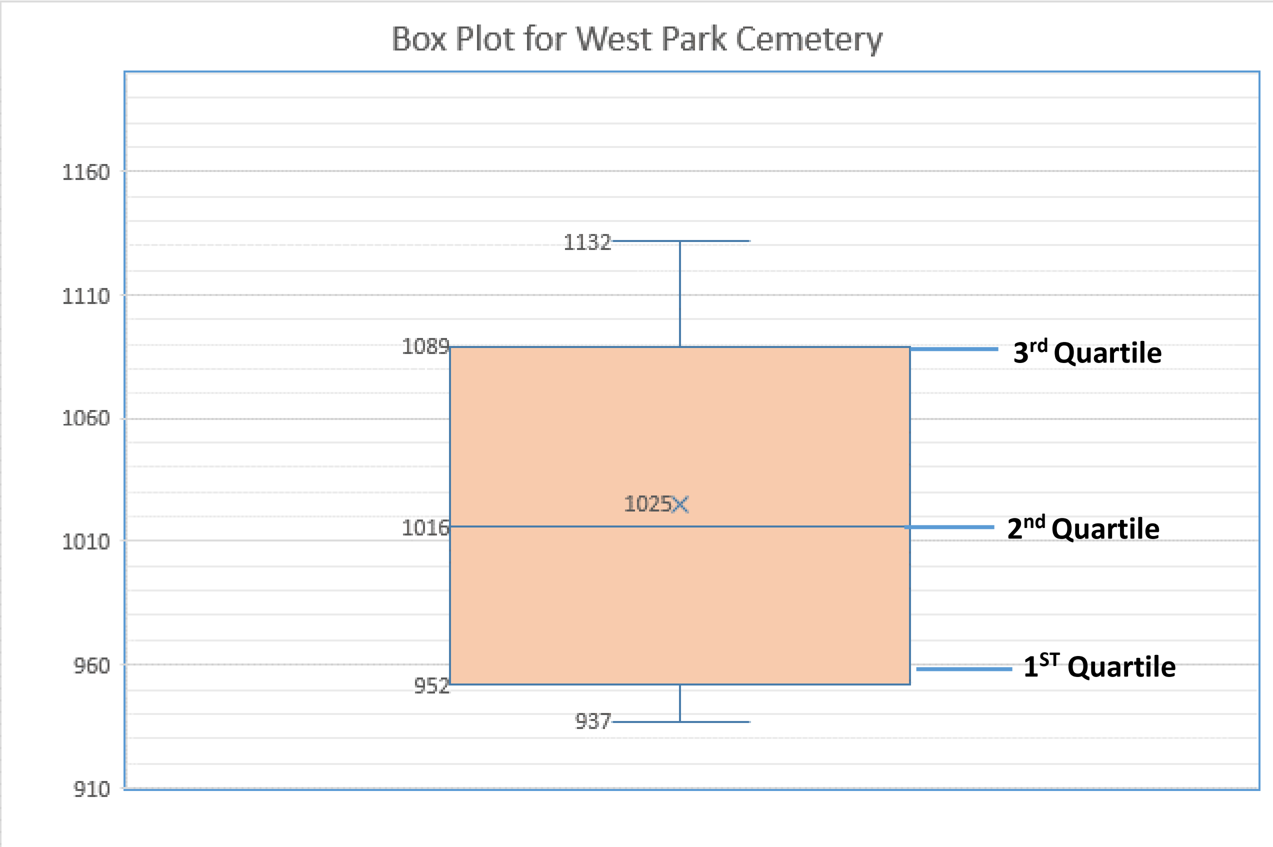

Figure 22: Box and Whisker diagram for West Park Cemetery.

Figure 23 shows the overall total of burials from first to the fourth quarters, excluding the year totals.

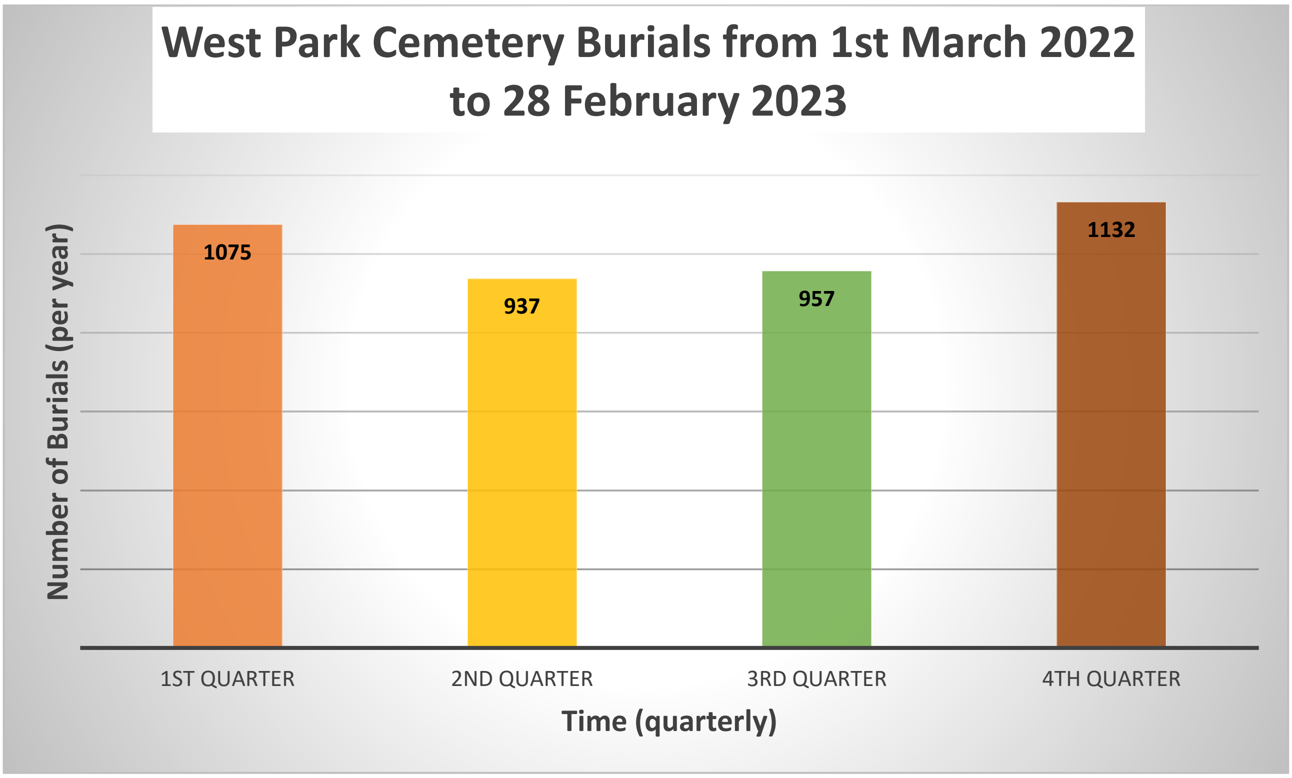

Figure 23: West Park Cemetery Burials from 1st March to 28 February 2023.

5.3 Cremations

Table 7: Total number of cremations in Johannesburg crematories for 5 years.

Total number of cremations over five years in Johannesburg		
Period	**Number of Deaths**	**Percentage of cremations (%)**
2018-2019	3107	16
2019-2020	3390	18
2020-2021	4368	23
2021-2022	5031	26
2022-2023	3139	16
Total	**19035**	**100**

The graph below, created using (Greaves, 2023) data, displays the total number of cremations conducted in the Johannesburg Crematoria.

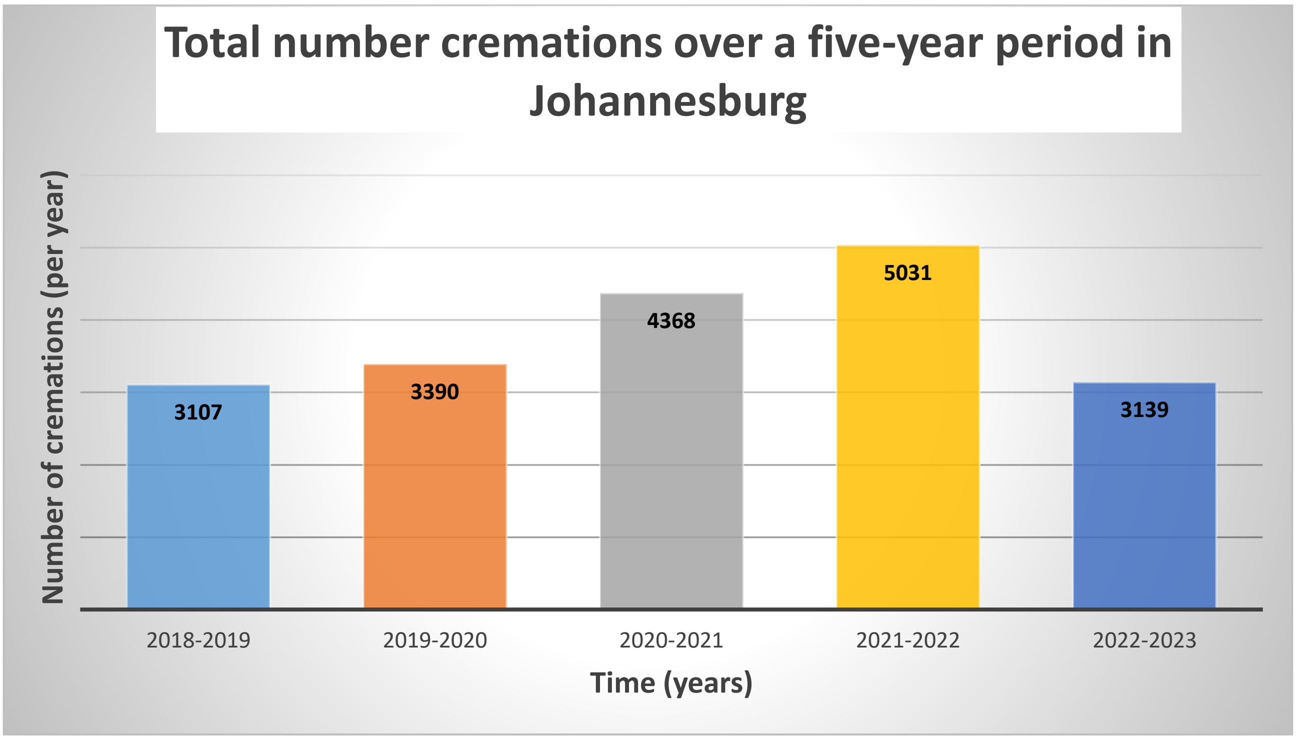

Figure 24: Total number of cremations done in Johannesburg Crematories.

The highest proportion of people who were cremated during five years occurred in 2021–2022, followed by 4368 in 2020 and 3390 in 2019–2022. This was due to the COVID-19 infectious disease, which spread rapidly and caused a large number of deaths. The number of cremations was almost identical in the years 2018–2019 (3107;16%) and 2022–2023 (3139;16%).

5.4 Water Quality

Table 8: West Park Cemetery Groundwater Levels

Groundwater Monitoring Boreholes						
Borehole No	**Depth to bottom of the well(m)**	**Latitude**	**Longitude**	**Sample Time**	**Depth to Water**	**Comment**
WES1	11	S26.16522	E27.99851	27-06-2023 10:06	9.2	Slightly turbid
WES2	10.77	S26.16230	E27.98446	27-06-2023 10:50	-	Dry
WES3	27	S26.16747	E27.99093	No access	-	Dry

At depths of 10.77 meters and 27 meters, respectively, boreholes WES2 and WES3 were reported to be dry during the site inspection. Figure 25 was taken from the prior report and shows the monitoring of groundwater levels at West Park Cemetery as of 2020.

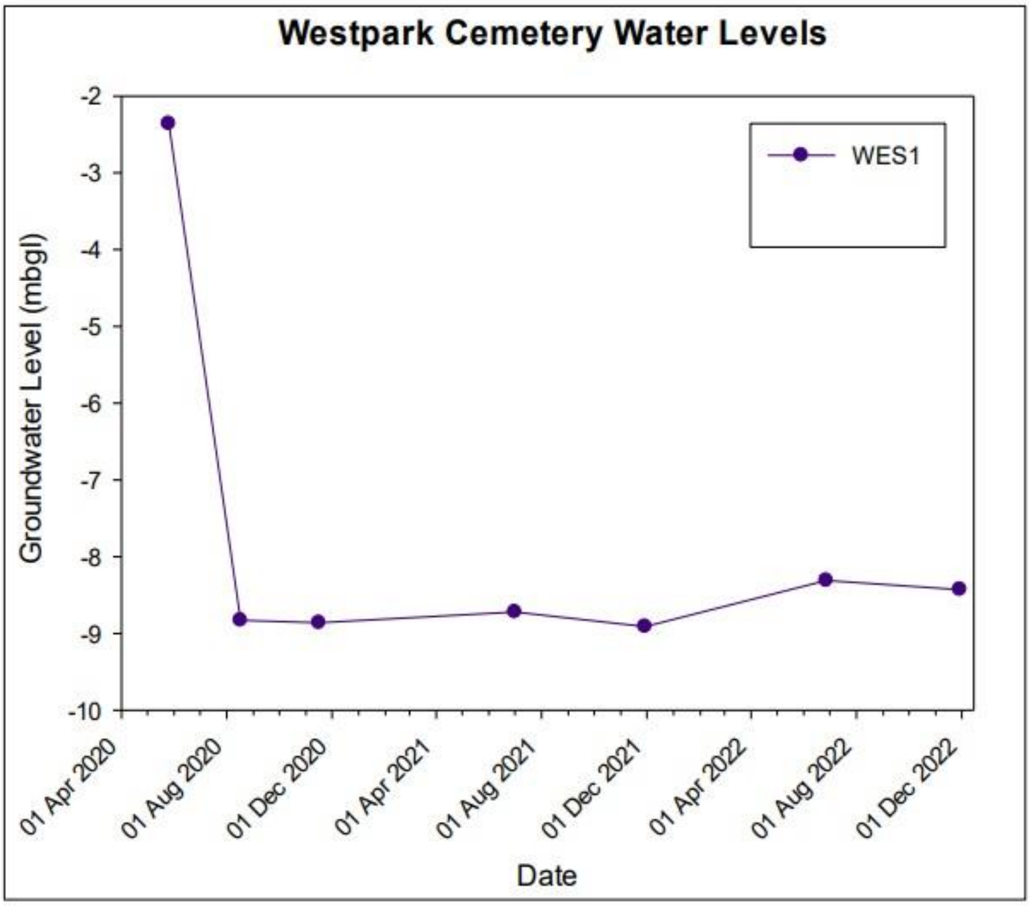

Figure 25: West Park groundwater levels obtained from *(Breedt, 2022)*.

Three water quality tests are performed annually in West Park: in April, August, and December according to the information given by the environmentalist. Due to the dryness and shallowness of the majority of the monitoring boreholes, only borehole WES1 is displayed. In August, there was an extremely high groundwater level reading at the beginning of the readings, as can be seen in the figure above. There are many potential causes for the high-level reading, including a recharge that occurred because January through April are the wettest months and experience the most precipitation, rain entering the borehole because there is no cap to prevent rain from entering on top, and an error that was the result of human or equipment.

The water levels varied between August 1st, 2021, and August 1st, 2022, due to variations in recharge (how quickly the groundwater is refilled) and season. The water levels began to rise on December 1, 2021, and continued until July 20, 2022. Due to the significant seasonal change, heavy rainfall, and lack of a good cab to prevent water or contaminants from entering the well, the rain was entering the borehole well from the top. We could conclude from these findings that the West Park Cemetery is situated in a region with rock features where precipitation recharges the aquifer slowly.

5.5 Groundwater Quality

An evaluation of groundwater quality is required because groundwater resources are under more stress due to anthropogenic activities and climatic variability. By assessing the current state of groundwater quality, awareness is raised, and the required actions can be taken. To identify any contaminants emanating from the burials, Table 9 displays the groundwater quality of West Park Cemetery for borehole WES1 using data from (Breedt, 2022).

Table 9: West Park Cemetery groundwater quality data adapted from *(Breedt, 2022)***.**

Variable	Units	Assessment 1	Monitoring Localities	Assessment 2	Monitoring Localities
		Leachable Concentration Threshold Limits- (mg/l)	WES1	SANS 24-1:2015 Drinking Water Standard (SABS, 2015)	WES1
pH @25°C	pH	-	6.49	5.0/9.7	6.49
Electrical conductivity (EC) @25°C	mS/m	-	42	170	42
Total Dissolved Solids @180°C	mg/l	1000	282	1200	282
Total alkalinity	mg $CaCO_3$/l	-	246	-	246
Calcium (Ca)	mg/l	-	40.1	-	40.1
Potassium (K)	mg/l	-	4.84	-	4.84
Magnesium (Mg)	mg/l	-	21.5	-	21.5
Sodium (Na)	mg/l	-	23.1	200	23.1
Chloride (Cl)	mg/l	300	8.62	300	8.62
Sulphate (SO_4)	mg/l	250	2.56	500	2.56
Nitrate (NO_3) as N	mg/l	11	<0.194	11	<0.194

Ammonium (NH_4) as N	mg/l	-	0.32	1.5	0.32
Orthophosphate (PO4) as P	mg/l	-	<0.005	-	<0.005
Fluoride (F)	mg/l	1.5	0.68	1.5	0.68
Iron (Fe)	mg/l	-	0.048	0.3	0.048
Manganese (Mn)	mg/l	0.5	4.8	0.1	4.8
Chemical oxygen demand (COD)	mg/l	-	18.2	-	18.2
E.coli	CFU/100ml	-	0	0	0
Total coliform	CFU/100ml	-	0	10	0
Temperature	°C	-	22.5	-	22.5
Oil and grease (SOG)	mg/l	-	<0.100	-	<0.100
Formaldehyde	mg/l	25	<0.100	-	<100

According to the data shown in the table above, the manganese (Mn) levels in the water at borehole WES1 exceeded both the Leachable Concentration Threshold (LTC) Limits and the SANS 241-1:2015 Drinking Water Standards. Metals like iron (Fe) and manganese (Mn) are found naturally in soils, rocks, and minerals. When groundwater in the aquifer comes into an interface with such solids, water tends to disintegrate them and release the minerals they contain, including iron and manganese, into the water (World Health Organization, 2011). Manganese dissolves in groundwater to an excessive or minor extent depending on the water's acidity and oxygen content. Manganese has a metallic taste when water concentrations for it surpass 0.05 mg/l. The geology, as well as metals leaching from the borehole casing, coffin decorations, or jewellery, may cause excessive manganese concentration in WES1 at West Park Cemetery. West Park Cemetery's groundwater is characterized as neutral and non-saline.

Chapter 6: Groundwater Transport Model

Figure 14 illustrates the geology of the West Park Cemetery, which is in the geological group of West Rand. The region is made up of quartzites, shale, subordinate lava, and small conglomerate. Due to a lack of available data, we were unable to identify the actual geology and lithology of the region; consequently, the equation was computed using the following two scenarios:

i. We will assume their geology does not have any retardation, therefore will solve using an advection-dispersion equation without a retardation factor.
ii. We will assume there is retardation with the geology, therefore we will solve using an advection-dispersion equation with retardation.

6.1 Advection-dispersion Equation without Retardation Factor

$$\begin{cases} \frac{\partial C(x,t)}{\partial t} = D\frac{\partial^2 C(x,t)}{\partial x^2} - v\frac{\partial C(x,t)}{\partial x} \\ C(x,0) = g(x) \\ C(0,t) = f(t) \\ C(0,0) = C_0 \end{cases} \tag{12}$$

To be more practical, we will assume that D and v are functions of space and will be determined accordingly.

$$\frac{\partial C(x,t)}{\partial t} = D(x)\frac{\partial^2 C(x,t)}{\partial x^2} - v(x)\frac{\partial C(x,t)}{\partial x} \tag{13}$$

We apply the integral on both sides to get,

$$C(x,t) = C(x,0) + \int_0^t \left[D(x)\frac{\partial^2 C(x,\tau)}{\partial x^2} - v(x)\frac{\partial}{\partial x}C(x,\tau)\right] d\tau \tag{14}$$

We put for simplicity.

$$F\big(x,t,C(x,t)\big) = D(x)\frac{\partial^2 C(x,t)}{\partial x^2} - v(x)\frac{\partial}{\partial x}C(x,t) \tag{15}$$

The simplified equation can be reformulated as

$$C(x,t) = C(x,0) + \int_0^t F\left(x,\tau,C(x,\tau)\right) d\tau \tag{16}$$

Equation *16* can be disintegrated using different approaches.

i. A simple Euler method will be applied to the time component and a suitable approach will be applied to the space component,

$$x \in [0, L];\ t \in [0, T]$$

Where L is the boundary of the cemetery and F is the longest time for the transport.

To accommodate readers who are not used to this approach, we present here the derivation with a general nonlinear ordinary differential equation: Let us consider the following Cauchy problem,

$$\begin{cases} y'(t) = f(y(t), t) \\ y(0) = 0 \end{cases} \qquad 17$$

It is assumed that the function $f(y(t), t)$ is nonlinear concerning the function $y(t)$, thus, the above initial value problem cannot be solved using any analytical technique. Numerical schemes are suitable candidates in this case. To solve this equation, we integrate both sides to obtain:

$$y(t) = y(0) + \int_0^t f(\tau, y(\tau))d\tau \qquad 18$$

We replace $t = t_{n+1}$ in the above to obtain.

$$y(t_{n+1}) = y(0) + \int_0^{t_{n+1}} f(\tau, y(\tau))d\tau \qquad 19$$

Here we replace $t = t_n$ to obtain.

$$y(t_n) = y(0) + \int_0^{t_n} f(\tau, y(\tau))d\tau \qquad 20$$

$$y(t_{n+1}) = y(t_n) + \int_0^{t_{n+1}} f(\tau, y(\tau))d\tau \qquad 21$$

We approximate $f\big(t, y(t)\big)$ between $[t_n, t_{n+1}]$, $f(t_n, y(t_n))$

$$y_{n+1} = y_n + \int_{t_n}^{t_{n+1}} f(t_n, y_n)d\tau \qquad 22$$

$$= y_n + f(t_n, y_n) \int_{t_n}^{t_{n+1}} d\tau$$

$$= y_n + f(t_n, y_n)[t]_{t_n}^{t_{n+1}} \qquad 23$$

Therefore,

$$y_{n+1} = y_n + f(t_n, y_n)h \qquad 24$$

We can now apply the above derivation to the advection-dispersion equation *12* starting from point (x_i, t_{n+1}), we have

$$C(x_i, t_{n+1}) = C(x_i, 0) + \int_0^{t_{n+1}} F\left(x_{i,}\tau, C(x_i, \tau)\right) d\tau. \quad 25$$

At the point (x_i, t_n)

$$C(x_i, t_{n+1}) = C(x_i, 0) + \int_0^{t_n} F\left(x_{i,}\tau, C(x_i, \tau)\right) d\tau \quad 26$$

On both points, we apply Euler on $F\left(x_{i,}\tau, C(x_i, \tau)\right)$ between $[t_n, t_{n+1}]$ to get

$$C_i^{n+1} = C_i^n + F(x_i, t_n, C_i^n)h \quad 27$$

Replacing $F(x_i, t_n, C_i^n)$ by its value produces

$$C_i^{n+1} = C_i^n + h\left[D(x_i)\frac{\partial^2}{\partial x^2}C(x_i, t_n) - v(x_i)\frac{\partial}{\partial x}C(x_i, t_n)\right]$$

28

Where

$$\frac{\partial^2}{\partial x^2}C(x_i, t_n) \cong \frac{C_{i+1}^n - 2C_i^n + C_{i-1}^n}{\Delta x^2}$$

$$\frac{\partial}{\partial x}C(x_i, t_n) \cong \frac{C_{i+1}^n - C_{i-1}^n}{2\Delta x}$$

Replacing equation *28* , we obtain

$$C_i^{n+1} = C_i^n + h\left[D_i\frac{C_{i+1}^n - 2C_i^n + C_{i-1}^n}{\Delta x^2} - v_i\frac{C_{i+1}^n - C_{i-1}^n}{2\Delta x}\right] \quad 29$$

However, if we consider the following approximation of Euler $F\left(x_{i,}\tau, C(x_i, \tau)\right) \cong F\left(x_{i,}t_{n+1}, C(x_i, t_{n+1})\right)$ between $[t_n, t_{n+1}]$, we will get

$$C_i^{n+1} = C_i^n + F(x_i, t_{n+1}, C_i^{n+1})h$$

$$C_i^{n+1} = C_i^n + h\left[D(x_i)\frac{\partial^2}{\partial x^2}C(x_i, t_{n+1}) - v(x_i)\frac{\partial}{\partial x}C(x_i, t_{n+1})\right] \quad 30$$

Here we have two cases,

i.

$$\frac{\partial^2}{\partial x^2}C(x_i, t_{n+1}) \cong \frac{C_{i+1}^{n+1} - 2C_i^{n+1} + C_{i-1}^{n+1}}{\Delta x^2}$$

$$\frac{\partial}{\partial x}C(x_i, t_{n+1}) \cong \frac{C_{i+1}^{n+1} - C_{i-1}^{n+1}}{2\Delta x}$$

$$C_i^{n+1} = C_i^n + h\left[D_i \frac{C_{i+1}^{n+1} - 2C_i^{n+1} + C_{i-1}^{n+1}}{\Delta x^2} - v_i \frac{C_{i+1}^{n+1} - C_{i-1}^{n+1}}{2\Delta x}\right] \quad 31$$

ii.

$$\frac{\partial^2}{\partial x^2} C(x_i, t_{n+1}) \cong \frac{C_{i+1}^{n+1} - 2C_i^{n+1} + C_{i-1}^{n+1}}{2\Delta x^2} + \frac{C_{i+1}^n - 2C_i^n + C_{i-1}^n}{2\Delta x^2} \quad 32$$

Replacing into the original equation

$$C_i^{n+1} = C_i^n + h\left[D_i \frac{C_{i+1}^{n+1} - 2C_i^{n+1} + C_{i-1}^{n+1} + C_{i+1}^n - 2C_i^n + C_{i-1}^n}{2\Delta x^2} - v_i \frac{C_{i+1}^{n+1} - C_{i-1}^{n+1}}{2\Delta x}\right] \quad 33$$

We have chosen i to begin at 1 to help with the reader's understanding.

6.2 Advection-dispersion Equation with Retardation Factor

In the earlier section, we have assumed that the geological formation underlying the cemetery does not have any retardation factor. In this section, we will consider the effect of retardation. To do this we introduce the retardation factor $\mathrm{R(x,t)}$ to obtain:

$$\begin{cases} \frac{\partial C(x,t)}{\partial t} = D\frac{\partial^2 C(x,t)}{\partial x^2} - v\frac{\partial C(x,t)}{\partial x} + R(x,t) \\ C(x,0) = g(x) \\ C(0,t) = f(t) \\ C(0,0) = C_0 \end{cases} \quad 34$$

We will presumptively determine D and v as functions of space.

$$\frac{\partial C(x,t)}{\partial t} = D(x)\frac{\partial^2 C(x,t)}{\partial x^2} - v(x)\frac{\partial C(x,t)}{\partial x} + R(x,t) \quad 35$$

We apply the integral on both sides to get,

$$C(x,t) = C(x,0) + \int_0^t \left[D(x)\frac{\partial^2 C(x,\tau)}{\partial x^2} - v(x)\frac{\partial}{\partial x}C(x,\tau) + R(x,\tau)\right] d\tau \quad 36$$

We put for simplicity.

$$F\left(x_i, t, C(x,t)\right) = D(x)\frac{\partial^2 C(x,t)}{\partial x^2} - v(x)\frac{\partial}{\partial x}C(x,t) + R(x,t) \quad 37$$

The above equation will be rewritten as

$$C(x,t) = C(x,0) + \int_0^t F\left(x,\tau,C(x,\tau)\right) d\tau \quad 38$$

When we apply the Simple Euler method on $F\left(x_i, \tau, C(x_i,\tau)\right)$ between $[t_n, t_{n+1}]$, we get.

$$C_i^{n+1} = C_i^n + F(x_i, t_n, C_i^n)h \quad 39$$

Substituting its value for $F(x_i, t_n, C_i^n)$ results in

$$C_i^{n+1} = C_i^n + h\left[D(x_i)\frac{\partial^2}{\partial x^2}C(x_i,t_n) - v(x_i)\frac{\partial}{\partial x}C(x_i,t_n) + R(x_i,t_n)\right] \qquad 40$$

Where,

$$\frac{\partial^2}{\partial x^2}C(x_i,t_n) \cong \frac{C_{i+1}^n - 2C_i^n + C_{i-1}^n}{\Delta x^2}$$

$$\frac{\partial}{\partial x}C(x_i,t_n) \cong \frac{C_{i+1}^n - C_{i-1}^n}{2\Delta x}$$

Replacing the above equations, we obtain

$$C_i^{n+1} = C_i^n + h\left[D_i\frac{C_{i+1}^n - 2C_i^n + C_{i-1}^n}{\Delta x^2} - v_i\frac{C_{i+1}^n - C_{i-1}^n}{2\Delta x} + R_i^n\right] \qquad 41$$

If we take into account, the following approximation of Euler.

$$F\left(x_{i,}\tau, C(x_i,\tau)\right) \cong F\left(x_{i,}t_{n+1}, C(x_i,t_{n+1})\right)$$

between$[t_n, t_{n+1}]$, we will get.

$$C_i^{n+1} = C_i^n + F(x_i, t_{n+1}, C_i^{n+1})h \qquad 42$$

Replacing $F(x_i, t_n, C_i^{n+1})$ by its value produces

$$C_i^{n+1} = C_i^n + h\left[D(x_i)\frac{\partial^2}{\partial x^2}C(x_i,t_{n+1}) - v(x_i)\frac{\partial}{\partial x}C(x_i,t_{n+1}) + R_i^n\right] \qquad 43$$

Following the discussion presented earlier, we shall consider several cases starting with

i.

$$\frac{\partial^2}{\partial x^2}C(x_i,t_{n+1}) \cong \frac{C_{i+1}^{n+1} - 2C_i^{n+1} + C_{i-1}^{n+1}}{\Delta x^2}$$

$$\frac{\partial}{\partial x}C(x_i,t_{n+1}) \cong \frac{C_{i+1}^{n+1} - C_{i-1}^{n+1}}{2\Delta x}$$

$$C_i^{n+1} = C_i^n + h\left[D_i\frac{C_{i+1}^{n+1} - 2C_i^{n+1} + C_{i-1}^{n+1}}{\Delta x^2} - v_i\frac{C_{i+1}^{n+1} - C_{i-1}^{n+1}}{2\Delta x} + R_i^n\right] \qquad 44$$

The second option is to use the well-known Crank-Nicolson

ii.

$$\frac{\partial^2}{\partial x^2}C(x_i,t_{n+1}) \cong \frac{C_{i+1}^{n+1} - 2C_i^{n+1} + C_{i-1}^{n+1}}{2\Delta x^2} + \frac{C_{i+1}^n - 2C_i^n + C_{i-1}^n}{2\Delta x^2} \qquad 45$$

Noting that the first derivative approximation is the same as previously presented, now replacing these into the main equation yields:

$$C_i^{n+1} = C_i^n + h\left[D_i \frac{C_{i+1}^{n+1} - 2C_i^{n+1} + C_{i-1}^{n+1} + C_{i+1}^n - 2C_i^n + C_{i-1}^n}{2\Delta x^2} - v_i \frac{C_{i+1}^{n+1} - C_{i-1}^{n+1}}{2\Delta x} + R_i^n\right] \quad 46$$

6.3 Numerical Solution with Crank Nicolson Method

The Crank Nicolson method is used to numerically solve the heat equation and related partial difference equations using the finite difference approach. The forward Euler method at n and the backward Euler technique at $n+1$ are combined to create the numerically stable Crank-Nicolson method equations (Crank & Nicolson, 1947; Fadugba, et al., 2012). An implicit finite difference is used to approximate the solution of the non-linear differential system that arises in heat flow issues (Morton & Mayers, 1994). To arrive at a numerical solution to the basic advection-dispersion equation, we will apply the well-known Crank-Nicolson method in this section. The general equation is as follows:

$$\frac{u_i^{n+1} - u_i^n}{\Delta t} = \frac{1}{2}\left[F_i^{n+1}\left(u, x, t, \frac{\partial u}{\partial x}, \frac{\partial^2 u}{\partial x^2}\right) + F_i^n\left(u, x, t, \frac{\partial u}{\partial x}, \frac{\partial^2 u}{\partial x^2}\right)\right] \quad 47$$

We will first apply Crank-Nicolson in the advection-dispersion equation without retardation, where function $F()$ is a linear advection-dispersion representing space changes.

$$\frac{C(x_i,t_{n+1}) - C(x_i,t_n)}{\Delta t} = \frac{D_x}{2}\left(\frac{C(x_{i+1},t_{n+1}) - 2C(x_i,t_{n+1}) + C(x_{i-1},t_{n+1})}{\Delta x^2} + \frac{C(x_{i+1},t_n) - 2C(x_i,t_n) + C(x_{i-1},t_n)}{\Delta x^2}\right) - v\frac{C(x_{i+1},t_n) - C(x_{i-1},t_n)}{2\Delta x} \quad 48$$

It is important to remember that the central approximation is used for the first-order space approximation and we obtain

$$\frac{C_i^{n+1} - C_i^n}{\Delta t} = \frac{D_x}{2}\left(\frac{C_{i+1}^{n+1} - 2C_i^{n+1} + C_{i-1}^{n+1}}{\Delta x^2} + \frac{C_{i+1}^n - 2C_i^n + C_{i-1}^n}{\Delta x^2}\right) - v\frac{C_{i+1}^n - C_{i-1}^n}{2\Delta x} \quad 49$$

It can also be written as

$$\frac{C_i^{n+1} - C_i^n}{\Delta t} = \frac{D_x}{2\Delta x^2}\left\{C_{i+1}^{n+1} - 2C_i^{n+1} + C_{i-1}^{n+1} + C_{i+1}^n - 2C_i^n + C_{i-1}^n\right\} - \frac{v}{2\Delta x}\left\{C_{i+1}^n - C_{i-1}^n\right\} \quad 50$$

To simplify the above equation, we will multiply both sides by Δt

$$C_i^{n+1} - C_i^{n} = \frac{D_x\Delta t}{2\Delta x^2}\{C_{i+1}{}^{n+1} - 2C_i^{n+1} + C_{i-1}{}^{n+1} + C_{i+1}{}^{n} - 2C_i^{n} + C_{i-1}{}^{n}\} - \frac{v\Delta t}{2\Delta x}\{C_{i+1}{}^{n} - C_{i-1}{}^{n}\} \quad 51$$

By factorization and making C_i^{n+1} the subject of the formula, the Crank-Nicolson final equation will be written as

$$C_i^{n+1}\left\{1 + \frac{D_x\Delta t}{\Delta x^2}\right\} = C_i^{n}\left(1 - \frac{D_x\Delta t}{\Delta x^2}\right) + C_{i+1}{}^{n+1}\left(\frac{D_x\Delta t}{2\Delta x^2}\right) + C_i^{n+1}\left(\frac{D_x\Delta t}{2\Delta x^2} - \frac{v}{2\Delta x}\right) + C_{i-1}{}^{n}\left(\frac{D_x\Delta t}{2\Delta x^2} + \frac{v}{2\Delta x}\right) \quad 52$$

To derive a numerical solution to the classical advection-dispersion equation with retardation factor, we will substitute the Crank-Nicolson equation to obtain.

$$\frac{C(x_i,t_{n+1}) - C(x_i,t_n)}{\Delta t} = \frac{D_x}{2}\left(\frac{C(x_{i+1},t_{n+1}) - 2C(x_i,t_{n+1}) + C(x_{i-1},t_{n+1})}{\Delta x^2} + \frac{C(x_{i+1},t_n) - 2C(x_i,t_n) + C(x_{i-1},t_n)}{\Delta x^2}\right) - v\frac{C(x_{i+1},t_n) - C(x_{i-1},t_n)}{2\Delta x} - RC(x_i,t_n) \quad 53$$

Applying first-order space approximation results to

$$\frac{C_i^{n+1} - C_i^{n}}{\Delta t} = \frac{D_x}{2}\left(\frac{C_{i+1}{}^{n+1} - 2C_i^{n+1} + C_{i-1}{}^{n+1}}{\Delta x^2} + \frac{C_{i+1}{}^{n} - 2C_i^{n} + C_{i-1}{}^{n}}{\Delta x^2}\right) - v\frac{C_{i+1}{}^{n} - C_{i-1}{}^{n}}{2\Delta x} - RC_i^{n} \quad 54$$

Thus, using the same process will result in the final equation being.

$$C_i^{n+1}\left\{1 + \frac{D_x\Delta t}{\Delta x^2}\right\} = C_i^{n}\left(1 - \frac{D_x\Delta t}{\Delta x^2} - R\right) + C_{i+1}{}^{n+1}\left(\frac{D_x\Delta t}{2\Delta x^2}\right) + C_i^{n+1}\left(\frac{D_x\Delta t}{2\Delta x^2} - \frac{v}{2\Delta x}\right) + C_{i-1}{}^{n}\left(\frac{D_x\Delta t}{2\Delta x^2} + \frac{v}{2\Delta x}\right) \quad 55$$

6.4 Von Neumann Stability Analysis

The Hungarian scientist and creator of the electronic computer John von Neumann created the stability analysis technique known as von Neumann stability analysis in the middle of the 20th century (Matlabgeeks, 2006). The von Neumann stability analysis is a method for evaluating the stability of finite difference schemes and is only applicable to linear finite difference schemes with constant coefficients (Eugene & Herbert, 1994). It is grounded on the breakdown of numerical errors of numerical approximations into Fourier series. Joseph Fourier was the first person to use a Fourier series, which is an expansion of a periodic function into a collection of trigonometric functions, to obtain answers to the heat equation.

Numerical analysis evaluates computation errors when applied to approximation equations or algorithms especially when used in infinitely digits to represent real numbers (Ralston & Rabinowitz, 2012). Truncation errors and round-off errors are both types of computation errors, often known as numerical errors. Real trigonometric functions are far more difficult to work with than complex exponentials therefore we have chosen complex exponentials to represent the errors. There are three key characteristics of a numerical scheme:

1. Consistency- this refers to the accuracy with which the partial difference equation is approximated by the finite difference equation as the range and time step sizes approach zero.
2. Stability - a numerical approach is said to be stable if mistakes from any source do not increase uncontrollably with time.
3. Convergence - as the grid interval and time step size are both decreased, the solution to a finite difference equation gets closer to the actual solution of the partial difference equation.

The numerical approach of the truncation error resolves an issue that is not a perfect match to the one we are attempting to solve. The one-dimensional equation below will represent the Crank-Nicolson approach and will show the von Neumann analysis to simplify and better explain how we will arrive at the stability analysis.

Let

$$\frac{\partial u}{\partial t} = \alpha \frac{\partial^2 u}{\partial x^2} \qquad 56$$

The forward time-centered space (FTCS) is applied to solve the equation, to give.

$$\frac{u_j^{n+1} - u_j^n}{\Delta t} = \alpha \frac{u_{j+1}^n - 2u_j^n + u_{j-1}^n}{\Delta x^2} \qquad 57$$

Let

$$r = \alpha \frac{\Delta t}{\Delta x^2}$$

The equation can be discretised as the following and the solution of the discrete equation approximates the analytical solution of the PDE on the grid.

$$u_j^{n+1} = u_j^n + r\left(u_{j+1}^n - 2u_j^n + u_{j-1}^n\right) \qquad 58$$

where r is the mesh ratio, j is the space index, and n is the time index.

Define the numerical approximation error as

$$\epsilon_j^n = N_j^n - u_j^n \tag{59}$$

Where N_j^n represents the numerical result derived using finite precision arithmetic and u_j^n represents the discretized equation solution if there were no round-off errors.

According to (Anderson, 1994), the error ϵ_j^n must fulfil the discretized equation because the precise solution u_j^n is required to precisely satisfy it. Therefore, we must assume that N_j^n also satisfies the equation to show the relationship of frequency for the error.

$$\epsilon_j^{n+1} = \epsilon_j^n + r\left(\epsilon_{j+1}^n - 2\epsilon_j^n + \epsilon_{j-1}^n\right) \tag{60}$$

The spatial changes of error for linear differential equations with periodic boundary conditions in a finite Fourier series can be described under the assumption of error amplitude E_m being time dependence and function of time as x falls inside the range L.

Let

$$M = \frac{L}{\Delta x}$$

and,

$$k_m = \frac{\pi m}{L}\ with\ m = -M, \dots, -2, -1, 0, 1, 1, \dots, M$$

The linear differential equation with periodic boundary conditions in a finite Fourier series is as follows.

$$\epsilon(x,t) = \sum_{m=-M}^{M} E_m(t) e^{ik_m x} \tag{61}$$

If the boundary condition is not periodic in a finite Fourier series, we apply the integral concerning x to obtain.

$$\epsilon(x,t) = \int_{k=-\frac{\pi}{\Delta x}}^{k=\frac{\pi}{\Delta x}} E_k(t) e^{ikx} dk \tag{62}$$

Given that the behaviour of every term in the series is like that of the series itself and that the difference equation of error is linear, the growth of error can be explained using two cases.

i. When a Fourier series is used

$$\epsilon_m(x,t) = E_m(t) e^{ik_m x} \tag{63}$$

ii. When a Fourier integral is used

$$\epsilon_k(x,t) = E_k(t)e^{ikx}dk \qquad 64$$

Replace $\epsilon_m(x,t)$ into the equation of ϵ_j^{n+1}, to determine how error varies over time.

$$\epsilon_j{}^n = E_m(t)e^{ik_m x}$$
$$\epsilon_j{}^{n+1} = E_m(t+\Delta t)e^{ik_m x}$$
$$\epsilon_{j+1}{}^n = E_m(t)e^{ik_m(x+\Delta x)}$$
$$\epsilon_{j-1}{}^n = E_m(t)e^{ik_m(x-\Delta x)}$$
$$\epsilon_{j+1}{}^{n+1} = E_m(t+\Delta t)e^{ik_m(x+\Delta x)}$$
$$\epsilon_{j-1}{}^{n+1} = E_m(t+\Delta t)e^{ik_m(x-\Delta x)}$$

6.4.1 Crank-Nicolson Method

Under the condition that the acquired numerical scheme is stable within the scope of the Von Neumann stability analysis, the Crank Nicolson discretization of the numerical solution will be determined. Both the discretization results from equation 46 and 55 will be subject to investigation. The analysis of Equation *52* is as follows:

$$C_i^{n+1}\left\{1+\frac{D_x\Delta t}{\Delta x^2}\right\} = C_i{}^n\left(1-\frac{D_x\Delta t}{\Delta x^2}\right) + C_{i+1}^{n+1}\left(\frac{D_x\Delta t}{2\Delta x^2}\right) + C_i^{n+1}\left(\frac{D_x\Delta t}{2\Delta x^2}-\frac{v}{2\Delta x}\right) + C_{i-1}^{n}\left(\frac{D_x\Delta t}{2\Delta x^2}+\frac{v}{2\Delta x}\right)$$

65

From the definition of ϵ_j^{n+1}, substitute the error equations into Crank Nicolson. Thus, we obtain.

$$E_m(t+\Delta t)e^{ik_m x}\left\{1+\frac{D_x\Delta t}{\Delta x^2}\right\} = E_m(t)e^{ik_m x}\left(1-\frac{D_x\Delta t}{\Delta x^2}\right) + \frac{D_x\Delta t}{2\Delta x^2}E_m(t+\Delta t)e^{ik_m(x+\Delta x)} + \left(\frac{D_x\Delta t}{2\Delta x^2}-\frac{v}{2\Delta x}\right)E_m(t)e^{ik_m(x+\Delta x)} + \left(\frac{D_x\Delta t}{2\Delta x^2}+\frac{v\Delta t}{2\Delta x}\right)E_m(t)e^{ik_m(x-\Delta x)} \qquad 66$$

Since we have a common factor, we will apply the product rule.

$$E_m(t+\Delta t)e^{ik_m x}\left\{1+\frac{D_x\Delta t}{\Delta x^2}\right\} = E_m(t)e^{ik_m x}\left(1-\frac{D_x\Delta t}{\Delta x^2}\right) + \frac{D_x\Delta t}{2\Delta x^2}E_m(t+\Delta t)e^{ik_m x}.e^{ik_m\Delta x} + \left(\frac{D_x\Delta t}{2\Delta x^2}-\frac{v}{2\Delta x}\right)E_m(t)e^{ik_m x}.e^{ik_m\Delta x} + \left(\frac{D_x\Delta t}{2\Delta x^2}+\frac{v\Delta t}{2\Delta x}\right)E_m(t)e^{ik_m x}e^{-ik_m\Delta x} \qquad 67$$

Remove the common factor $e^{ik_m x}$ and collect like terms.

$$E_m(t+\Delta t)\left\{1+\frac{D_x\Delta t}{\Delta x^2}\right\} - \frac{D_x\Delta t}{2\Delta x^2}E_m(t+\Delta t)e^{ik_m\Delta x} = E_m(t)\left(1-\frac{D_x\Delta t}{\Delta x^2}\right) + \left(\frac{D_x\Delta t}{2\Delta x^2}-\frac{v}{2\Delta x}\right)E_m(t)e^{ik_m\Delta x} + \left(\frac{D_x\Delta t}{2\Delta x^2}+\frac{v\Delta t}{2\Delta x}\right)E_m(t)e^{-ik_m\Delta x} \qquad 68$$

Simplify the above equation we obtain.

$$E_m(t+\Delta t)\left\{\left(1+\frac{D_x\Delta t}{\Delta x^2}\right)-\left(\frac{D_x\Delta t}{2\Delta x^2}e^{ik_m\Delta x}\right)\right\}=E_m(t)\left\{\left(1-\frac{D_x\Delta t}{\Delta x^2}\right)+\left(\frac{D_x\Delta t}{2\Delta x^2}-\frac{v}{2\Delta x}\right)e^{ik_m\Delta x}+\left(\frac{D_x\Delta t}{2\Delta x^2}+\frac{v\Delta t}{2\Delta x}\right)e^{-ik_m\Delta x}\right\} \quad 69$$

Divide both sides by $\mathrm{E_m(t)}$

$$\frac{E_m(t+\Delta t)}{E_m(t)}=\frac{\left(1-\frac{D_x\Delta t}{\Delta x^2}\right)+\left(\frac{D_x\Delta t}{2\Delta x^2}-\frac{v}{2\Delta x}\right)e^{ik_m\Delta x}+\left(\frac{D_x\Delta t}{2\Delta x^2}+\frac{v\Delta t}{2\Delta x}\right)e^{-ik_m\Delta x}}{\left(1+\frac{D_x\Delta t}{\Delta x^2}\right)-\left(\frac{D_x\Delta t}{2\Delta x^2}e^{ik_m\Delta x}\right)} \quad 70$$

Considering the equation above, let

$$A_1=\frac{D_x\Delta t}{2\Delta x^2}-\frac{v}{2\Delta x}$$
$$A_2=\frac{D_x\Delta t}{2\Delta x^2}+\frac{v\Delta t}{2\Delta x}$$
$$A_3=\frac{D_x\Delta t}{2\Delta x^2}$$

Rewrite the equation.

$$\frac{E_m(t+\Delta t)}{E_m(t)}=\frac{\left(1-\frac{D_x\Delta t}{\Delta x^2}\right)+A_1e^{ik_m\Delta x}+A_2e^{-ik_m\Delta x}}{\left(1+\frac{D_x\Delta t}{\Delta x^2}\right)-\left(A_3e^{ik_m\Delta x}\right)}$$

71

Using Euler's formula $e^{ix}=\cos x+\mathrm{i}\sin x$, define the trigonometry identities as

$$\cos\theta+\mathrm{i}\sin\theta=e^{i\theta}$$
$$\cos\theta-\mathrm{i}\sin\theta=e^{-i\theta}$$

Thereafter, substitute the identities in *71*

$$\frac{E_m(t+\Delta t)}{E_m(t)}=\frac{\left(1-\frac{D_x\Delta t}{\Delta x^2}\right)+A_1(cos(k_m\Delta x)+i\,sin(k_m\Delta x))+A_2(cos(-k_m\Delta x)+i\,sin(-k_m\Delta x))}{\left(1+\frac{D_x\Delta t}{\Delta x^2}\right)-\left(A_3(cos(k_m\Delta x)+i\,sin(k_m\Delta x))\right)}$$

$$\frac{E_m(t+\Delta t)}{E_m(t)}=\frac{\left(1-\frac{D_x\Delta t}{\Delta x^2}\right)+(A_1+A_2)\,cos(k_m\Delta x)+i(A_1-A_2)\,sin(-k_m\Delta x)}{\left(1+\frac{D_x\Delta t}{\Delta x^2}\right)-\left(A_3(cos(ik_m\Delta x)+i\,sin(ik_m\Delta x))\right)} \quad 72$$

The notation displayed below can be used to simplify the above equation.

$$\left(1-\frac{D_x\Delta t}{\Delta x^2}-R\right)+(A_1+A_2)\,cos(k_m\Delta x)=a_1$$

$$i(A_1-A_2)\,sin(-k_m\Delta x)=b_1$$

$$\left(1+\frac{D_x\Delta t}{\Delta x^2}\right)-(A_3\,cos(k_m\Delta x))=a_2$$

$$A_3 i\,sin(-k_m\Delta x)=b_2$$

The exaggeration factor G is given as

$$\frac{E_m(t+\Delta t)}{E_m(t)}$$

To obtain the stability of the equation, let

$$\frac{E_m(t+\Delta t)}{E_m(t)}=\frac{a_1+ib_1}{a_2+ib_2} \tag{73}$$

Crank Nicolson method will be considered to be stable when.

$$\left|\frac{E_m(t+\Delta t)}{E_m(t)}\right|<1$$

And

$$\left|\frac{a_1+ib_1}{a_2+ib_2}\right|<1$$

Substituting back into the stability equation, the advection-dispersion without retardation analysed using Crank Nicolson method will only be stable if.

$$\left|\frac{\left(1-\frac{D_x\Delta t}{\Delta x^2}\right)+\left(\frac{D_x\Delta t}{2\Delta x^2}-\frac{v}{2\Delta x}+\frac{D_x\Delta t}{2\Delta x^2}+\frac{v\Delta t}{2\Delta x}\right)cos(k_m\Delta x)+i\left(\left(\frac{D_x\Delta t}{2\Delta x^2}-\frac{v}{2\Delta x}\right)-\left(\frac{D_x\Delta t}{2\Delta x^2}+\frac{v\Delta t}{2\Delta x}\right)\right)sin(-k_m\Delta x)}{\left(1+\frac{D_x\Delta t}{\Delta x^2}\right)-\left(\frac{D_x\Delta t}{2\Delta x^2}cos(k_m\Delta x)\right)+i\,sin(k_m\Delta x)}\right|<1 \tag{74}$$

$$|a_1+ib_1|<|a_2+ib_2|$$

We shall recall that.

$$|a+ib|=\sqrt{a^2+b^2} \tag{75}$$

The above can be used to obtain the condition for 74.

6.5 Numerical simulations and prediction

In this chapter, we will use the Mittag-Leffler mathematical model to demonstrate how the decay process works. The mathematical model of Mittag-Leffler considers systems that exhibit nonlocal behaviour. It can predict where crossover will happen, assess the mass during the decay process at an early stage, and demonstrate the skeleton's extremely slow deterioration. We will use the mass we obtained from the previous section Chapter 3**: Groundwater contamination in cemeteries** to achieve this.

The decay process with a classical differential operator is described by a well-known mathematical equation as follows:

$$\begin{cases} m'(t) = -\lambda m(t) \\ m(t_0) = m_0 \end{cases} \quad 76$$

And the precise solution to the equation, where λ is the decay rate, is

$$m(t) = m(0)\, exp(-\lambda t) \quad 77$$

Below is the precise solution to the decay equation using the classical derivative, where $m\,(0)$ =1 and $\lambda = 2$.

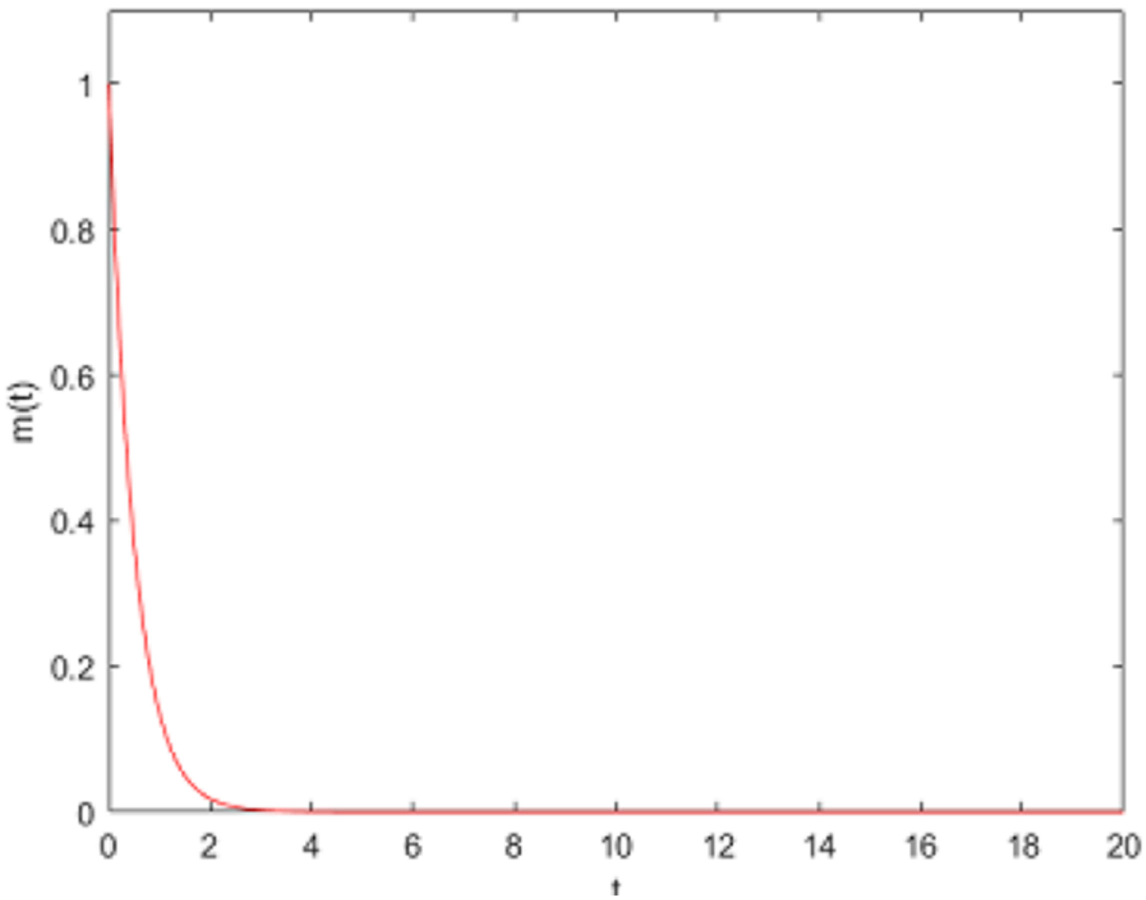

Figure 26: The exact solution of decay solution using classic derivative extracted from *(Igret Araz & Atangana, 2022)*.

The outcome above demonstrates the homogeneity of the decay process. The flesh and blood degrade more quickly than the skeleton when we examine the anatomy of a human body, which goes against the conclusions drawn from using classical derivative. To find the exact equation, we shall therefore replace the classical derivative with the power law-based derivative.

Given:

$$ {}_0^C D_t^\alpha \, m(t) = -\lambda m(t) \tag{78} $$

By definition:

$$ {}_0^C D_t^\alpha \, m(t) = \frac{1}{\Gamma(1-\alpha)} \int_0^t m'(t)(t-\tau)^{-\alpha} d\tau \tag{79} $$

Which can be reformatted as:

$$ {}_0^C D_t^\alpha \, m(t) = m'(t) * \frac{t^{-\alpha}}{\Gamma(1-\alpha)} \tag{80} $$

Where " $*$ " is the convolution operator and described as:

$$ v * u = \int_0^t v(\tau)u(t-\tau)d\tau \tag{81} $$

$$ \mathcal{L}(v * u) = \mathcal{L}(v)\mathcal{L}(u) \tag{82} $$

Applying the equation

$$ \mathcal{L}\left({}_0^C D_t^\alpha m(t)\right) = \mathcal{L}\left(m'(t)\right) * \mathcal{L}\left(\frac{t^{-\alpha}}{\Gamma(1-\alpha)}\right) $$

$$ \mathcal{L}\left(f(t)\right) = \int_0^\infty e^{-st} f(t)dt \tag{83} $$

Where

$$ \mathcal{L}\left(m'(t)\right) = sM(s) - m(0) \tag{84} $$

$$ \mathcal{L}\left(\frac{t^{-\alpha}}{\Gamma(1-\alpha)}\right) = s^{\alpha-1} $$

$$ \mathcal{L}\left({}_0^C D_t^\alpha m(t)\right) = \left(sM(s) - m(0)\right)s^{\alpha-1} $$

$$ = \left(s^\alpha M(s) - m(0)\right)s^{\alpha-1} \tag{85} $$

We will apply the Laplace equation on both sides to obtain.

$$ s^\alpha M(s) - s^{\alpha-1}m(0) = -\lambda M(s) $$

$$ M(s)(s^\alpha + \lambda) = s^{\alpha-1}m(0) $$

$$ M(s) = \frac{s^{\alpha-1}m(0)}{s^\alpha + \lambda} \tag{86} $$

Applying the inverse Laplace transform

$$\mathcal{L}^{-1}(M(s)) = m(t) = m(0)\mathcal{L}^{-1}\left(\frac{s^{\alpha-1}}{s^{\alpha}+1}\right)$$

$$= m(0)\, E_{\alpha}(-\lambda t^{\alpha}) \quad 87$$

Therefore, the final solution of the decay equation by replacing the classical derivative with the power law-based derivative is given by

$$m(t) = m(0)\, E_{\alpha}(-\lambda t^{\alpha}) \quad 88$$

We shall present below some graphical representation of the above solution and compare it with the decay of a dead body. Here we considered $m(0) = 1$ and performed the simulations for different values of fractional orders.

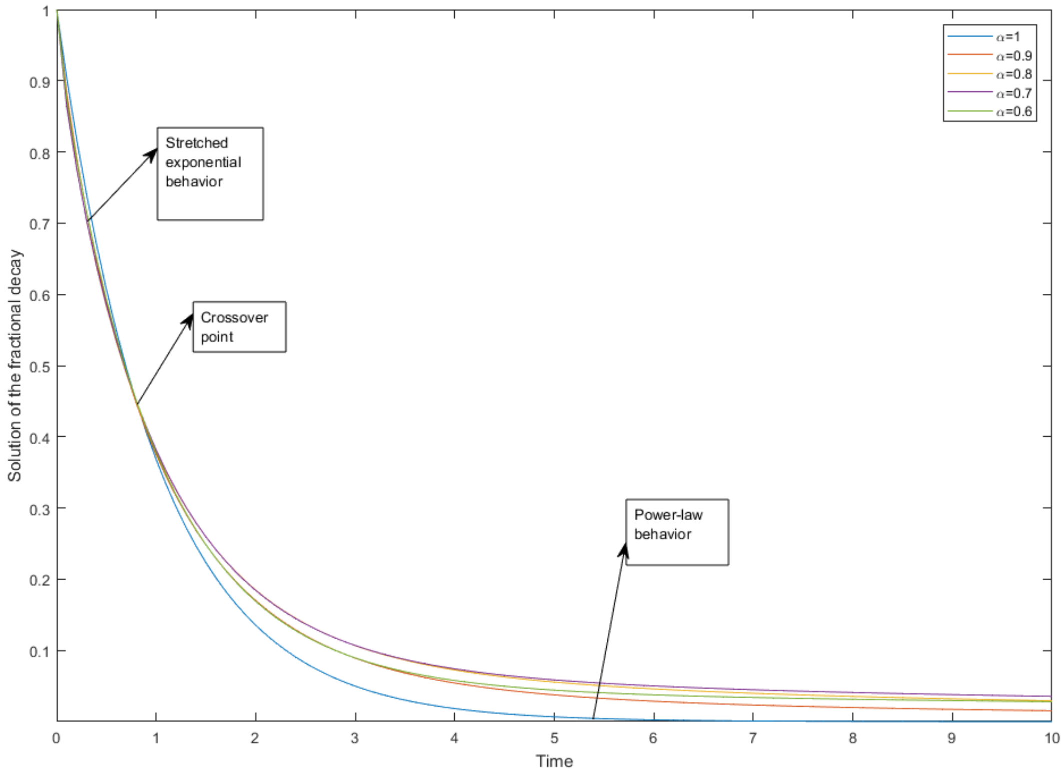

Figure 27: Numerical solution of the fractional decay equation for different fractional order

The above figure shows that for a fractional order, there is a crossover behaviour from stretched exponential to power law. Thus, the decomposition of the flesh, blood, and water from the dead body can be compared to the stretched exponential behaviour, and the decomposition of the bones, which can take years, can be compared to the power law behaviour. One can therefore draw the conclusion that the Mittag-Leffler function derived here as the solution of the fractional decay model replicates the decay of the death body more accurately than the exponential function which is the solution of the classical decay model. According to our study, by selecting a specific initial condition or initial mass, such as $m(0)$, one may determine the mass that goes underground by evaluating the mass at the transition point (t_{st}), where the graph exhibits a long tail behaviour. This point is the end of the advanced decay that was described in chapter 3. In conclusion, the mass $m(0) - m(t_{st})$ represents the whole mass that went into the geological formation. The mass $m(0) - m(t_{st})$ will be converted into a concentration as a function of time and space and utilized as the initial concentration for the advection-dispersion equation. We shall present first graphical representation of the advection dispersion about. To do this, we will consider the following theoretical parameters: We first start with the following, T =4000*24 which is the total time per hour. The dispersion coefficient D=($1E^{-6}$)*3600 with unit m^2/h, the velocity V=(1E^-7)*3600 m/hr, the total length considered here is L=100 m, we chose the partial grid to be N=20, a temporal grid M=40 m, spatial spacing $\Delta t = T/M$ and $\Delta x = L/N$ our initial concentration is C=100. The numerical simulations are presented in Figure 28, Figure 29,Figure *30*, Figure 31, andFigure *32* below:

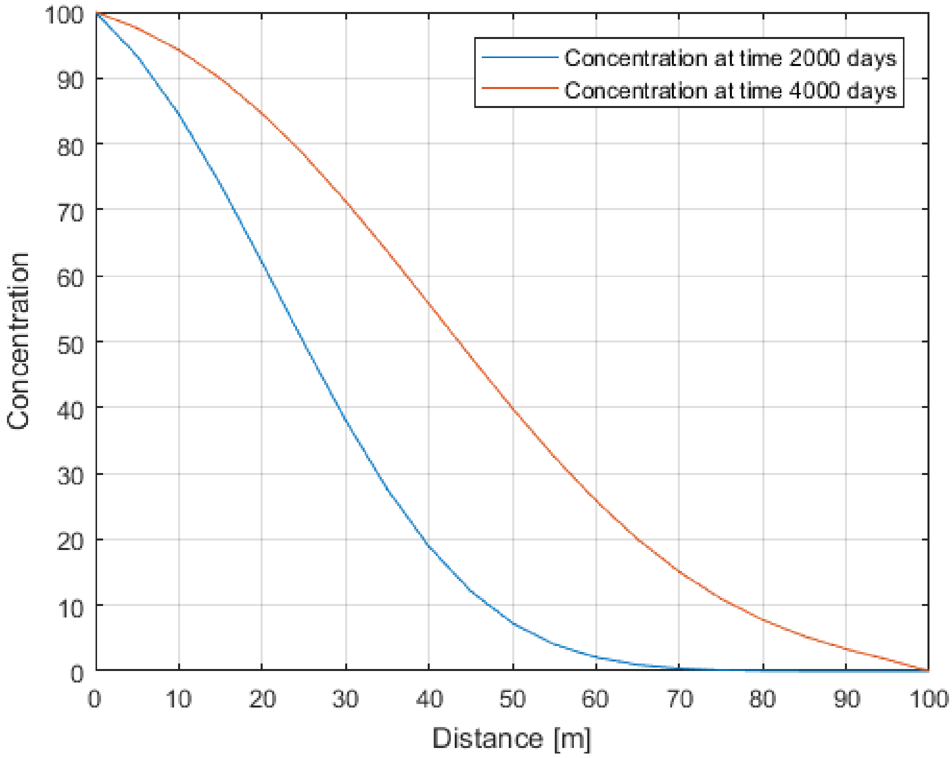

Figure 28: Numerical simulation of concentration against distance.

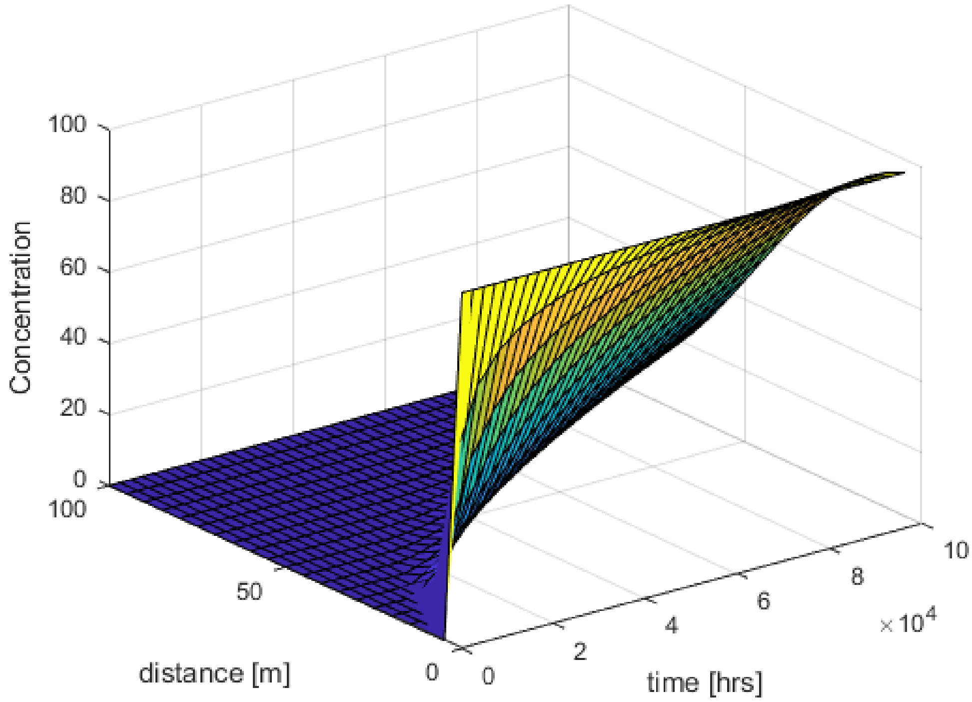

Figure 29: Numerical simulation of concentration as function of space and time.

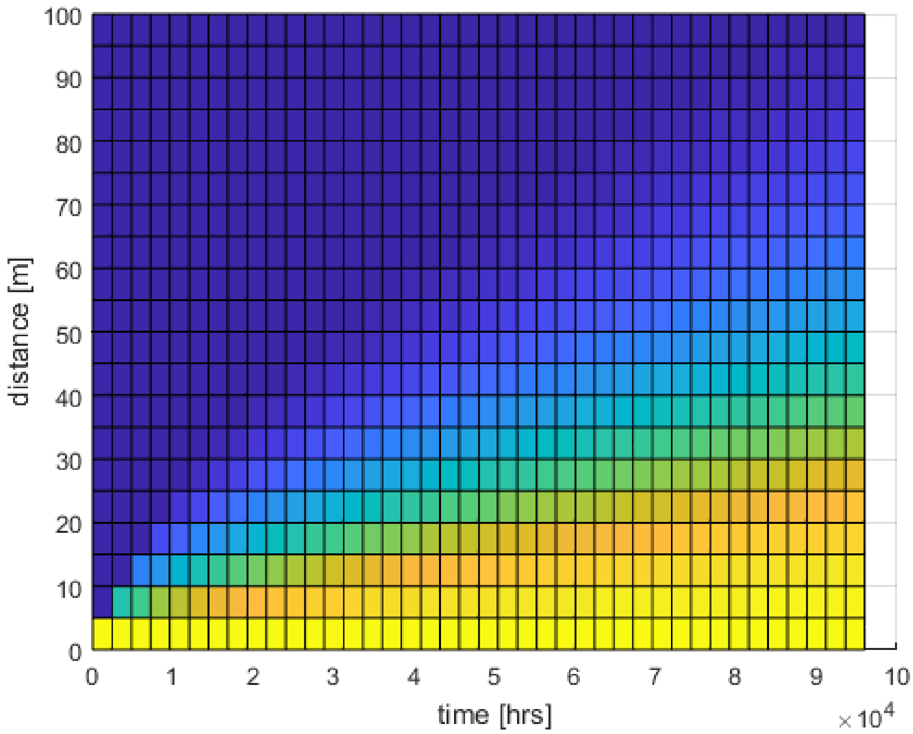

Figure 30: Contour-plot representation of the concentration.

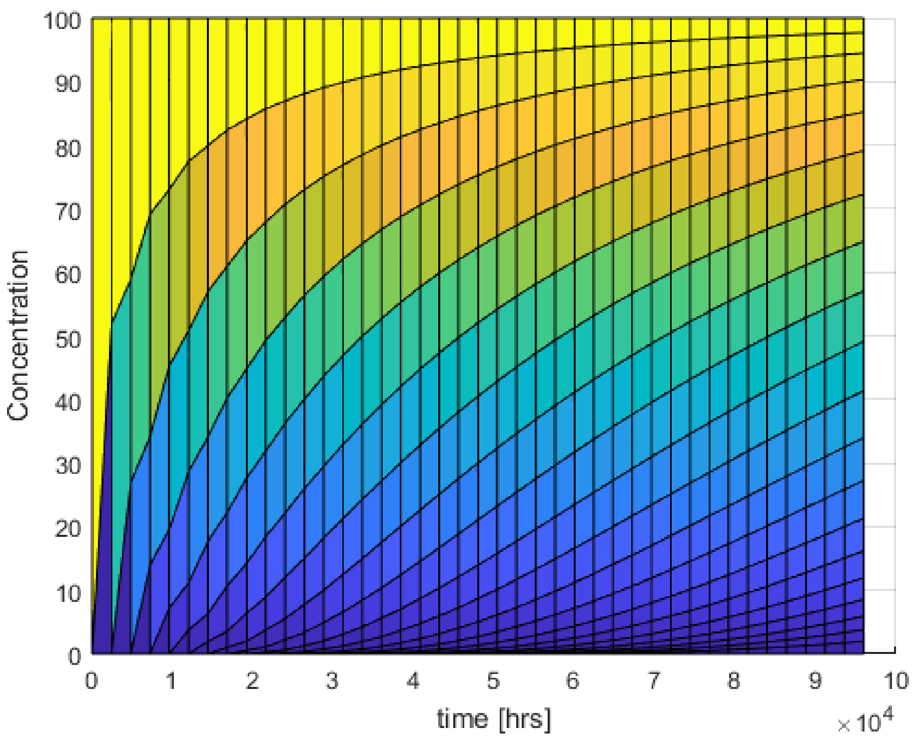

Figure 31: Simulation of concentration over time.

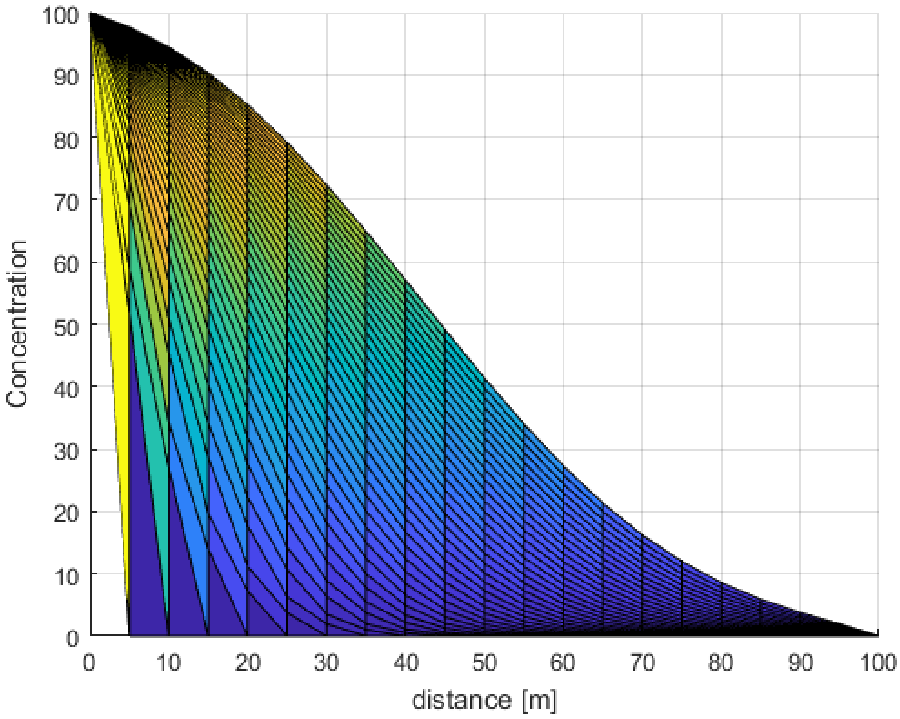

Figure 32: Numerical simulation of concentration over distance.

The above numerical solutions are for the advection-dispersion equation without retardation factor. It is assumed that the geological formation where the transport takes place is homogeneous. We shall now present numerical simulations for an advection dispersion equation with a retardation factor. To do this we consider the retardation function to be $R(x,t) = RC(x,t)$ with R as the retardation constant. We retain the same theoretical parameters but chose R to be 0.05, obtained numerical simulations are depicted in Figure Figure 33, **Error! Reference source not found.**,Figure *35*, Figure *36*Figure 37.

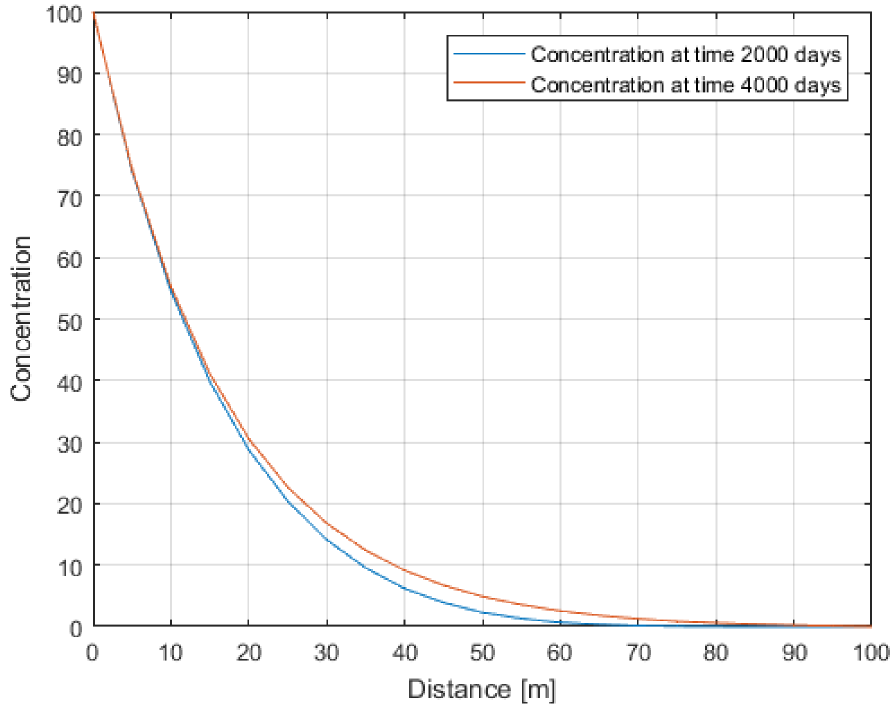

Figure 33: Numerical simulation of concentration against distance.

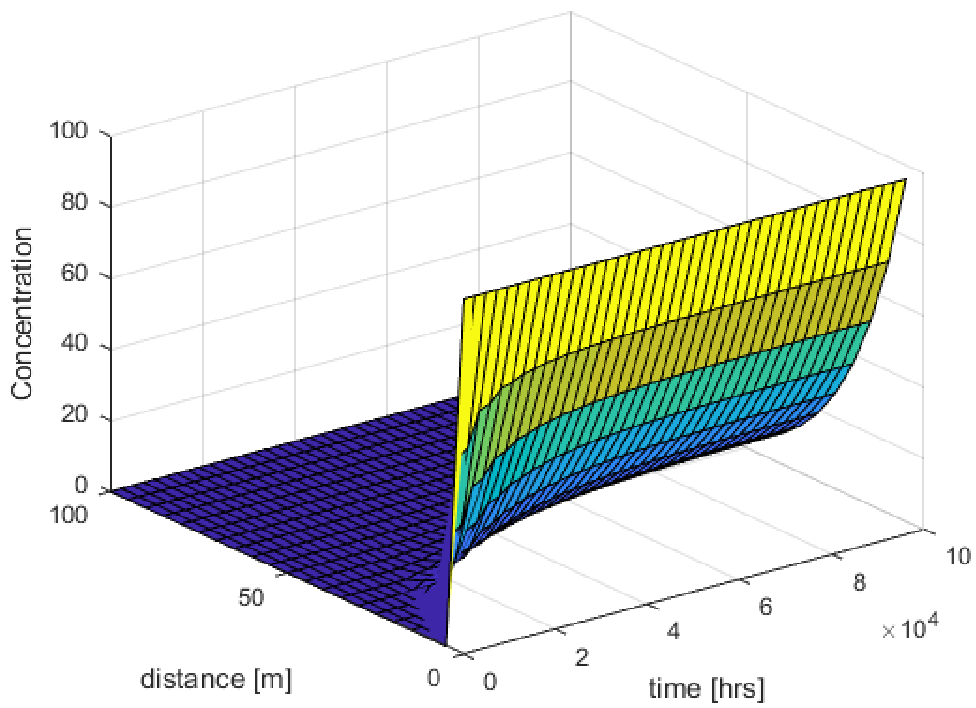

Figure 34: Numerical simulation of concentration as a function of space and time.

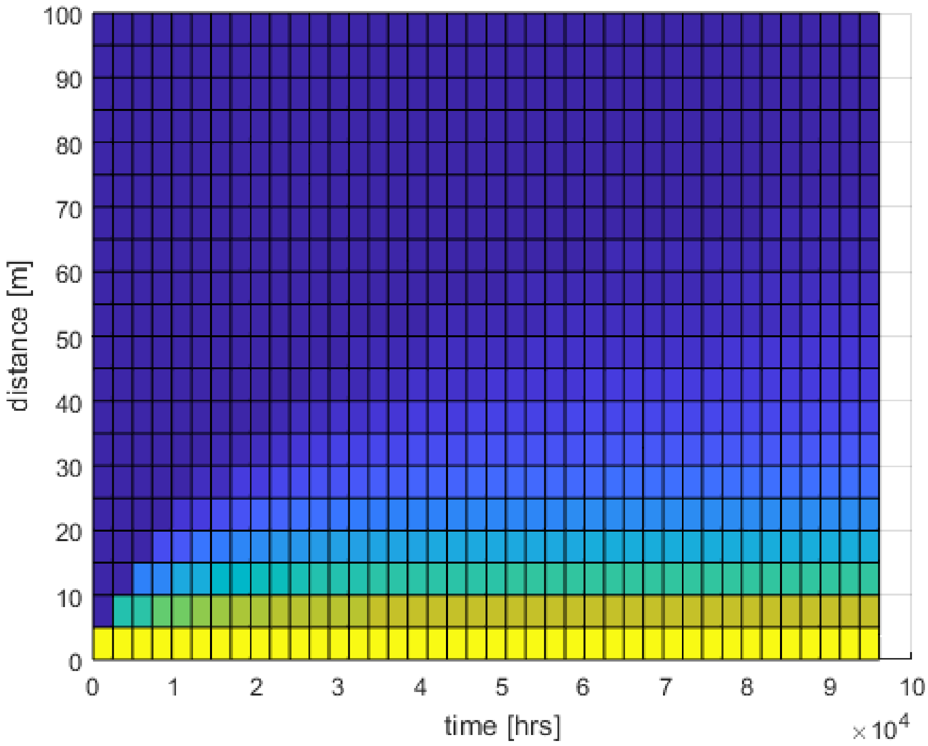

Figure 35: Plot displaying simulation of distance over time.

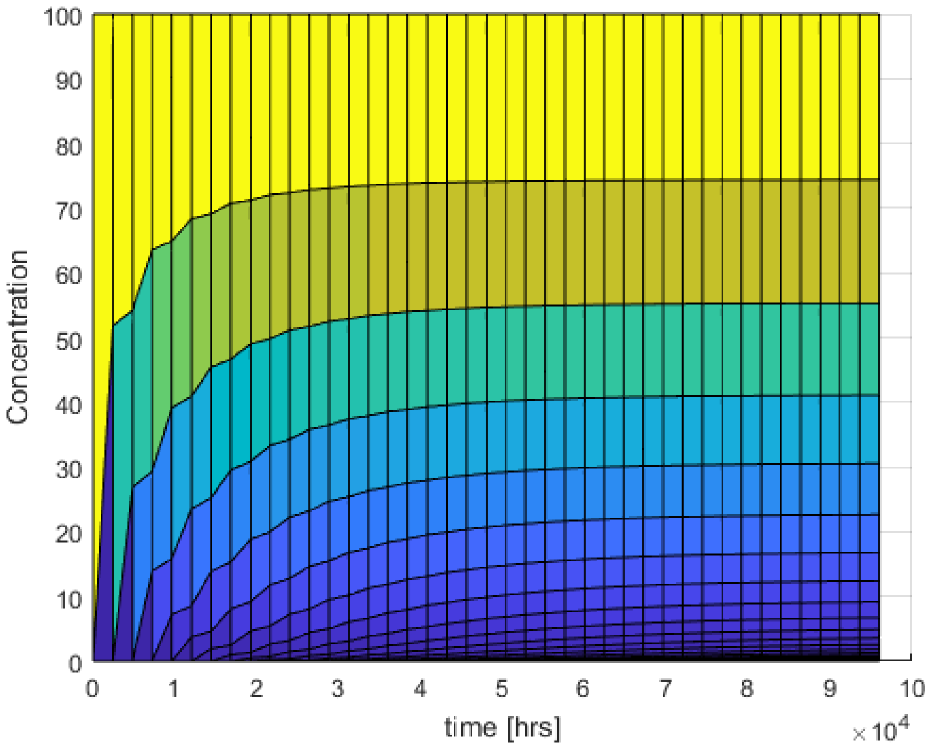

Figure 36: Simulation of concentration over time.

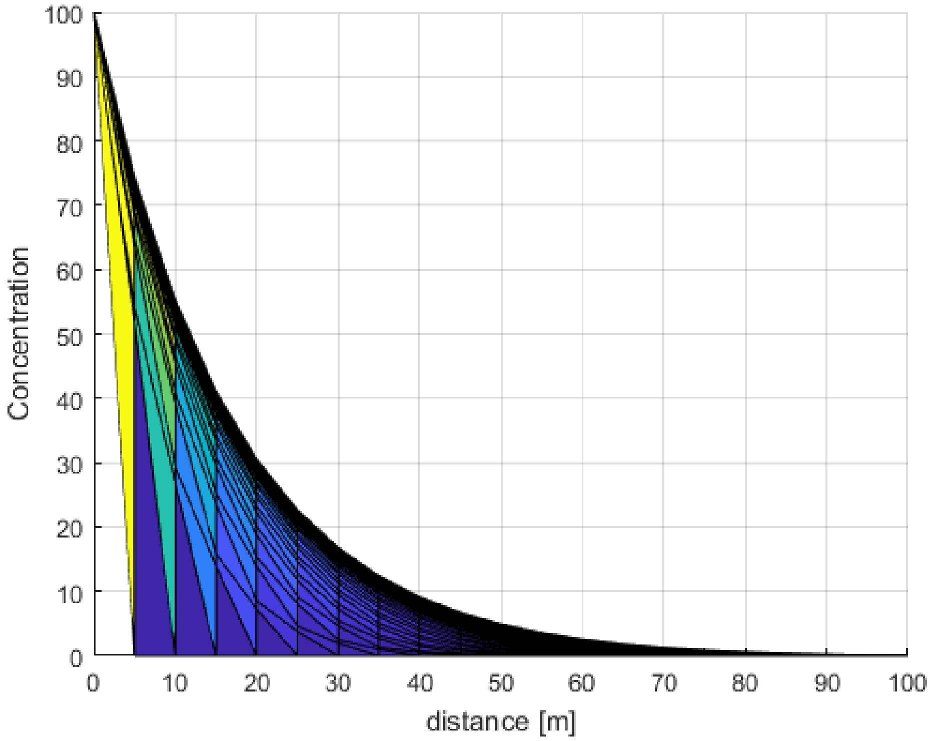

Figure 37: Numerical simulation of concentration versus distance.

Chapter 7: Discussion, Recommendation and Conclusion

7.1 Discussion

Leachate, a liquid containing microorganisms produced by the decomposition of human remains, contaminates the environment and groundwater, causing infectious illnesses and harmful chemicals to spread. Due to the rise of infectious diseases like COVID 19, the years 2020–2022, in Johannesburg, had the largest number of burials over a five-year period. Between March 1st, 2018 and February 28th, 2023, 88440 people were laid to rest in graves. The West Park Cemetery had a 25% burial rate, whereas the Olifantsvlei Cemetery had a 38% burial rate. Rapid urbanization and the growing population in cities have increased demand for burial space, resulting in overcrowded cemeteries and a shortage of room for burials. The majority of these cemeteries are situated close to residences, water sources, and educational institutions. According to the Johannesburg cemeteries manager, there is a need for alternatives because the cemeteries are overcrowded and under pressure.

7.1.1 Water quality

Groundwater levels at West Park Cemetery are inspected three times a year as of 2020. There are three monitoring boreholes; boreholes WES2 and WES3 are dry at depths of 10.77 meters and 27 meters, respectively, while well WES1 contained minimal water at a depth of 9.2 meters. There was some turbidity in borehole WES 1. The dry boreholes may be a result of the boreholes shallow depth, which prevents them from crossing any cracks or water-bearing rocks, or it may be because West Park is in a location with rock formations where precipitation slowly recharges the aquifer. According to estimates, the aquifer yields in the vicinity of West Park Cemetery range between 0.1 and 0.5 l/s, which are poor to minor (SRK, et al., 2013).

7.1.2 Groundwater quality

(Breedt, 2022) conducted a groundwater quality examination to find any contaminants coming from the cemeteries, and the results revealed that manganese (Mn) was the only component that was found to be above the Leachable Concentration Threshold Limits and SANS 241:2015 Drinking Water Standards. There was no evidence of contamination originating from the cemetery; this may be due to the local geology, where the leachate disperses or becomes trapped. The boreholes may have been built in an area without any interconnections to allow pollution emanating from the graves to enter the boreholes.

7.1.3 Groundwater transport

The advection-dispersion equation was used to analyse the leachate of the corpse degradation emanating from the burial sites. Due to the lack of precise geology and lithology in the area, two scenarios—the advection-dispersion equation with retardation and the advection-dispersion equation without retardation—were used to analyse the transport of contaminants. By using Crank-Nicolson approach, which is the most stable method, we were able to determine the numerical solution to the advection-dispersion problem. Later, we used von Neumann Stability analysis to show the equation's stability. When the following inequality $|a_1 + ib_1| < |a_2 + ib_2|$ was obtained, it was discovered that the advection-dispersion equation was stable.

The fractional decay model was used to show how the degradation process operates before calculating the contamination distribution. We were able to draw the conclusion that classical derivatives cannot give us the precise answer to the decay problem since it shows that the human body entirely degrades rapidly, including the skeleton, which takes time to dissolve. Later, we substituted the classical derivatives for power law-based derivatives, which resulted in a fractional decay model solution that replicates the decay of the dead body with greater accuracy than the exponential classical decay model solution. The advection-dispersion equation used the mass as the initial concentration. According to the graphs, the pollutant plume moved from highly concentrated to less concentrated places. Despite geological heterogeneities, the contamination from the graves dissipates over time.

7.2 Recommendation

The biggest challenge facing the cemetery sector in South Africa is the availability of land, insufficient budget for cemeteries, high rates of traditional and community resistance to alternative forms of burials. Cemeteries are also located on unsuitable land and in some municipalities cemeteries are located near water resources and non-adherence to burial standards regarding grave depths. The following recommendations are made:

1. Eliminate the stigma attached to cremation. Cemeteries need to promote cremation as a substitute option and use crematories powered by renewable energy sources.
2. Headstones should be used instead of tombstones since they take up less space. Compared to traditional memorialization, headstones have less influence on the environment and may use less area.

3. Aquamation implementation.
4. It is important to undertake a hydrogeological survey and keep records
5. New boreholes should be drilled in West Park Cemetery, and monthly monitoring should be carried out.
6. To avoid digging dry boreholes, it is strongly advised to do a geophysical research before selecting a drilling site.

7.3 Conclusion

The study investigated a more precise groundwater flow and transport model which could forecast unusual behaviours in the flow and movement of pollution from cemeteries. We performed numerical analysis on the well-known advection-dispersion equation.

The purpose of this study is to get a detailed understanding of how cemeteries affect groundwater and the movement of human remains underground. Cemetery pollution results in the spread of illness and dangerous chemicals. Water percolates through cemeteries carrying human remains, and the variety of the hydrogeology and geology found at various cemetery sites affects the movement of these dissolved elements into the environment. Human decomposition produces a saline contamination plume that moves beneath the graves in the direction of the hydraulic gradient. The risks to the environment are increased by the use of chemicals like formaldehyde during funeral preparations. The water found in West Pack Cemetery fall within acceptable limits of SANS 241-1:2015 standard, however, further analyses should be conducted. It is not advisable to drink the water directly from the boreholes, appropriate treatment should be conducted.

The Mittag-Leffler function, a solution of the fractional decay model, as opposed to the classic decay model with a solution exponential function, is a more precise representation of the fraction decay that reflects the breakdown of the human body. The three stages of the fractional decay solution are stretched exponential behavior, crossover point, and power-law behavior. In MATLAB, the advection-dispersion was used to illustrate the spread of the human remains, and the stability and accuracy of the equation were obtained. In relation to the decay rate, we found that the dispersion coefficient and velocity are quite sensitive.

References

Abiye, T. A., Mengistu, H. & Demlie, M. B., 2011. Groundwater Resource in the Crystalline Rocks of the Johannesburg Area, South Africa. *Journal of Water Resource and Protection,* Volume 3, pp. 199-212 .

Abiye, T., Masindi, K., Mengistu, H. & Demlie, M., 2018. Understanding the groundwater-level fluctuations for better management of groundwater resource: A case in the Johannesburg region. *Groundwater for Sustainable Development,* Volume 7, pp. 1-7.

Abubakr, K., 2012. The evaluation and determination of infiltration Models. *Australan Journal of Basic and Applied Sciences,* 6(6), pp. 94-98.

Adelaide Cemeteries Authority, 2021. *A Comparison of GHG Emissions due to Burials and Cremations,* Adelaide: Adelaide Cemeteries Authority Board.

Adindu, R. U., Igbokwe, K. K. & Dike, I. I., 2015. Philip Model Capability to Estimate Infiltration for Soils of Aba, Abia State. *Journal of Earth SSciences and Geotechnical Engineering,* 5(2), pp. 63-68.

Akhtar, N., Ishak, M. I. S., Bhawani, S. A. & Umar, K., 2021. Various Natural and Anthropogenic Factors Responsible for Water Quality Degradation: A Review. *Water,* 13(19), p. 35.

Alley, W. M., Healy, R. W., LaBaugh, J. W. & Reilly, T. E., 2002. Flow and Storage in Groundwater Systems. *Science,* 296(1985).

Amuno, S. A. & Amuno, M. M., 2014. Spatio-temporal variation of trace element contents in Rwanda necrosols. *Environmental Earth Science,* Volume 71, pp. 659-674.

Anderson, J. D. J., 1994. *Computational Fluid Dynamics: The Basics with Applications.* s.l.:McGraw Hill.

Borstel, C. L. N. C., 2000. *Testing Procedure for Historic Cemeteries,* Lexington, KY, USA: Cultural Resource Analysts, inc.

Bosma, W. J. P., van der Zee, S. E. A. T. M. & van Dujin, C. J., 1996. Plume development of a nonlinearly sorbing solute in heterogeneous formations. *Water Resources Research,* 32(6), pp. 1569-1584.

Bouwer, H., 1978. *Groundwater Hydrology.* New York: McGraw-Hill Inc.

Bouwer, H., 1978. *Groundwater Hydrology.* New York: McGraw-Hill, Inc.

Breedt, N., 2022. *Bi-annual Surface- and Groundwater Quality Evaluation for Johannesburg City Parks – Cemeteries,* Johannesburg: Aquatico Scientific.

Carol, B., 2009. Groundwater flow through fractured rocks. In: *Groundwater.* s.l.:EOLSS Publications, pp. 22-42.

Carrillo-Rivera, J. J. & Cardona, A., 2012. Groundwater Flow Systems and Their Response to Climate Change: A Need for a Water-System View Approach. *American Journal of Environmental Sciences,* 8(3), pp. 220-235.

Charles, R. F., 2002. Groundwater: the Big Picture. In: *Groundwater Science.* London: Academic Press, pp. 1-17.

Cheremisinoff, N. P., 1997. 3 - Principles of Hydrogeology. In: N. P. Cheremisinoff, ed. *Groundwater Remediation and Treatment Technologies.* s.l.:William Andrew Publishing, pp. 85-126.

Chiappelli, J. & Chiappelli, T., 2008. Drinking Grandma: The Problem of Embalming. *Journal of Environmental Health,* 71(5), pp. 24-28.

Cohen, A., 2023. *BioSoCal.* [Online] Available at: https://biosocal.com/what-are-the-stages-of-human-decomposition/ [Accessed 26 April 2023].

Commonwealth War Graves Commission, 2023. *Johannesburg (West Park) Cemetery.* [Online] Available at: https://www.cwgc.org/visit-us/find-cemeteries-memorials/cemetery-details/101545/johannesburg-west-park-cemetery/
[Accessed 25 June 2023].

Crank, J. & Nicolson, P., 1947. A practical method for numerical evaluation of solutions of partial differential equations of the heat-conduction type. *Mathematical Proceedings of the Cambridge Philosophical Society,* 43(1), pp. 50-67.

Cremation Institute, 2023. *Muslim Funeral Traditions: 10 Things You Should Know.* [Online] Available at: https://cremationinstitute.com/muslim-funeral-traditions/ [Accessed 10 July 2023].

Danielopol, D., Grievler, C., Gunatilaka, A. & Notenboom, J., 2003. Present state and future prospects for groundwater ecosystems. *Environment Conservation,* 30(2), pp. 104-130.

Darcy, H., 1856. *Exposition and application of the principles to be followed and the formulas to be employed in questions of the distribution of water.* 1st ed. Victor Dalmont, Paris: The public fountains of the city of Dijon.

Dent, B. B., Forbes, S. L. & Stuart, B. H., 2004. Review of human decomposition processes in soil. *Environmental Geology,* Volume 45, p. 576–585.

Dent, B. B. & Knight, M. J., 1998. Cemeteries: a special kind of landfill. The context of their sustainable management. Groundwater: sustainable solutions. *Conference of the International Association of Hydrogeologists,* pp. 451-456.

Department of Water and Sanitation, 2000. *THE JOHANNESBURG BROCHURE.* [Online] Available at: https://www.dws.gov.za/Groundwater/maps/jhbbrochure.pdf [Accessed 10 May 2023].

Department of Water and Sanitation, 2016. *National Groundwater Strategy,* Pretoria: Department of Water and Sanitation Strategy.

Durand, J. F., 2012. The impact of gold mining on the Witwatersrand on the rivers and karst system of Gauteng and North West Province, South Africa. *Journal of African Earth Sciences,* Volume 68, pp. 24-43.

Dutfield, S. & Rettner, R., 2021. *Live science.* [Online] Available at: https://www.livescience.com/37009-human-body.html [Accessed 24 April 2023].

Engelbrecht, J. F. P., 1993. *An assessment of health aspect on the impact of domestic and industrial waste disposal activities on groundwater resources,* Pretoria: Water Research Commission.

Eugene, I. & Herbert, B. K., 1994. *Analysis of Numerical Methods.* s.l.:Courier Corporation.

Fadugba, S. E., Adefolaju, F. H. & Akindutire, O. H., 2012. On the Stability and Accuracy of Finite Difference Method for Options Pricing. *Mathematical Theory and Modeling ,* 2(6), pp. 101-105.

Fitts, C. R., 2013. 2 - Physical Properties. In: C. R. Fitts, ed. *Groundwater Science (Second Edition).* s.l.:Academic Press, pp. 23-45.

Foster, S. S. & Chilton, P. J., 2003. Groundwater: the processes and global significance of aquifer degradation. *Philosophical Transactions of the Royal Society of London. Series B: Biological Sciences,* 358(1440), pp. 1957-1972.

Fourie, C., 2018. *Westpark Cemetery a resting place for thousands.* [Online] Available at: https://northcliffmelvilletimes.co.za/269779/westpark-cemetery-resting-place-thousands/
[Accessed 11 July 2023].

Franco, D. S. P., 2022. The environmental pollution caused by cemeteries and cremations: A review. *Chemosphere ,* Volume 307.

Gatrad, A. R., 1994. Muslim customs surrounding death, bereavement, postmortem examinations, and organ transplants. *BMJ,* Volume 309, pp. 521-523.

Gill-King, H., 1997. Chemical and ultrastructural aspects of decomposition. In: W. D. Hagland & M. H. Sorg, eds. *Forensic taphonomy: the postmortem fate of human remains.* Florida: CRC Press LLC, pp. 93-108.

Goeppert, N. & Goldscheider, N., 2011. Transport and Variability of Fecal Bacteria Carbonate Conglomerate Aquifers. *Groundwater,* 1(49), pp. 77-84.

Goodman, A. M., 2003. *A Plain Pine Box: A Return to Simple Jewish Funerals and Eternal Traditions.* s.l.:Ktav Publishing House.

Gray, D. A., Mather, J. D. & Harrison, J. B., 1974. Review of groundwater pollution from waste disposal sites in England and Wales with provisional guidelines for future site selection. *The Quarterly Journal of Engineering Geology,* Volume 7, pp. 181-196.

Greaves, C., 2023. *Cemeteries and Crematoria Management,* Johannesburg: City Parks and Zoo House.

Groffman, P., Law, N., Belt, K. B. L. E. & Fisher, G. T., 2004. Nitrogen fluxes and retention in urban watershed ecosystems. *Ecosystems,* Volume 7, pp. 393-403.

Häggström, M., 2022. *Skeletonization.* [Online] Available at: https://en.wikipedia.org/wiki/Skeletonization#/media/File:Postmortem_interval_changes_(stages_of_death).png
[Accessed 27 April 2023].

Hanzlick, R., 1994. Embalming, body preparation, burial and disinterment. An overview for forensic pathologists. *The American Journal of Forensic Medicine and Pathology,* Volume 15, pp. 122-131.

Herzog, K., 2016. *A different way to die: the story of a natural burial.* [Online] Available at: https://www.vox.com/2016/5/29/11775976/natural-green-burial [Accessed 14 July 2023].

Igret Araz, S. & Atangana, A., 2022. Step forward in epidemiological modeling: Introducing the indicator function to capture waves. *Results in Physics,* Volume 30.

Iyyanki, V. M. & Valli, M., 2017. Chapter Eleven - Principles and Design of Water Treatment. In: V. M. Iyyanki & M. Valli, eds. *Environmental Management.* India: Butterworth-Heinemann, pp. 209-248.

Janaway, R. C., Percival, S. L. & Wilson, A. S., 2009. Chapter 14: Decomposition of Human Remains. In: S. L. Percival, ed. *Microbiology and Aging .* New York: Humana Press, pp. 313-334.

Jenifer, A. M. & Jha, M. K., 2018. Comprehensive risk assessment of groundwater contamination in a weathered hard-rock aquifer system of India. *Journal of Cleaner Production,* Issue 201, p. 853–868.

Jha, M. K., Chowdhury, A., Chowdary, V. M. & Peiffer, S., 2007. Groundwater management and development by integrated remote sensing and geographic information systems: prospects and constraints. *Water Resources Management,* Volume 21, pp. 427-467.

Ji, Y. et al., 2020. easonal variation of drinking water quality and human health risk assessment in Hancheng City of Guanzhong Plain, China. *Exposure and Health,* Issue 12, p. 469–485.

Jones, D., 2013. *To Bury or to Burn? Cremation in Christian Perspective.* [Online] Available at: https://www.thegospelcoalition.org/article/to-bury-or-to-burn-cremation-in-christian-perspective/
[Accessed 9 July 2023].

Jonker, C. & Olivier, J., 2012. Mineral contamination from cemetery soils: case study of Zandfontein Cemetery, South Africa. *International Journal of Environmental Research and Public Health,* Volume 9, pp. 511-520.

Jonker, C. & Olivier, J., 2012. Mineral Contamination from Cemetery Soils: Case Study of Zandfontein Cemetery, South Africa. *International journal of environmental research and public health,* 9(2), pp. 511-520.

Kaapu, M., 2021. *Joburg Cemeteries.* [Online]
Available at: https://www.jhbcityparksandzoo.com/services-facilities/cemeteries/joburg-cemeteries
[Accessed 17 August 2023].

Kapulu, M., 2012. *Iron Removal in Borehole Water: A Case Study of Luapula Province,* Zambia: University of Zambia.

Kaur, L., Rishi, M. S. & Siddiqui, A. U., 2020. Deterministic and probabilistic health risk assessment techniques to evaluate non-carcinogenic human health risk (NHHR) due to fluoride and nitrate in groundwater of Panipat, Haryana, India. *Environmental Pollution,* 259(1137112), pp. 1-11.

Kazmeyer, M., 2023. *Seattlepi.* [Online]
Available at: https://education.seattlepi.com/stages-human-decomposition-process-4705.html
[Accessed 26 April 2023].

Keijzer, E., 2017. The environmental impact of activities after life: life cycle assessment of funerals. *International Journal of Life Cycle Assessment,* 22(5), p. 715–730.

Kemerich, P. D. ,. d. C. et al., 2014. *Chemical Changes in Soil Occupied for Cemetery Horizontal in Rio Grande Do Sul,* North: s.n.

Knight, M. J. & Dent, B. B., 1995. A Watery Grave - The Role of Hydrogeology in Cemetery Practice. *Australian Cemeteries & Crematoria Association,* Volume 2, pp. 19-22.

Kruger, A. C. & Mbatha, S., 2021. *Regional Weather and Climate of South Africa: Gauteng,* Gauteng: South African Weather Service, SAWS.

Landrot, G. & Sparks, D. L., 2022. Sorption–desorption kinetics. In: *Reference Module in Earth Systems and Environmental Sciences.* s.l.:Elsevier.

Leketa, K., Abiye, T. & Butle, M., 2018. Characterisation of groundwater recharge conditions and flow mechanisms in bedrock aquifers of the Johannesburg area, South Africa. *Environmental Earth Sciences,* 77(22), p. 727.

Li, P., Karunanidhi, D., Subramani, T. & Srinivasamoorthy, K., 2021. Sources and Consequences of Groundwater Contamination. *Archives of Environmental Contamination and Toxicology ,* Volume 80, pp. 1-10.

Li, P., Tian, R., Xue, C. & Wu, J., 2017. Progress, opportunities and key fields for groundwater quality research under the impacts of human activities in China with a special focus on western China. *Environmental Science and Pollution Research,* Volume 24, p. 13224–13234.

Li, P. et al., 2018. Geochemistry, hydraulic connectivity and quality appraisal of multilayered groundwater in the hongdunzi coal mine, Northwest China. *Mine Water and the Environment,* Volume 37, p. 222–237.

Long, J. C. S. et al., 1996. *Rock Fractures and Fluid Flow: Contemporary Understanding and Applications.* Washington: National Academy of Sciences.

Lyu, X. et al., 2019. Transport and retention of perfluorooctanoic acid (PFOA) in natural soils: importance of soil organic matter and mineral contents, and solution ionic strength. *Journal of Contaminant Hydrology,* Volume 225.

Matlabgeeks, 2006. *Von Neumann Stability Analysis Presentation.* [Online] Available at: https://matlabgeeks.weebly.com/uploads/8/0/4/8/8048228/von_neumann_stability_analysis-presentation-v5.pdf
[Accessed 30 August 2023].

Mattern, S., Sebilo, M. & Vanclooster, M., 2011. Identification of the nitrate contamination sources of the Brusselian sands groundwater body (Belgium) using a dual-isotope approach. *Isotopes in Environmental and Health Studies,* 47(3), pp. 297-315.

Matthews Cremation Division, 2006. *Cremation Equipment Operator Training Program,* Apopka (FL): Matthews Cremation Division.

McCarthy, T. S., 2006. The Witwatersrand Supergroup. *The Geology of South Africa,* Volume 1, pp. 155-186.

Morton, K. W. & Mayers, D. F., 1994. *Numerical Solution of Partial Differential Equations.* United Kingdom: Cambridge University Press.

Murray, E. & Douglas, M., 2001. Predicting Impacts of Groundwater Contaminantion. */ ENVIRONMENTAL SCIENCE & TECHNOLOGY,* 35(3).

Mvandaba, V. et al., 2019. *Green Book. The impact of climate change on South Africa's future groundwater availability,* Pretoria: CSIR.

Neckel, A. et al., 2021. Hazardous elements in the soil of urban cemeteries; constructive solutions aimed at sustainability. *Chemosphere,* Volume 262.

Norman, N. & Whitfield, G., 2006. Geological Journeys. In: Cape Town: Struik Publishers.

Oliveira, B. et al., 2013. Burial grounds' impact on groundwater and public health: an overview. *Water and Environmental Journal,* 27(1), pp. 99-106.

Özkan, B., Küçükerba, E., Kaplan, A. & Aslan, N., 1996. *Open-Green Area And Planning and Design of Cemeteries as Recreation Areas In the Example of Izmir City of Problems and Solution Opportunities Searching for,* Bornova, zmir: Ege University Research Fund Research Report,Project No: 1994/006.

Pacheco, A. et al., 1991. Cemeteries - A Potential Risk to Groundwater. *Water Science and Technology,* 24(11), pp. 97-104.

Ralston, A. & Rabinowitz, P., 2012. A First Course in Numerical Analysis. In: 2nd, ed. *Dover Books on Mathematics.* s.l.:Courier Dover Publications, pp. 2-4.

Rance, D. et al., 2006. *Feasibility Study for the Burnstone Gold Project, Balfour, Mpumulanga Province, Republic of South Africa,* Balfour: Behre Dolbear and Company Ltd.

Saravanan, S., Parthasarathy, K. S. S. & Sivaranjani, S., 2019. Chapter 10 - Assessing Coastal Aquifer to Seawater Intrusion: Application of the GALDIT Method to the Cuddalore Aquifer, India. In: M. Ramkumar, A. R. James, D. Menier & K. Kumaraswamy, eds. *Coastal Zone Management.* s.l.:Elsevier, pp. 233-250.

Schraps, W. G., 1972. The importance of the filtering properties of the soil for the creation of cemeteries. *Society,* Volume 16, pp. 225-229.

Shackelford, C. D., 1993. Contaminant transport. In: D. E. Daniel, ed. *Geotechnical Practice for Waste Disposal.* London: Chapman & Hall.

Silliman, S. & Simpson, E., 1987. Laboratory evidence of the scale effect in dispersion of solutes in porous media. *Water Resources Research,* Volume 23, pp. 1667-1673.

Silva, F. C. B., Haberland, N. T. & Filho, P. C. O., 2011. Cemeteries as a source of contamination of groundwater and watercourses. In: *Book of Abstracts.* Brazil, Santa Cruz: Integration week teaching, research and extension, pp. 1-4.

Silva, R. B. P. d. et al., 2020. Concentration of heavy metals in soils under cemetery occupation in amazonas, Brazil. *Soil sediment contamination. An International Journal,* Volume 29, pp. 192-208.

Simmons, C. T., Fenstemaker, T. R. & Sharp Jr, J. M., 2001. Variable-density groundwater flow and solute transport in heterogeneous porous media: approaches, resolutions and future challenges. *Journal of Contaminant Hydrology,* Volume 52, pp. 245-275.

Singh, M. & Kaur, S., 2003. Groundwater Pollution: An overview. *Journal of the IPHE,* Volume 2.

Slichter, C., 1905. Field measurements of the rate of movement of underground waters. *US Gelogical Survey Water-Supply and Irrigation Paper,* Volume 140.

Spongberg, A. L. & Becks, P. M., 2000. Inorganic soil contamination from cemetery leachate. *Water Air and Soil Pollution,* 117(1-4), pp. 313-327.

SRK, C., Aurecon, Solutions, S. & Turner, T., 2013. *Feasibility Study for a Long-Term Solution to address the Acid Mine Drainage associated with the East, Central and West Rand underground mining basins. Assessment of the Water Quantity and Quality of the Witwatersrand Mine Voids,* Pretoria: Department of Water Affairs.

Stewart, R. A., Reimold, W. U. & Charlesworth, E. G., 2004. Tectonosedimentary model for the Central Rand Goldfield, Witwatersrand Basin, South Africa. *South African Journal of Geology,* Volume 107, pp. 603-618.

Sukop, M. C. & Dentz, M., 2022. Solute transport. In: *Reference Module in Earth Systems and Environmental Sciences.* s.l.:Elsevier.

Talabi, A. & Kayode, T., 2019. Groundwater Pollution and Remediation. *Journal of Water Resource and Protection,* Volume 11, pp. 1-19.

Toride, N., Inoue, M. & Leij, F. J., 2003. Hydrodynamic Dispersion in an Unsaturated Dune Sand. *Soil Science Society of America Journal,* Volume 67, pp. 703-712.

Tornevi, A., Bergstedt, O. & Forsberg, B., 2014. Precipitation Effects on Microbial Pollution in A River: Lage Structures and Seasonal Effect Modification. *PLOS One,* 9(5).

Toth, J., 1963. A theoretical analysis of groundwater flow in small drainage basins. *Journal of Geophysical Research,* 68(16), p. 4795e4812.

Tóth, J., 1970. A conceptual model of the groundwater regime and the hydrogeologic environment. *Journal of Hydrology,* Volume 10, pp. 164-176.

Trick, J. K. W., Noy, G. M., Moore, D. J. & Reeder, Y. S., 1999. *Pollution Potential of Cemeteries: Impact of the 19th century Carter Gate Cemetery, Nottingham,* Nottingham: Technical Report WE/99/4.

Trozzi, C. et al., 2019. *MEP/EEA Air Pollutant Emission Inventory Guidebook: Cremation,* Copenhagen, Denmark: European Environment Agency.

Tucker, R. F., Viljoen, R. P. & Viljoen, M. J., 2016. A Review of the Witwatersrand Basin - The World's Greatest Goldfield. *Episodes,* 39(2), pp. 106-129.

Tumagole, K. B., 2006. *Geochemical survey of underground water pollution at Ditengteng northern cemetery within city of Tshwane municipality,* Johannesburg: University of Johannesburg.

Tumagole, K. B., 2009. *Geochemical survey of underground water pollution at Ditengteng northern cemetery within city of Tshwane municipality,* Johannesburg: University of Johannesburg.

Üçisik, A. S. & Rushbrook, P., 1998. *THE IMPACT OF CEMETERIES ON THE ENVIRONMENT AND PUBLIC HEALTH,* Europe: World Health Organization.

United States Agency, 2012. *Climate Change Adaptation in Southern Africa,* United States: USAID.

United States Geological Survey, U., 2021. *Geological Influences on the Quality of Groundwater Used for Domestic Supply in the Northern Sierra Nevada Foothills,* Colifonia: Water Boards.

van Allemann, S., Dippenaar, M. A. & Olivier, J., 2019. A laboratory study of the leachate composition of selected metals in cemeteries (South Africa). *Environmental Earth Sciences ,* 74(518).

van Allemann, S., Olivier, J. & Dippenaar, M. A., 2018. A laboratory study of the pollution of formaldehyde in cemeteries (South Africa). *Environmental Earth Sciences,* 77(1).

Van Haaren, F. W. J., 1951. Cemeteries as sources of groundwater contamination. *Water,* 35(16), pp. 167-172.

Vermeulen, T. & Heister, N. K., 1952. Ion-Exchange Chromatography of Trace Components. *Industrial & Engineering Chemistry Research,* 44(3), pp. 636-651.

Viljoen, G. & Bosman, C., 2022. *Some Legal Options to Ensure the Protection of South Africa's Utilisable Groundwater Resources.* [Online] Available at: http://dx.doi.org/10.17159/1727-3781/2022/v25i0a13483 [Accessed 08 February 2023].

Wang, C.-Y. & Manga, M., 2021. Groundwater Flow and Transport. In: G. M. Friedman & A. Seilacher, eds. *Water and Earthquakes.* United Kingdom: Springer, pp. 9-22.

Wilkinson, T., 2016. *Typology: Crematorium,* s.l.: EMAP Publishing LTD.

Witthüser, K. T. & Holland, M., 2008. *Hydrogeology of the Cradle of Humankind World Heritage Site, South Africa.* Goa, India, IACMAG.

Woessner, W. W. & Poeter, E. P., 2020. Properties of Aquifers and Confining Units. In: *Hydrogeologic Properties of Earth Materials and Principles of Groundwater Flow.* Canada: Groundwater Project, p. 205.

World Climate Guide, 2023. *Climate - Johannesburg (South Africa).* [Online] Available at: https://www.climatestotravel.com/climate/south-africa/johannesburg [Accessed 26 June 2023].

World Health Organization, 2011. *Manganese in Drinking-water: Background document for development of WHO Guidelines for Drinking-water Quality,* Switzerland: WHO Press.

Wright, A., 1999. *Groundwater contamination as a result of developing urban settlement. Report to the water research commission: WRC Report No. 514/1/99,* Pretoria: Cape water Programme Environmental CSIR.

Young, C. P., Blackmore, K. M., Reynolds, P. J. & Leavens, A., 1999. *Pollution Potential of Cemeteries – Draft Guidance,* Bristol, United Kingdom: R&D Technical Report P223, Environment Agency.

Zhou, Y. & Li, W., 2011. A review of regional groundwater flow modeling. *Geoscience Frontiers,* 2(2), pp. 205-214.

Zhuang, L. et al., 2021. Unsaturated flow effects on solute transport in porous media. *Journal of Hydrology,* Volume 598.